8-2-2017

Efficient Template-Based Nanomanufacturing of Carbon Nanotube Arrays for Cell Applications

Adeel Ahmed
aa5925@rit.edu

Efficient Template-Based Nanomanufacturing of Carbon Nanotube Arrays for Cell Applications

by

Adeel Ahmed

A Thesis Submitted in Partial Fulfillment of the Requirements for the Degree of Master of Science in Mechanical Engineering

Supervised By

Associate Professor Dr. Michael Schrlau

Department of Mechanical Engineering

Kate Gleason College of Engineering

Rochester Institute of Technology

Rochester, New York

August 2nd, 2017

Approved By:

Dr. Michael Schrlau, Associate Professor

Thesis Adviser, Department of Mechanical Engineering

Dr. Kathleen Lamkin-Kennard, Associate Professor

Committee Member, Department of Mechanical Engineering

Dr. Thomas Gaborski, Associate Professor

Committee Member, Department of Biomedical Engineering

Dr. Agamemnon Crassidis, Professor

Department Representative, Department of Mechanical Engineering

Abstract

Carbon nanotube arrays have been found to be highly effective at carrying out intracellular delivery of cargo at high efficiencies while ensuring cell viability. Template based chemical vapor deposition is a commonly used process to fabricate these arrays. However, current etching methods used to expose carbon nanotubes from templates are expensive and time consuming. The high cost and time-consuming processes currently required to fabricate such arrays are factors which limit the commercialization of this technology and inhibit scope for larger research programs. In this thesis, alternative nanofabrication methods were explored with the aim of making the fabrication of CNT arrays cost effective and efficient. Mechanical polishing coupled with wet chemical etching is shown as a feasible alternative option to dry etching. The effects of process variables on physical properties of CNT arrays have been studied and quantified in order to demonstrate control over the process. Scanning Electron Microscopy has been used to qualitatively understand the differences between CNT arrays fabricated using dry etching and the alternative process. Cell culture has been demonstrated on the CNT arrays and the potential to use 3D printing to fabricate a nanofluidic device is also demonstrated. The alternative process can save etching time by 97% while maintaining a similar level of control over the process. This study therefore, opens the path to quicker production of CNT arrays at low cost for biomedical use.

Acknowledgements

I would like to thank my adviser and mentor, Dr. Schrlau for guiding me along a long and winding path with much patience and diligence. This work would not have been possible without your mentorship, support and resourcefulness. Thank you for letting me be a part of the NBIL and supporting me through thick and think during this project.

I am also deeply delighted to have worked with the friendliest, most supportive lab mates -Masoud, Olivia, Anna, Ryan, Peter, Devarsh, Christina, James, Koby and Schkenca. Your continued stories of raccoons and wild turkeys coupled with our escapades to Indian buffet to posting embarrassing updates on my Facebook when I was not looking helped me keep my morale up and gave me a much-needed level of personal support. Also, I would like to acknowledge that you were all excellent storehouses of knowledge and ideas during my project.

Dr. Ian Dickerson walked me through working with cells and never ran out stories about BMWs. Thank you for guiding me and having the patience to put up with my rookie mistakes and often erratic schedule.

Lastly, I would like to extend my heartfelt gratitude to my parents, Amra and Nadeem, who have supported me unconditionally, showered me with blessings I cannot even count and always believed in me. My brother Fauzan, for constantly distracting me with his stories of school and love for video games and my late brother Adnan who was my motivation to work in this field. You were a source of joy to our family and will forever be missed. I hope someday technology like the one discussed in this study will prevent many from the pain and suffering you endured in this world.

Contents

List of Figures

List of Abbreviations

DOTMA	1,2-di-O-octadecenyl-3-trimethylammonium propane
AIDS	Acquired immune deficiency sydnrome
AAO	Anodized aluminum oxide
CNT	Carbon nanotube
CNTFET	Carbon nanotube field effect transistor
CHO	Chinese Hamster Ovary
cDNA	Complementary deoxyribonucleic acid
DNA	Deoxyribonucleic acid
DWNT	Double wall carbon nanotube
EDS	Electron dispersive spectroscopy
GFP	Green Fluorescent Protein
HEK	Human embryonic kidney cells
HIV	Human immunodeficiency virus
MSC	Mesenchymal stem cell
MWCNT	Multi wall carbon nanotube
NADH	Nicotinamide adenine dinucleotide
PI	Propidium Iodide
RIE	Reactive ion etching
RNA	Ribonucleic acid
SEM	Scanning electron microscopy
SCID	Severe combined immunodeficiency disease
SWNT	Single wall carbon nanotube
TB-CVD	Template based chemical vapor deposition

1. Introduction

According to the American Medical Association, the cause of more than 4000 serious diseases can be attributed to gene disorders [1]. These diseases include cancer, acquired immune deficiency syndrome (AIDS), cystic fibrosis, Parkinson's and Alzheimer's diseases. The cause may be gene mutations or missing genes caused due to external factors such as radiation, viruses or in many cases, mutations during deoxyribonucleic acid (DNA) replication. Most of these diseases are known to be incurable in the true sense of the word. Although there exist methodologies to slow down the spread of diseases like cancer and Parkinson's, they are far from perfect, often resulting in harmful side effects and severely limiting the patient's abilities and reducing quality of life.

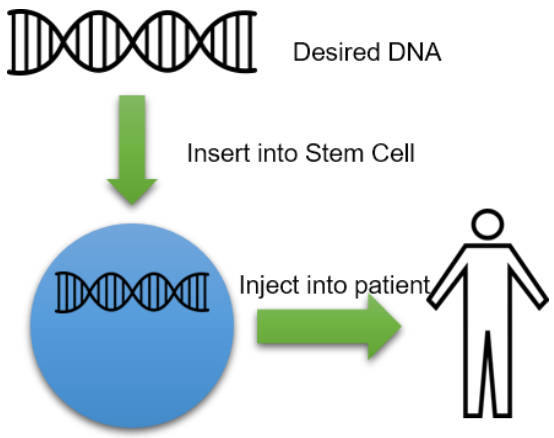

Figure 1.1: Mechanism of gene therapy

In the 1980's, multiple studies were carried out on animal models to study the feasibility of transferring healthy genes into cells which upon expression *in vivo* would result in the development of healthy cells. This method of healing is known as gene therapy. It has in recent times been explored as a cure for cancer [2, 3], cystic fibrosis [4], HIV [5, 6] and color blindness [7] with highly encouraging results. The crux of gene therapy is to transfect stem cells with DNA or other proteins *in vitro*, depicted in Fig. 1.1. These cells, once genetically modified can repair, replace or inhibit the action of a specific DNA strand. The altered cells are then capable of developing immunity against attacking viruses causing the disease, express DNA which was earlier deficient to overcome a genetic disability or grow into enhanced macrophages which can further fight the disease in question. It can be concurred that the most important element of gene therapy is to develop a method for transfecting of cells with the DNA or protein in question without inducing harmful side effects and ensuring cell viability.

Transfection into cells for gene therapy conventionally has been carried out using viral vectors or lipids [6, 8-12]. Viruses have the unique ability of expressing their genetics in the cells they infect. This ability of viruses has been taken advantage of by modifying viruses to express a desirable genetic code rather than a harmful one. However, side effects such as immunological attacks on viruses, homologous recombination and cytopathic effects must be considered when using viruses for transfection [10]. Other commonly methods of transfection being used include electroporation – the application of an electric field to cells allowing charged particles to move into cell [13, 14]; particle bombardment – bombardment of particles onto the cell membrane at high velocity with the intent of them breaking through the cell membrane [15]; and the use of micro needles and wires to inject into individual cells [16].

Each of these methods has been successful in transfecting cells with appreciable efficiency yet they pose multiple issues which are yet to be resolved:

- Ensuring cell viability post transfection process
- Controlling the amount of cargo delivered to cells
- Cost effectiveness
- Transfection into different cell types
- Ensuring long expression times

The above issues, most notably, ensuring cell viability post transfection process has been one of the biggest limiting factors for further expanding research in gene therapy and large-scale implementation of this technology. A number of researchers have explicitly expressed the importance of safer, more viable transfection technologies to accelerate research in gene therapy and for large scale applications [11, 12, 17].

"The message we have extracted from a history of anticipation and disappointment is that the future success of gene therapy will be founded on a thorough understanding of vector biology and pharmacology (Kay et al, 2003)." [10]

"The success of gene therapy is largely dependent on the development of a vector or vehicle that can selectively and efficiently deliver a gene to target cells with minimal toxicity (Li. et al, 2000)" [18]

"we are still far from the perfect gene carrier suitable for clinical use (Niidome et al, 2002)."[15]

In 2013, Golshadi et al [19]. were able to manufacture an ordered array of carbon nanotubes (CNTs) by carrying out template based chemical vapor deposition (TB-CVD) of anodized aluminum oxide (AAO) and applied it to nanofluidic transport applications. The CNT array thus developed consisted of highly ordered, vertical carbon nanotubes, open from both ends and supported by an AAO template. This CNT array showed encouraging results when utilized to transfect cells by culturing cells on the device [20], shown in fig. 1.2. Compared to current state of the art methods such as particle bombardment, electrochemical methods and micro-injections, CNT arrays are minimally intrusive**,** caused no damage to

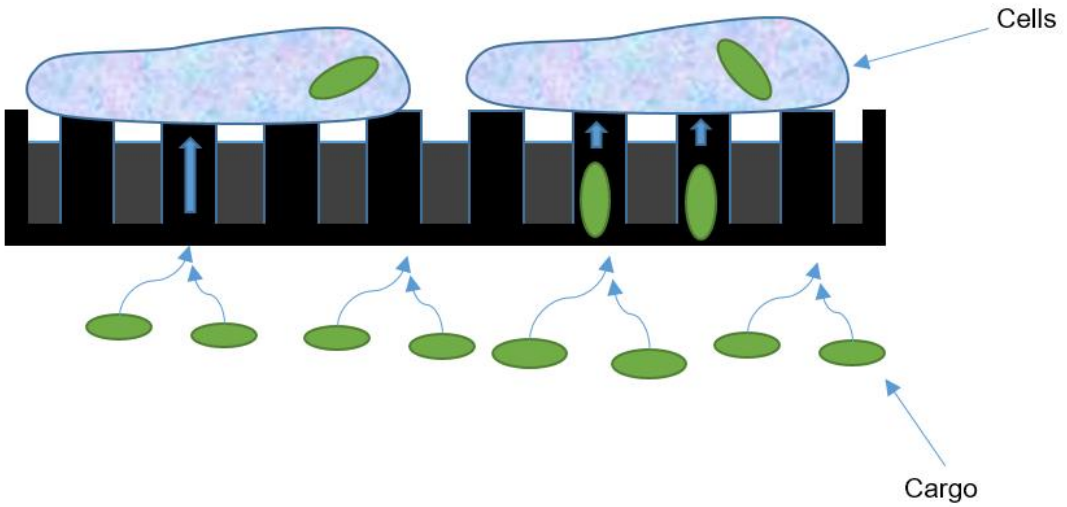

Figure 1.2: Schematic of CNT array device for intracellular delivery

the cells and achieved higher transfection efficiency. This is a breakthrough invention for biologists and genetic engineers working on drug delivery, gene therapy, cell therapy and studying the effects of novel synthetic genetic material on cells. CNT arrays also present the advantage of being able to interface with multiple cells in parallel, allowing for injections at a larger scale compared to individual injections.

CNT arrays offer the following advantages over current technologies:

- High transfection efficiency
- Controlled volume of delivery
- Cell viability
- Ability to transfect multiple cells in vitro
- Potential to transfect cells such as neural cells and stem cells

A limiting factor for CNT array technology is the current fabrication procedure for CNT arrays. Being time consuming and requiring specialized processes is hindering large scale fabrication and exploration in further areas of research which can exploit CNT arrays to their full potential. In order to explore large scale manufacturing feasibility and bring down costs, it is important to study the fabrication methods available to make these devices and suggest potential improvements.

Fabrication of the CNT array device currently involves the following steps, schematically depicted in fig. 1.3:

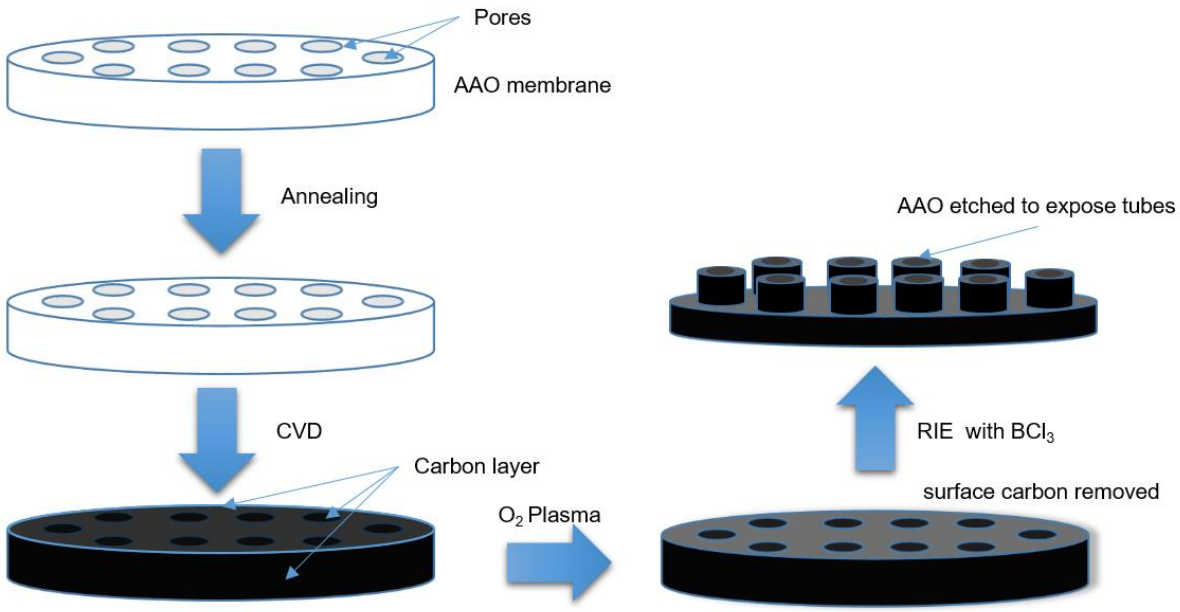

Figure 1.3: Stepwise fabrication of carbon nanotube array

Annealing of template: The template used to manufacture the CNT device is an anodized aluminum oxide membrane (AAO membrane) which is 13mm in diameter and 60µm in thickness. The membranes are annealed prior to CVD to prevent distortion during the high temperature CVD process.

Template based chemical vapor deposition: The membranes after annealing are ready for CVD. During CVD, the membranes are exposed to a continuous flow of ethylene in a sealed, high temperature furnace. The CVD set up used is depicted in fig. 1.4. Breakdown of ethylene leads to the deposition of carbon on the membrane surface and pores. The carbon deposited inside the pores of the membrane forms tubes. Carbon is deposited in its amorphous form and is not graphitic.

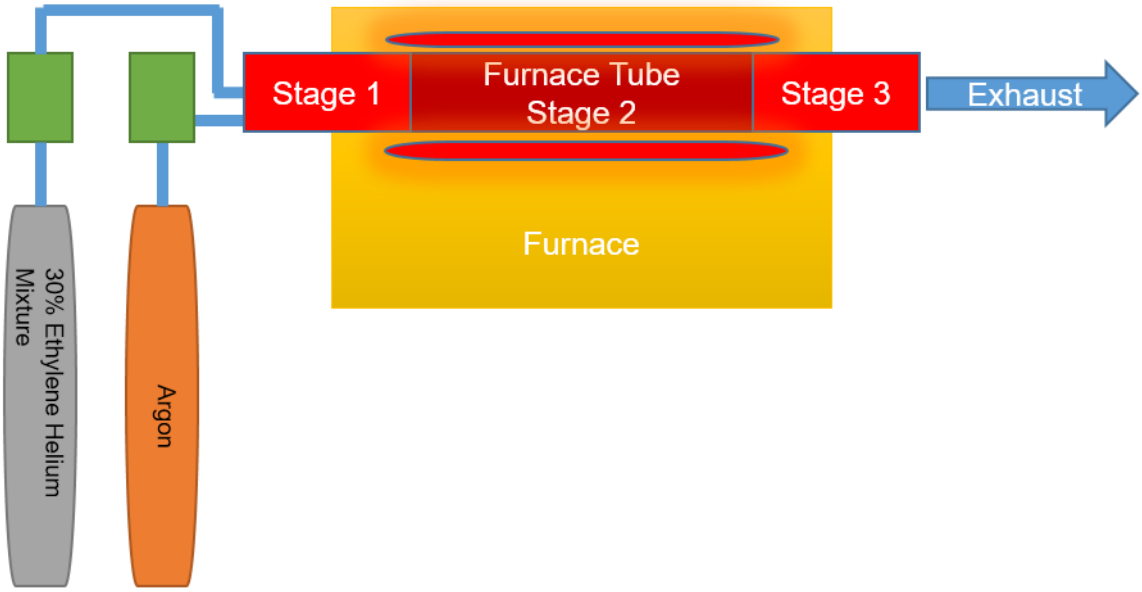

Figure 1.4: Schematic showing chemical vapor deposition (CVD) set up

Oxygen plasma etching: Before aluminum oxide can be etched away to expose tips of nanotubes, the layer of amorphous carbon deposited on the surface must be cleaned to expose aluminum oxide for etching. Oxygen plasma is used to selectively remove only the carbon layer and prepare the device for reactive ion etching.

Reactive ion etching using boron trichloride (BCl_3): Reactive ion etching (RIE) is a combined physical and chemical etching method carried out in a weakly ionized plasma. BCl_3 plasma is used to selectively etch aluminum oxide in a controlled manner. Etching is carried out to achieve an exposed length of ~250nm of nanotubes.

The device has demonstrated impeccable transfection into cells with minimal damage [20], however, there is scope for greater research such as studying the effects of variations in physical array dimensions on transfection, the method by which interfacing of device and cell occurs, transfection into a variety of cells and its application on tissue. These experiments require a large number of expendable CNT arrays. Also, the CNT arrays need to be produced quicker and with greater ease to make them feasible for large scale use in laboratories.

fig 1.5. Shows graphically the time consumed in each manufacturing process.

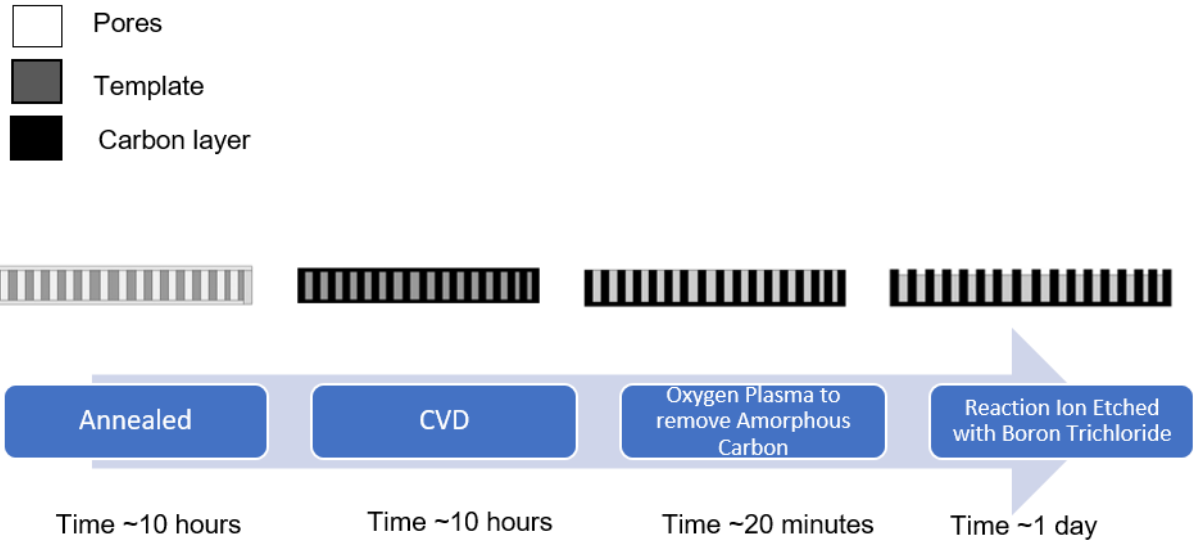

Figure 1.5: Breakdown of time required to fabricate CNT arrays

- The annealing process: Annealing takes up approximately 10 hours to anneal 10 membranes
- The CVD process: The CVD process requires another 10 hours to coat 7 membranes
- Oxygen plasma etching of amorphous carbon layer is a 20-minute process

- Reactive ion etching using BCl_3 is a 6 -12-hour long process which required specialized equipment and trained personnel to operate this equipment. BCl_3 is also a highly toxic gas which is described as hazardous.

Currently the process to fabricate these membranes can take up to 4 days for a batch size of 7 membranes. While the process can be scaled up using more sophisticated, large-scale equipment and parallel processing of batches, it is hindered by multiple issues which cannot easily be addressed.

A dry etching process is also resource intensive. This hinders large scale economic production of these arrays since setting up of such equipment is extremely costly which makes the commercialization of these devices difficult.

CVD and RIE processes, unlike conventional manufacturing processes are dependent on physical equipment variables such as size of chamber, voltage, power and position of substrate in the plasma chamber. A set of manufacturing parameters resulting in desirable outcomes on a certain set of equipment cannot be guaranteed to reproduce similar outcomes on a different set up. Equipment based variability is a major obstacle in ensuring repeatable results and preventing manufacturing errors. This is also a major obstacle in scaling up the current manufacturing system since a complete parametric study will be required with any type of equipment before it can be set up.

This thesis explores alternative nano-fabrication processes to overcome the above-mentioned drawbacks associated with the current process. Ease of scale-up, control over physical dimensions of CNTs and ease of access were considered while exploring alternative fabrication processes. A combination of mechanical polishing and wet chemical etching is presented as a feasible alternative with the potential to reduce etching time from the range of 6-12 hours to 10-40 minutes. The process variables affecting CNT properties have also been studied and quantified in detail followed by a qualitative assessment of device quality using scanning electron microscopy.

2. Background

2.1 Gene Therapy

The method of gene therapy is gaining popularity in treating diseases which have a genetic background. According to the American Medical Association, more than 4000 diseases have their root causes in genetic mutations or alterations caused due to microbes [1], external factors such as radiation, environment or errors during reproduction. Gene therapy in its most basic forms aims to rectify the problem by delivering the missing or dysfunctional gene into a patient's cells to allow for propagation of healthy cells and genetics.

One of the most comprehensive definitions for gene therapy is given by the European Medical Agency: [21]

"A gene therapy medicinal product is a biological medicinal product which fulfills the following two characteristics: (a) it contains an active substance which contains or consists of a recombinant nucleic acid used in or administered to human beings with a view to regulating, repairing, replacing, adding or deleting a genetic sequence; (b) its therapeutic, prophylactic or diagnostic effect relates directly to the recombinant nucleic acid sequence it contains, or to the product of genetic expression of this sequence. Gene therapy medicinal products shall not include vaccines against infectious products."

Gene therapy, as defined above, aims to deliver into cells the missing or deficient genes to enable expression of proteins which can act therapeutically against the disease in question. The most common mechanism employed in clinical trials around the world today is depicted in fig. 2.1 below: [22]

Step 1: Blood cells or stem cells are extracted from the patient and incubated. Stem cells can differentiate into a variety of specialized cells and hence, they are preferred for gene therapy. Through injection of the missing genetic material, stem cells can be made to differentiate into healthy cells with the ability to fight

disease such as enhanced macrophages. In some cases, they are modified to prevent a certain microbe from entering the cell, as in the case of gene therapy for the human immunodeficiency virus (HIV).

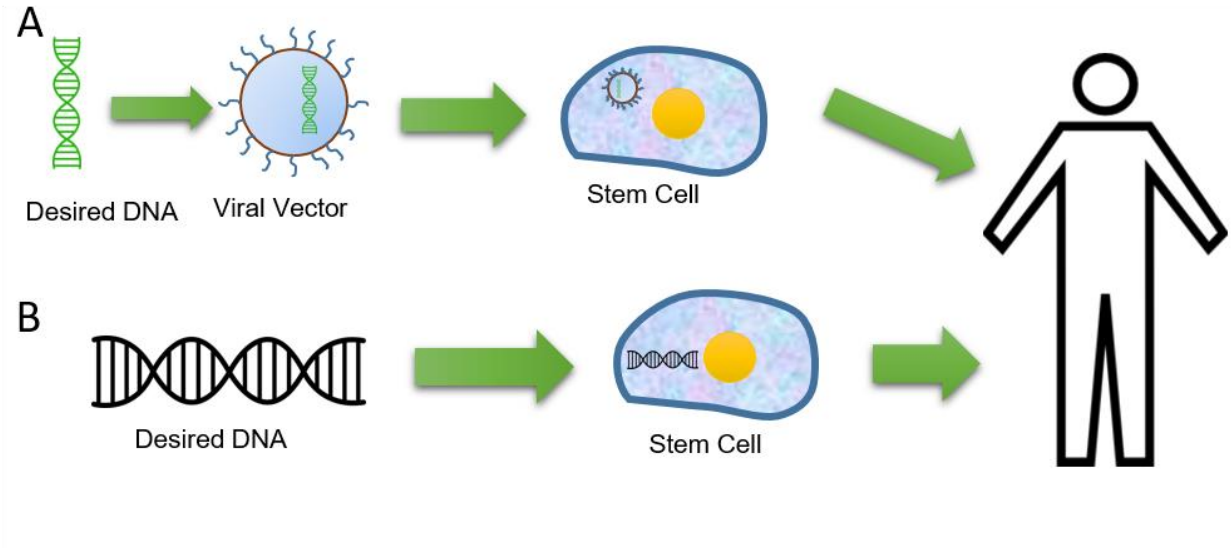

Figure 2.1: Process of gene therapy **(A)** using a viral vector **(B)** using non-viral vector

Step 2: The required cargo to be delivered is packaged inside a 'vector'. The vector is a carrier with the ability to permeate the cell membrane and deliver cargo without damaging either cell or cargo. The vector should satisfy the following conditions:

- Be able to permeate the cell membrane
- Not induce any cytopathic effects in cells
- Not induce homologous recombination [1]
- Be non-toxic
- Should not initiate immunogenic response against itself
- Be a safe carrier for cargo
- Carry required amount of cargo

[1] Exchange of nucleotides between similar DNA

The most common vectors used for gene therapy have been viruses which were genetically modified from their original form to be non-toxic and satisfy to an extent the conditions listed above.

Step 3: Cells collected from step 1 are infected with viruses modified in step 2 using techniques which will be briefly discussed in the next section. The viruses express the modified DNA they carried as cargo in the infected cell, leading to the creation of genetically modified cells. These cells upon division will now express the effects of the infected gene.

Step 4: Injection of genetically modified cells back into the patient. The cells once injected into the patient will now follow instructions coded in the cargo delivered to them. This will allow cells to differentiate into specialized cells to fight diseases or produce proteins which can mitigate the effect of disease.

2.1.1 Conventional Gene Transfection Technologies

It can be seen from the above section that designing an efficient vector is one of the most critical elements of a gene therapy based healing process. In fact, the first trials of gene therapy were made possible only after Roger and Pfuderer [23] showed proof of concept for genetic transfer into mammalian cells using viruses. Ever since, viruses have been used as vectors for transduction in gene therapy clinical trials for a number of diseases such as cancer [2, 3, 24], HIV [6] and others [4, 25, 26].

Viruses are microorganisms which are highly efficient in gaining access to cells and introducing viral DNA into their host cells. With this method, viruses are able to hijack the host cell into creating more copies of the virus. In the case of gene therapy, the ability of a virus to infect cells with its DNA is an advantageous capability. However, the viral DNA leading to toxicity and replication should be deleted and replaced by desirable cargo, depicted in fig. 2.2 before the virus can be allowed to infect the cell [27]. Sequences governing the functioning of the virus are left untouched but viral genes which lead to disease and toxicity are deleted. The protein to be expressed is cloned into the viral backbone in place of deleted genomes.

The viral vector particles also require purification which is often carried out using density gradient centrifugation. This step is often difficult to carry out and results in damage to the viral vectors, decreasing the number of viruses which can infect cells. Column chromatographic methods are also implemented and have overcome many drawbacks of centrifugation. [10]

Some of the viruses commonly used in gene therapy are as follows:

Lentiviral Vectors: Lentiviral vectors are derived from the HIV virus [27]. They have been used in gene therapy for the correction of β-thalassemia and X-linked [25, 28] adrenoleukodystrophy [29]. They have

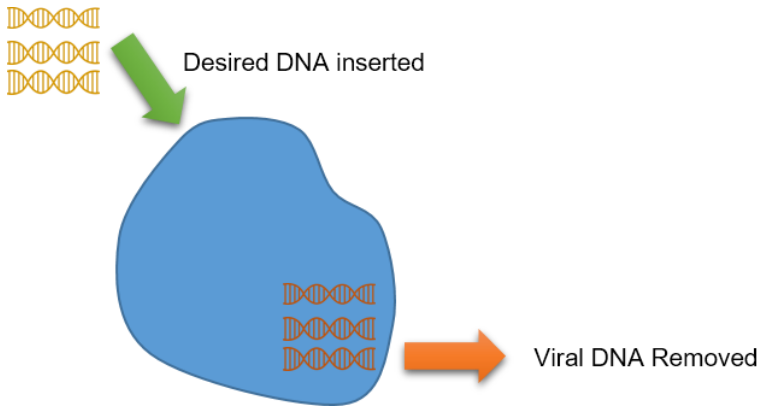

Figure 2.2: Modification of virus to create a viral vector

been used in earlier gene therapy trials owing to an ability to very well transcribe their ribonucleic acid (RNA) into cDNA[2] of host cells which makes them good gene carriers into target cells [11]. However, lentiviruses and retroviruses still pose significant toxicity to the host cells. Lentiviral vectors were used in a gene therapy trial which was published in April 2000 to treat severe combined immunodeficiency (SCID)-XI disease. A leukemia like disorder in two of the patients was observed and led to much anxiety in the field of gene therapy. The retrovirus genome had inserted itself near a cancer-causing protein in the LIM domain[3], activating its expression. [30]

[2] Complementary DNA
[3] Structural protein domain playing important role in organ development, oncogenesis and cytoskeletal organisation

Adenovirus Vectors*:* Adenoviruses are different from lentiviruses in the sense that they do not integrate into the genome of the cell [8], thus limiting the expression of their cargo to only limited number of cell generations before transduction is required again. Adenoviral vectors have also been popularly used for transfection in a number of clinical trials but have had their share of side effects. In 1999, 18 year old Jesse Gelsinger was part of a clinical trial at the University of Pennsylvania [31] aimed at treating ornithine transcarbylamase[4] deficiency. This deficiency can cause an accumulation of ammonia in the bloodstream leading to an ammonium buildup in the brain which is a fatal condition. Gelsinger developed high fever within 4 hours after delivery of the viral vector and died 4 days later due to multi organ failure. The vector had accumulated in the spleen, lymph nodes and bone marrow, resulting in intravascular coagulation. Subsequent studies have shown that the adenovirus capsid protein can elicit an early inflammatory cytokine cascade.

It is thus shown that viral vectors pose a number of dangers to patients who take part in gene therapy such as eliciting immunological responses against viruses and destroying the vectors, inflammation, limited transduction capabilities such as being able to transduce non-dividing cells only, oncological effects, limited packaging capacity and others [32]. Viral vectors also present a challenge in terms of storage, handling and scaling up of operations for commercial use. It is of importance to develop a method of transfection which can achieve the same functionality without the above-mentioned side effects.

To overcome these effects, the prospect of using non-viral vectors has caught up recently with a number of non-viral vectors being developed for use such as lipids, polymers, nanoparticles combined with physical means including injection, electroporation and gene gun [18]

[4] Enzyme responsible for safe removal of nitrogen from amino acids and proteins

Lipofection

Lipid refers to a class of special organic molecules, often fats, waxes, glycerides and oils that are soluble in water. In biological reference, lipids are the main constituent of the cell membrane. They are also used in the body as energy storage, signaling devices and to a lesser extent, for transportation.

Lipofection is a lipid mediated method of transfection wherein a lipid-DNA complex is formed, ready to be accepted by the cell membrane. Often anionic molecules are bonded to positively charged lipids in order to maintain a net positive charge on the complex. The cell membrane accepts this complex since the membrane itself is a phosphobilipid layer with an overall negative charge. The anionic cell membrane and cationic lipid-DNA complex are attracted to each other and form lipoplexes due to electrostatic interactions. This leads the complex being taken up by the cell through endocytosis and the cargo subsequently being released inside the cell.

This was first demonstrated in 1987 by Felgner et al [33] who used DOTMA for high efficiency gene transfer into kidney cells and fibroblasts. They demonstrated that 100% of the DNA was encapsulated by DOTMA in a 5:1 lipid to DNA ratio by weight. The transfection efficiency with varying concentrations of DNA and lipid was observed to be as high as 100% but a significant downside mentioned is that the DOTMA DNA complex would prove to be toxic beyond a certain concentration.

Lipofectamine, manufactured by Invitrogen is one of the commercially available lipofection agents available and in widespread use. It is a cationic molecule which can form complexes with anionic nucleic acids. Although high transfection efficiencies have been observed using lipofectamine, it still poses toxic dangers to the cell. Madeira et al. [34] attempted transfection of green fluorescent protein (GFP) into human mesenchymal stem cells (MSCs) and observed up to 35% efficiency but noticed decreasing cell viability with an increased volume of lipid. Another drawback of using lipofection is that neutral cargo such as quantum dots must be bonded to a charged protein before it can be used as cargo for lipofection.

Microinjection

Microinjection can be viewed as a precursor to nanoscale devices. It refers to the physical injection of material into the cell by physically penetrating the cell membrane using a micro-sized injection device such as a needle or syringe. Fig. 2.3 shows microinjection into a single cell. The cargo to be delivered is coated on the needle which subsequently penetrates the cell membrane and delivers cargo inside the cell. Microinjection has widely been used in the creation of genetically modified animals such as pigs [35] and expression of genes in mouse progeny by injection into mice eggs [36]. These are cases of small scale transfection where a limited number of cells were injected with the required gene.

This method is victim to two major disadvantages:

a. Low cell viability due to invasiveness of the method: A microinjection device has dimensions in the micrometer range which makes it invasive into the cell and reduces cell viability

b. Limited throughput: Transfection done on a cell by cell basis is prohibitively slow. For gene therapy purposes, hundreds of thousands of cells need to be transfected. In such cases, microinjection is limited by its low throughput.

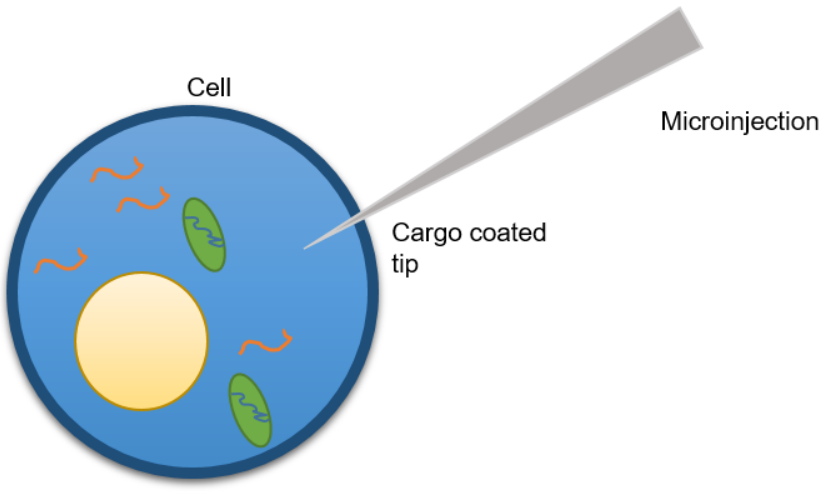

Figure 2.3: Microneedle injection into single cell using a cargo covered microneedle

An interesting, alternative use of microneedles or microneedle arrays is in the field of transdermal drug delivery. Drug delivery through hypodermic needles is often associated with pain and irritation, requiring specialized personnel for injection. Oral drug delivery is subject to reduced efficacy due to first pass metabolism in the body before the drug can reach its specified target. Microneedle arrays have been shown to be a potential candidate for alternative drug delivery [16, 37-39]. They are associated with a lack of pain, reduced dosage due to increased drug efficacy and easy delivery to intended site through skin. These results are encouraging when it comes to applying carbon nanotube arrays for injection into tissue.

Electroporation

Electroporation is a method of transfection in which an electric field is applied across the cell [14], allowing it to take up charged DNA or other molecules which would under normal conditions not diffuse across the cell membrane.

Under a short, high voltage electric field, phospholipid bilayers which are responsible for the integrity of cell membranes open, depicted in Fig. 2.4, allowing charged molecules to flow into the cell. These pores close immediately upon the removal of electric field. Electroporation has been found to work on a variety of cells and is also applicable for transfection *in vivo*, it does present a number of disadvantages which need to be overcome:

- Collateral cell damage during electroporation is significantly higher.
- Electroporation cannot permeate the cell nucleus.
- The efficiency of electroporation depends on the electrical properties of cells being transfected.

- Limited control over the amount of material delivered into cells.

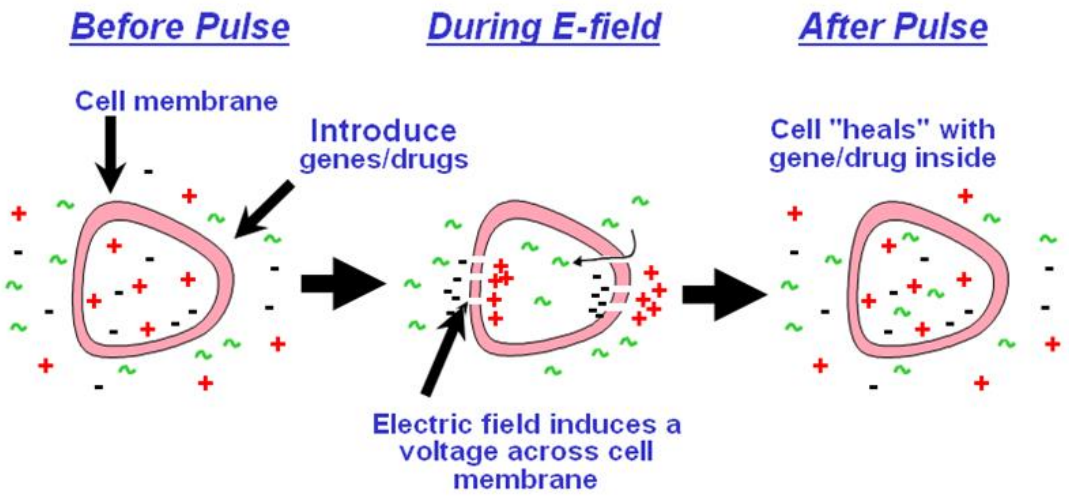

Figure 2.4: Schematic of electroporation. Adapted from [77]

Gene Gun (Particle Bombardment)

The gene gun utilizes high speed nanoparticles of heavy metals such as gold, platinum, titanium dioxide or polymers coated with the cargo [40, 41]. These nanoparticles upon impact with the cell are able to break through the cell membrane and thus deliver their cargo, shown in Fig. 2.5. The gene gun is effective in the transfection of hard to transfect cells such as plant cells but with the advent of more controlled methods, the use of particle bombardment has seen a decline. Some of the drawbacks of particle bombardment are as follows:

- Ability of the targets to resist damage due to high speed particles
- Little control over amount delivered into cells
- Potential toxicity of nanoparticle carriers
- Damage to cells

- Low efficiency (20-30% expression)

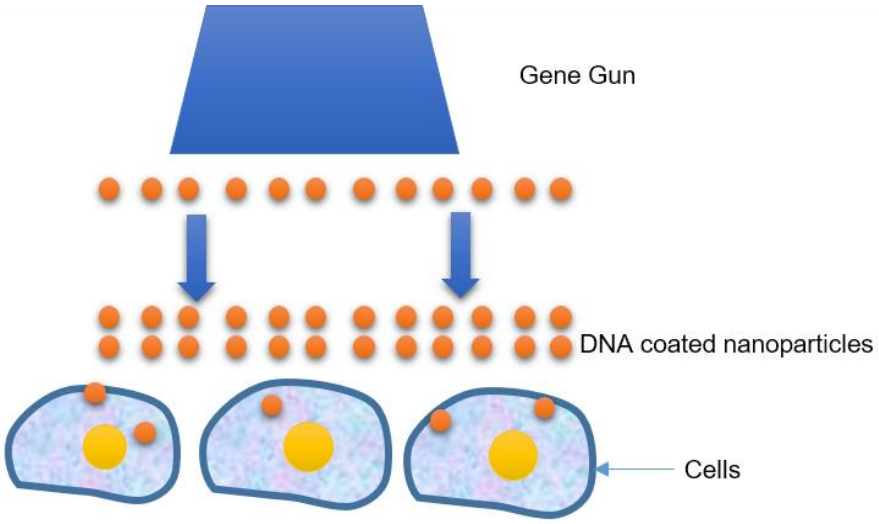

Figure 2.5: Process of particle bombardment

The potential to overcome the above limitations set forth by viral and non-viral vectors can be explored using injection devices which have been designed specifically to inject into cells with high efficiency without damaging the cell membrane. Work in the field of nanotubes, nanowires and their arrays has shown that these devices are capable of achieving transfection into cells. Researchers have different approaches for transfection with these structures. A common approach is to use high aspect ratio nano-needles or pillars with a height ranging from 2-6μm and a tip diameter in the tens of nanometers. Cargo is usually coated on the surface of these pillars with the help of an amphiphilic coating [42, 43] and then delivered into the cell when the needle or pillar penetrates the cell membrane by physically breaking through it. The cells might penetrate the device under their own weight or in some cases, physical pressing or centrifugation [44] is utilized to accelerate the process. Results from selected previous works are presented below.

3.1.2 Nano Structures for Transfection

In 2007, Kim et al [43]. prepared Si nanowire arrays with the intent of physically transferring material into the cell by rupturing the cell membrane using nanowires. The nanowires were 90nm in diameter and 60μm in length. Human Embryonic Kidney Cells (HEK293T) were grown on the clusters of nanowires which seemed to penetrate the cell easily without any external force. Cargo was coated on the Si nanowire

array and delivered into the cell through physical piercing of the cell membrane. This required functionalizing the nanowires to bind cargo. The nanowire arrays were fabricated using gold nanoparticles seeds planted on Si (111) wafers subject to CVD. The Si needle diameters were controlled via etching in HF after oxidation. This was one of the earliest transfection attempts using Si nanowires. Cell viability was observed at 78% with cells surviving a maximum of 3 days (Mouse embryonic stem cells). Primary attempts at transfection were carried out on HEK293 cells with DNA electrostatically attached to SiNWs. An efficiency of less than 1% was observed but this was attributed to the strong bonding between SiNW and DNA.

In 2009, Shalek et al [42] were able to manufacture vertical SiNW arrays for transfection into cells with the difference being mainly in the dimensions of nanowires. Although not explicitly reported, the SEM micrographs convey wire lengths of 1μm and diameter in the 50nm range. They used a similar manufacturing method as Kim et. al. Transfection was attempted using multiple cell types such as HeLa, human fibroblasts and rat hippocampal neurons. Regardless of the type of cells used, they claim to have observed a 95% transfection efficiency in all cells within 1 hour. They also utilized surface functionalization to bind their cargo to the nanowires and the mode of delivery was mechanical piercing of cells.

VanDersarl et al. in 2012 [45] developed silicon ‘nanostraws’ for direct fluidic access into cells. The nanostraws were hollow, 100nm in diameter and 1μm in height. Poly-carbonate membranes were used as templates for aluminum oxide deposition. Alumina specific reactive ion etch followed by a poly-carbonate specific etch were used to expose nanostraws. They used membrane impermeable dyes to demonstrate transfection and observed 3-10% transfection rate of the cells pierced by the nanostraws. Array devices fabricated by various researchers are shown in Fig. 2.6.

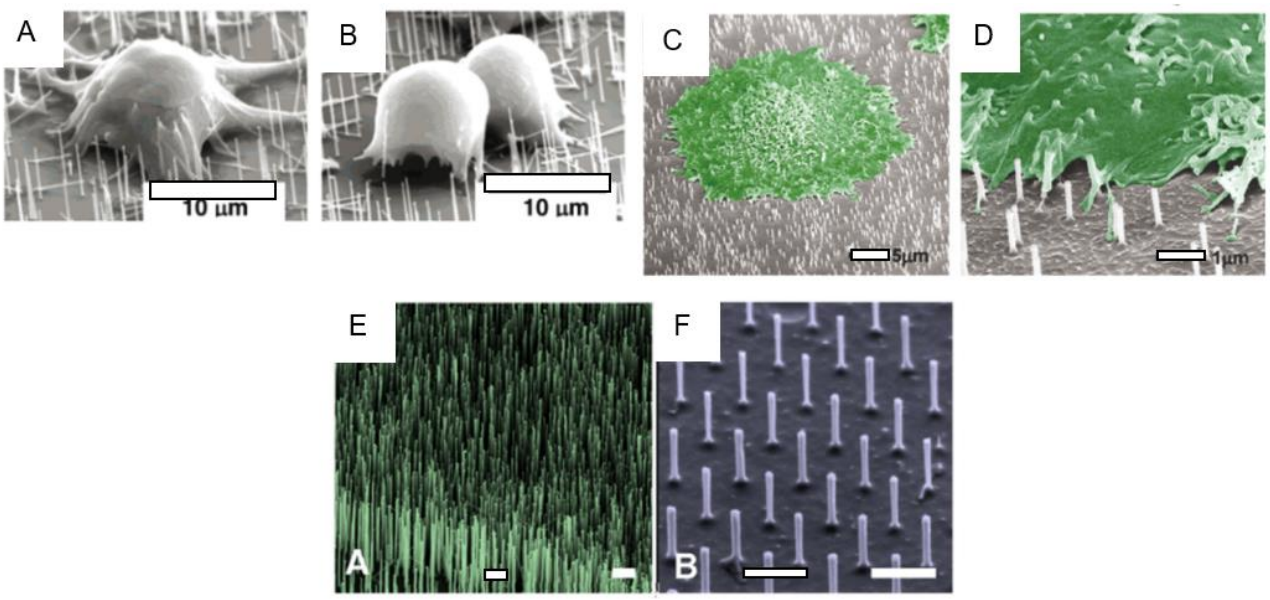

Figure 2.6: Devices fabricated by other researchers (A, B) Nanowires by Kim et al [43] (C, D) Silicon nanostraws by VanDersarl et. al [45] (E, F) Silicon nanowire arrays by Shalek et al [42], scale bar 1μm

The above are examples of using devices in the microscale for cell transfection. It is observed that even though extremely high aspect ratio devices do facilitate transfection, the efficiency of transfection and cell viability observed has been generally low (Table 1) and not feasible when compared to traditional methods such as lipofection or electroporation. The fact that these methods rely on puncturing the cell membrane to physically interface with it begs greater study on whether a tight seal is formed around the cell – structure interface or contents of the cell are in danger of leaking out. Smaller structures or a lower aspect ratio, such as the carbon nano syringe array developed in 2008 by Park et al [46] have been shown to exhibit higher transfection efficiencies. The carbon nano syringe arrays were fabricated with a diameter

of 50nm and heights of 80 and 120nm using TB-CVD process followed by ion milling and wet etching, which is a method very similar to the one employed by Golshadi et al. However, nano syringe arrays differ in the fact that they only have one open end, thus requiring preloaded cargo inside tubes before cells can be seeded on them. They were able to achieve 85% cell viability compared to the control and 37% overall gene expression. Golshadi et al. [20] demonstrated transfection using carbon nanotube array on HEK293 cells with propidium iodide (PI). They confirmed 98% cell viability using flow cytometry and observed 99% transfection within viable cells. This study shows us that carbon nanotube arrays with a lower aspect ratio are a more feasible method to transfect cells. Hence, in this study, we focus on the low cost fabrication of a device similar to the one developed by Golshadi et al.

Table 1: Comparison between array devices developed for transfection

Device	**Type**	**Cell Transfected**	**Cargo**	**Viability**	**Efficiency**
Kim et al.	6µm tall wires, 90nm tip diameter	HEK293	DNA-GFP	-	<1%
Park et al.	120nm tall, 50 nm diameter. Carbon Nanosyringe	NIH3T3 Cells	pEGFP	85%	30%
McKnight et al.	7µm tall carbon nanofibers, 30nm tip diameter	CHO cells	Plasmid DNA (pGreenLantern-1)	-	<1 %
Golshadi et al.	CNT array 205nm diameter 176nm high	HEK293	PI EYFP	98% 84%	99% 100%

Irrespective of the results obtained, we can observe that most devices developed required forms of reactive ion etching, silicon microfrabrication techniques or other methods which can hinder their large-scale development either due to lack of equipment availability or prohibitive costs. We thus wish to explore a low cost; high throughput manufacturing technique will make these devices available to researchers in need of such technology en masse.

Another advantage of carbon nanotube based devices is the possibility of adding multifunctional capabilities through functionalization to convert them into sensors while being able to transfect into cells. Section 3.3.1 mentions the applications of carbon nanotubes for sensing through chemical functionalization.

2.2. Carbon Nanotubes – Properties and Applications

Carbon nanotubes are a unique fullerene type allotrope carbon. They can be in the form of ordered, rolled up sheets of graphene or have an amorphous crystal structure depending upon their manufacturing technique. Carbon nanotubes, due to their varied atomic arrangements, exhibit mechanical, optical and electronic properties which can vary across a large spectrum. This also makes them useful for a wide variety of nanobiological applications such as tissue engineering, drug delivery, in vivo sensing applications, gene therapy and cancer treatments.

Atomic Structure of CNTs

Carbon nanotubes are classified as shown in Fig. 2.7:

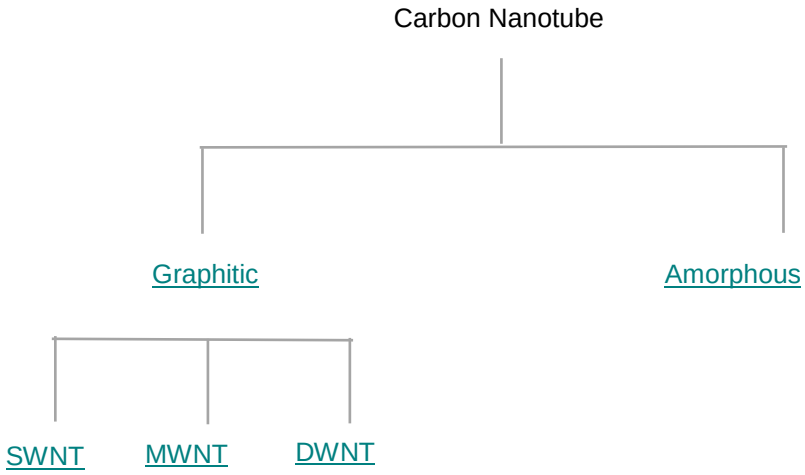

Figure 2.7: Classification of carbon nanotubes

Amorphous CNTs have no long-range crystal structure and are basically amorphous carbon in a tubular shape. Graphitic CNTs are further classified as single walled nanotube (SWNT), multiwall nanotube (MWNT), double wall nanotube (DWNT). They can be visualized as rolled up sheets of graphene. SWNTs are a single tube while DWNT and MWNTs are visualized as concentric, multiple tubes. DWNTs are often classified as a separate category from MWNTs since they can be obtained with high purity. MWNT samples often have SWNTs present and vice versa. SWNTs have a diameter of 3-7nm while MWNTs can be up to 25nm in diameter. The lengths of CNTs have been observed in the order of microns. During template based CVD, the dimensions of CNTs produced depend upon the template used.

The structure of graphitic CNTs can be described by the 'Chiral Vector' for CNTs made out of rolled graphene sheets. In Fig. 2.8, the chiral vector is made of the components *ma 1* and *na 2* with a 1 lying across the carbon atoms and a 2 in the direction of the reflection of a 1 over the 'arm chair vector' which divides

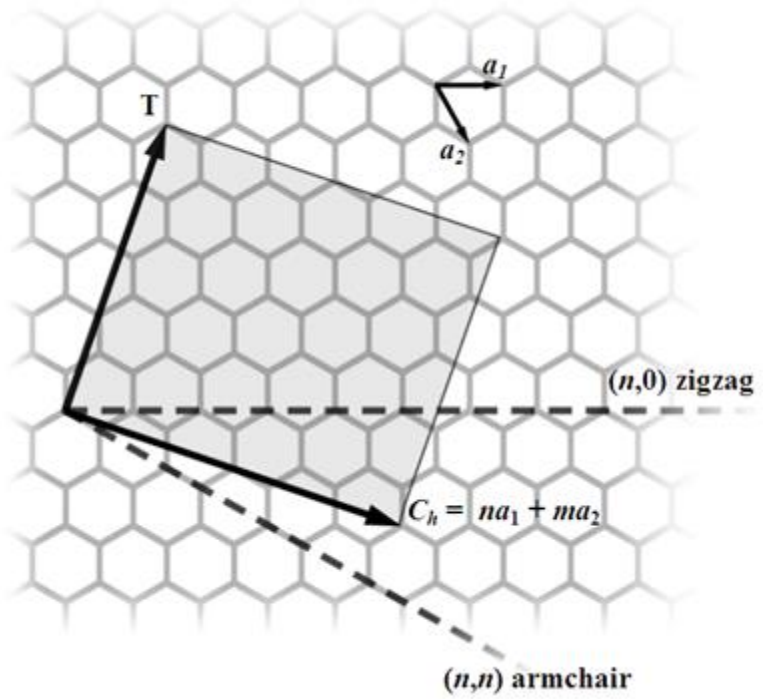

Figure 2.8: Chirality of graphitic carbon nanotube [78]

all hexagons in half. The wrapping angle is defined at the angle between the chiral vector and arm chair vector. If ϕ=0, the tube is known as an armchair tube, if ϕ=30, it is a zigzag type and for $0<\phi<30$, it is a chiral tube. The values of *m* and *n* describe the chirality of the tubes and also its diameter. The chirality can be used to deduce the mechanical, electrical and optical properties of a nanotube. A single walled nanotube will exhibit conductive properties if *n-m is a multiple of 3* and otherwise semiconducting. Carbon nanotubes have also been fabricated in an amorphous carbon form by multiple researchers. Carbon nanotubes formed after CVD are usually in the amorphous form since graphitization of carbon requires temperatures above 1200°C. Amorphous nanotubes differ from their graphitic counterparts in having lower electrical and thermal conductivity. The physical properties of amorphous tubes cannot be controlled by adjusting parameters such as chirality. However, for our application, amorphous nanotubes are easier to manufacture due to the lower CVD temperature and time needed. Dimensions of amorphous carbon nanotubes can be controlled by changing the template dimensions, leading to easy control of size over the resulting tubes.

2.2.1. In Composite Materials

Mechanical studies on CNTs have shown them to be the strongest materials known to mankind. They also possess an extremely high young's modulus. This makes CNTs especially attractive in structural applications. Lau et al [47] have demonstrated the use of CNTs in epoxy composites. They observed that despite their high strength and stiffness, CNTs did not offer satisfactory interfacial bonding at the CNT-epoxy interface. This work was further supplemented by Kim et al. who used surface modifications to improve interfacial bonding and showed the feasibility of using CNTs in epoxy composites. Nano-biological applications of carbon nanotubes can greatly benefit from the high strength of carbon nanotubes in applications pertaining to cellular injections using CNT probes. Also, since cells can be of varying mass and sizes, stronger structures minimized the risk of yielding or breakage of tubes inside cells or within the extracellular matrix, eliminating chances of cytotoxicity.

CNTs can also be looked at as the most idealized and defect free form of carbon fiber, with mechanical properties close to theoretically predicted values of properties for carbon fiber. Gojny et al. showed that even an addition of 0.1 wt.% CNTs in epoxy to led to an increase in Young's modulus from 3.29 to 3.50 GPa. [48]

3.2.2 In Electronics:

As consumer electronics continue to shrink with more functionality being added to smaller circuits, CNTs are looked up to replace metallic wires which cannot be shrunk down to the nano-scale. From an electronics point of view, nanotubes offer the following advantages:

- Conventional metals and semiconductors have in their lattice structures multiple defects, holes and dangling bonds. This leads to collisions and scattering of charge carriers which in turn produces heat and reduces the maximum current density that can be carried by the conductors. Carbon nanotubes possess near perfect structures with all chemical bonds satisfied, this implies

that conduction is possible with lesser heat dissipation and at maximum current density of 10^9 A/cm^2 compared to 10^4 A/cm^2 for metallic conductors [49]

- CNTs have high mechanical and thermal stability. This is due to the strong covalent bonding between carbon atoms.
- They can be made to behave as both metals and semiconductors depending upon their atomic arrangement. This property of CNTs can be utilized to make complete electronic circuits with both transistors and interconnects using only nanotubes.

High conductivity and small size makes carbon nanotubes worthy of use in cellular electrochemistry, further enhancing their use as sensors and adding multifunctional capabilities to them.

Nanoscale field effect transistors and gates have been developed using SWCNTs. It has been shown that CNTFETs even at a nascent stage of development are competitive compared to the current state of the art technology available. IBM expects nano electronics to be realized within this decade as an alternative to silicon microstructures. CNT are also being looked into for use in Li-ion batteries and fuel cells [50-52]. They have a high surface area to volume ratio, offer more intercalation sites in the form of interstitial spaces and tube cavities. CNTs also have an affinity for hydrogen adsorption which makes them a potential candidate for use in fuel cells and replace traditional platinum catalysts.

2.3 Carbon Nanotubes in Nano-Biotechnology applications

Unique and flexible mechanical, chemical, optical and fluid transport properties have found CNTs a prominent spot in biomedical research.

The use of carbon nanotubes in biomedical applications includes using them as drug carriers [53, 54], for transfection of DNA and proteins into cells [46], miniature biosensors with high selectivity and sensitivity, targeted enzyme delivery, cell tracking and labelling, building of tissue matrices and as imaging contrast agents. [49, 55, 56]

2.3.1 Bio sensing

The nano-dimensions of CNTs make them suitable for interacting with individual cells. The possibility of being able to monitor cell behavior, analyzing cell chemistry, ion transport, enzyme behavior and secretions will be advantageous in comprehending many mysteries of drug behavior, physiological responses at the larger scale and identifying disorders or unnatural behavior with greater accuracy.

Wang et al [57] have been at the forefront of exploring the use of CNTs as biosensors. They have shown the applications of CNT/Teflon composite electrodes in detecting hydrogen peroxide and NADH. Experiments also showed favorable response of the electrolyte over the complete potential range. The CNT/Teflon electrode also responds very rapidly to changes in the level of hydrogen peroxide and NADH and low noise levels. Wang et al also developed the first sensor with a CNT based electrode for amperometric and voltammetric determination of insulin. They observed increased electron transfer kinetics using CNTs.

In another study, Li et al [58]. were able to fabricate a CNT array embedded in SiO_2 for ultrasensitive DNA detection and were able to detect lower than a few attamoles of oligonucleotide targets. These applications using carbon nanotubes provide encouraging results to utilize CNT arrays as multifunctional devices for sensing, while at the same time behaving as drug delivery or transfection vectors.

2.3.2 Cell tracking, labelling

With the advent of artificial tissue constructs, it becomes important to be able to analyze the progress of tissue growth in-vivo and visualize cell migration, cell multiplication. This needs to be carried out with minimal intrusion to prevent external factors from influencing results. Conventional methods such as flow cytometry or fluorescence microscopy are either complex and time intensive methods [59]. CNTs can provide an alternative to these methods. Cherukuri et al [60] demonstrated the use of SWCNTs in optical labelling. Excitation of SWCNTs dispersed in a pluorinc surfactant incubated with mouse peritoneal macrophage-like cells resulted in a structured fluorescence spectrum. In vivo optical imaging is often

hampered due to tissues that absorb light, narrow optical absorption and broad emissions. CNTs possess optical transitions in the near infrared range which allows for greater penetration owing to lesser absorption.

Nanotubes were also observed to have remained in cells after repeated cell divisions. This observation encourages the application of CNTs in studying cell divisions and stem cell differentiation.

2.3.3 Imaging Contrast Agents and Radiotracers

Carbon nanotubes being composed purely of carbon provide poor contrast in MRI. This is overcome by taking advantage of their ability to be functionalized. Heavy atoms such as gadolinium can be attached to the surface of the tubes or caged inside them. The 'Gadonanotubes' thus produced displayed proton relaxivities 40 times above $Gd[(DTPA)(H_2o)]^{-2}$ which is a standard clinical contrast agent.

Singh et al. [61] were able to demonstrate the in vivo biocompatibility of CNTs by functionalizing them with radiotracers and studying their movement through the bloodstream. Indium (^{111}In) was covalently bound to SWNTs and administered to mice. The CNTs did not show a tendency to accumulate in a certain organ and were cleared from the blood via renal excretion. They could also be visually observed in urine. No mortality or toxic side effects were noted. This showed that CNTs can be used in vivo without eliciting harmful side effects in the bloodstream and are excreted.

2.3.4 Tissue Engineering

Regenerative medicine is a method of healing that involves rebuilding damaged organs and body parts using stem cells or genetic modifications. Cells when grouped together create around themselves their own supporting structure called the extra cellular matrix or tissue scaffold which acts as a medium for signaling molecules between cells. Through proper understanding of the requirements of cells and tissues, there exists scope to modify or rebuild damaged tissues. [55, 62, 63]

CNTs have simplified methods to track cells, understand development of the tissue and study its viability. Optical labelling of cells carried out using functionalized CNTs which easily permeate the cell membrane

has the potential to track cells without using expensive, complex methods such as flow cytometry or intravital microscopy. CNTs do not require specialized equipment or extraction of cells from the body to detect cells but can be used in vivo. The chemical functionalization of CNTs can be carried out using chemical methods only which greatly simplifies the process. CNTs with functional groups attached to them can be detected by Raman spectroscopy [53]. When inside a tissue matrix, the chemical changes in functional groups can be used to study microenvironments around the cell.

Implantable biosensors which can relay information in real time about vital tissue parameters such as pH and glucose levels are also being explored [57, 64]. With a high surface area to volume ratio, the active area available for analysis is large, which allows for higher sensitivity. Since CNT array devices can interface with a number of cells in parallel, with the proper functionalization, they have the potential to monitor a large number of cells in vivo and provide substantial amounts of data regarding cell behavior.

Another area of interest is the use of CNTs as structural support for tissue matrix [55, 63, 65]. The matrix is a critical component of tissues and greatly affects its development. Conventional matrix materials are usually synthetic polymers such as PLA, which lack the required mechanical strength. CNTs dispersed in chitosan, a biopolymer, showed improved mechanical properties.

Gene Transfection

Carbon nanotube arrays have been used to achieve transfection into cells of different kinds. Park et al. demonstrated transfection into fibroblast cells with up to 35% efficiency. Golshadi et al. demonstrated transfection into HEK293 and were able to achieve 99% transfection in live cells. Carbon nanotube arrays have also demonstrated the ability to transfect dye, DNA and quantum dots into cells, proving that they can be used in a versatile manner.

2.4 Fabrication

The success of carbon nanotube devices is in part contingent upon their ease of fabrication and accessibility. It was observed earlier that most array devices are manufactured using techniques which

cannot easily be adapted to commercial scale fabrication with reasonable costs. In order to develop a more feasible nanofabrication method, it becomes important to look at viable alternative techniques used in micro-nano fabrication. Given the variety of applications requiring the use of CNTs, researchers have formulated novel methods to fabricate them and control their physical dimensions. Some of the most prominent ones are mentioned below.

2.4.1 Chemical vapor deposition

Chemical vapor deposition is a method of applying thin film coatings to materials and also to produce high purity bulk materials.

It requires flowing a precursor gas over the heated object to be coated. High temperatures are maintained by keeping the target item in a furnace. As the precursor gas flows over the target material, chemical reactions occurring over it result in the deposition of a thin film on the surface. CVD provides multiple advantages over other deposition processes such sputtering or physical vapor deposition.

Because precursor gases used in the processes can be obtained in very high purities, the deposited material is devoid of contaminations, making CVD one of the most reliable methods to obtain a pure film. The gaseous nature of active material means that all crevices, pores and open surfaces are deposited with an even and continuous layer of film without breaks or large variations in thickness. It is also one of the few methods which can deposit material films with nanoscale precision.

Apart from obtaining controlled and pure film depositions, CVD equipment and set ups are easier to use and operate. Unlike sputtering, there is no line of sight requirement for CVD, as long as the precursor can access the object to be coated. Regular CVD works without the requirement of plasma, ions or lasers but these methods are often employed for specialized applications to improve yield or reduce time for CVD.

Depending upon the application, substrate requirement, material to be deposited, cost, precursors and deposition requirement, different kinds of CVD reactors are available.

1. Hot wall Reactor: These represent the more common and less complex CVD systems. They essentially consist of a chamber containing the target substrate, with the chamber surrounded by a heat source. Walls of the chamber are not cooled but heated by the heat source, thus the name ‘Hot Wall Reactor’. The chamber can be of different sizes depending upon the number of parts to be held, with shelves or might be as simple as a ceramic tube. Temperatures in these reactors are usually very high, limiting factor being the materials used in the process or construction of reactor. Their advantages include being able to maintain uniform temperatures resulting in even film thicknesses. On the downside, due to a heated chamber walls, some deposition occurs on the walls of the chamber and gas inlets or exhausts, requiring frequent cleaning. This may also lead to higher energy and precursor requirements. The CVD process used by Golshadi et al. utilizes a hot wall reactor due to ease of use, even thickness of deposited film and availability.
2. Cold wall reactor: These are another major category of CVD reactors. In this type, the chamber walls are cooled by running coolant through them and only the substrate holder is allowed to heat up. The holder may be heated using resistance heaters, induction or lamp heated. They are often used in high pressure applications with more reactive precursors. Although they present the advantages of reduced deposition on walls and lower thermal loads on substrate due to faster heat up and cool down times and consequently lower energy consumption, they do present more complicated disadvantages which requires careful process monitoring.
    - Non-uniform temperature distribution on the substrate, leading to non-uniform film thicknesses
    - Thermal stresses in case of quick heating and cooling
    - Smaller batch sizes compared to hot wall reactors

The use of TB CVD to grow nanotubes was first shown by Che et al in 1997 [66]. They showed that CNTs could be grown inside AAO membranes and develop into highly ordered arrays. Precursors used in the process were ethylene and pyrene. They also demonstrated the use of catalysts such as Ni, Fe and Co upon the CVD process and resulting nanotubes.

The compatibility of the nanotubes thus produced was not tested on biological systems since their primary focus was on applying them to the anode of a Li-ion battery. They observed that carbon nanotubes inside formed using ethylene as a precursor on Ni catalyzed AAO membranes were ordered and formed without any macroscopic defects. It is also observed that further exposure to higher temperatures after CVD converts the atomic structure of amorphous CNTs to ordered graphite.

Fe and Co were also explored as catalysts with ethylene as a precursor as 580°C for 30 minutes. In the Co catalyzed membranes, CNT structures were formed but were not ordered or symmetric and fused together. Fe catalyzed membranes did not show any sign of CNTs in them.

This study provides important insights for increasing the rate of CVD and possibly shortening fabrication times. The observation that CNTs thus formed were conductive motivated the idea of applying them as sensors.

Xu et al. [67] also demonstrate the growth of carbon nanotubes on AAO membranes while using cobalt as a catalyst. They different from the devices manufactured by Che et al. since their CNTs grew out of the membranes onto its surface. They go a step ahead to show how CNTs produced can be modified to eliminate the effects of the catalyst on their applications by using ultrasonification to chop off the excess CNT lengths from above the membrane. The AAO membranes utilized by them had an average pore diameter of 60 nm and interpore spacing of 100nm. Co was deposited using electrodeposition and CNTs grown using CVD with ethylene as a precursor at 650°C. Etching of AAO membrane was carried out using an aqueous mixture solution of $CuCl_2$ and HCl

TB-CVD is thus a well-established method for fabrication of nanotubes with different sizes and for a variety of applications. The use of a hot wall reactor is selected for this study due to availability, uniform film deposition thickness and ease of use.

2.4.2 Etching technologies

Wet Etching

Alumina is an amphoteric oxide which can react well with both acids and bases. It has been established in a number of studies that AAO can be fully dissolved using dilute NaOH, H_3PO_4 and HF. Researchers have commonly used NaOH to release CNTs formed using TB CVD to release CNTs from the template [68-70].

The following reactions take place when AAO reacts with an acid or base:

$$2OH^- + Al_2O_3 \longrightarrow 2AlO_2^- + H_2O$$

$$6H^+ + Al_2O_3 \longrightarrow 2Al^{3+} + 3H_2O$$

There have been multiple studies carried out on wet etching of AAO membranes [68, 70-73]. The most common etchants include NaOH, H_3PO_4, Hu. et al [70] have investigated the etching of AAO with H_3PO_4 and NaOH and reported linear mass dissolution rates for both. NaOH is also reported to be a stronger etchant whereas the slower etch rate of H_3PO_4 makes it more suitable for exposing nanotubes due to better control over exposed lengths. Golshadi et al. also carried out studies using wet etching with varied concentrations and reported similar trends as Hu et al. They also observed a decrease in etch rate with temperature. Lee et al. [74] who used AAO as a template to create gold tipped nano arrays also utilized wet etching to eliminate the AAO template. They utilized a mixture of H_3PO_4 (6wt%) and Cr_2O_3 (1.8%wt) at 60°C for 1 day.

Dry Etching

Dry etching is commonly used in microfabrication to selectively remove material. In template based manufacturing of array devices, dry etching has been used to selectively etch the template and expose carbon nanotubes from template [20, 75]. Dry etching can be both reactive and non-reactive. Material

removal achieved by exposing material to highly energized plasma. Plasma of reactive gases such as boron trichloride, oxygen and fluorocarbons might be used to achieve a combined reactive and physical etching mechanism, known as reactive ion etching (RIE). In other cases, non-reactive, heavy gases such as argon or gallium are used to achieve a purely physical etching, called sputtering or ion milling.

Mechanism of dry etching

A dry etching set up typically looks like the one shown in Fig. 2.9. The plasma chamber is a sealed, vacuum chamber with electrodes on the top and bottom. The lower electrode is where a sample to be etched is placed. It is connected to an RF power supply and a blocking capacitor. When the process is started, a vacuum pump evacuates the chamber down to low pressures (~5 MPa) and allows the required etching gas to flow into the chamber. An alternating electric field is set up inside the chamber using the RF supply. The most commonly used frequency for the electric field is 13.56MHz. At this time, electrons being lighter, move with the electric field. During this rapid movement, they strike other atoms with high energy which is usually higher than the ionization energy leading to either excitement of electrons in the atoms or ejection of electrons, which leads to formation of more ions. As the population of electron grows, cascade reactions take place which results in the formation of more and more ions. The plasma formed in a reactive ion etching chamber is a weakly ionized plasma, also known as a glow discharge plasma. An important characteristic of the glow discharge plasma is lack of thermal equilibrium between electrons and ions. The temperature of electrons is related to their Kinetic energy through the relation: [76]

$$½m_e v_e = \frac{3}{2} kT_e$$

Where k is the Boltzmann's constant. Thus $T_e >> T_g$, and the gas remains at approximately room temperature. Because glow discharge plasma is a weak plasma, the number of electrons is lesser than the number of ions, keeping the chamber at room temperature. The lower electrode upon which sample is placed experiences a negative DC bias due to the presence of a capacitor. This leads to repulsion of

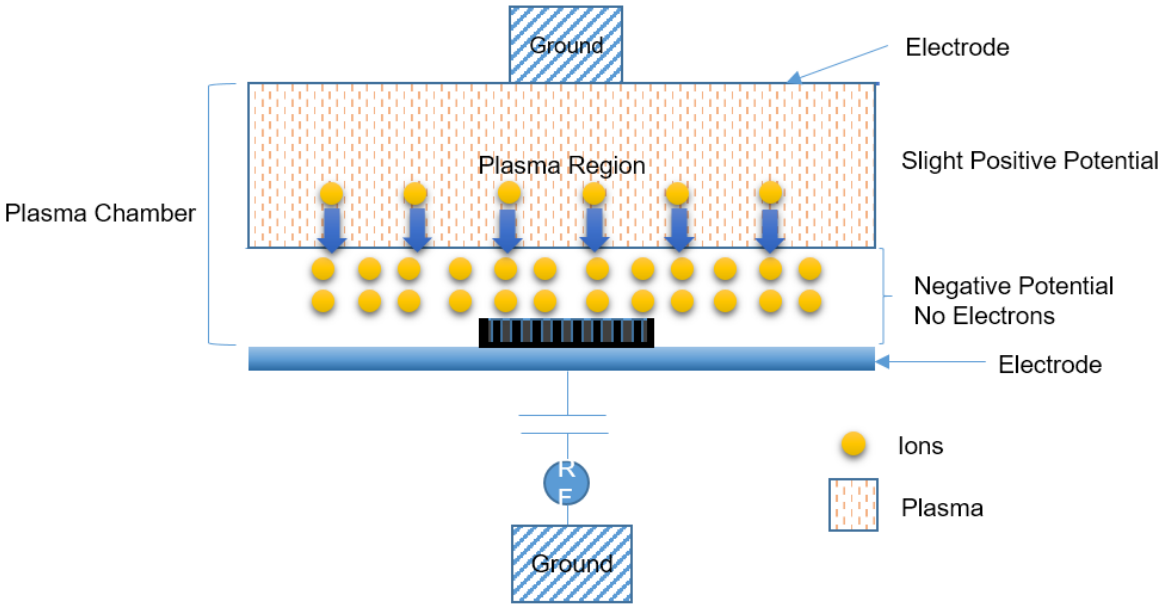

Figure 2.9: Mechanism of dry etching

electrons from the region near the lower electrode. Since no electron-ion interactions take place here, this area is referred to as the dark region. As positive ions approach this region, they are accelerated due to the local negative potential created at the lower electrode. These ions gain energy and are responsible for the directional etching profiles obtained through dry etching. In our case, this process is able to uniformly etch away the AAO membrane, leaving behind a smooth surface with no debris.

Ion Milling

Ion milling is a non-reactive method of dry etching and can be used to etch away the template in template based fabrication techniques. It is not material specific, since the mechanism of dry etching is purely physical. Unlike focused ion beam (FIB) milling or electron beam milling, ion milling is used for material

removal over larger surface areas without specific targeting. Ion milling is a form of dry etching characterized by the use of inert gases for etching. Most dry etching processes are some form of reactive ion etching processes which involve chemical and well as physical interaction between ions and sample material. The chemical reactions aid in etching, thereby accelerating the etch rate. However, the gases used in reactive ion etching such as boron trichloride and carbon tetrafluoride are toxic and hazardous. These gases require special handling considerations while at the same time etch much slower compared to wet etchants such as NaOH or phosphoric acid.

Ion milling relies purely on the physical interaction between ions and the sample for material removal. In its simplest form, it can be thought of as a method of ‘sandblasting using ions’. Energy transferred from ions to atoms of the surface of the material allows atoms at the surface to gain enough energy to break away from the crystal structure, resulting in material ablation. A lower pressure allows more ions to impact the surface since the mean free path is inversely proportional to the ambient pressure. This also decreases scattering of ions thus leading to a more directional etching profile, making ion milling applicable to a variety of materials without much variation in etch rate. Milling using argon is inexpensive and simple to carry out.

2.4.3 The AAO template

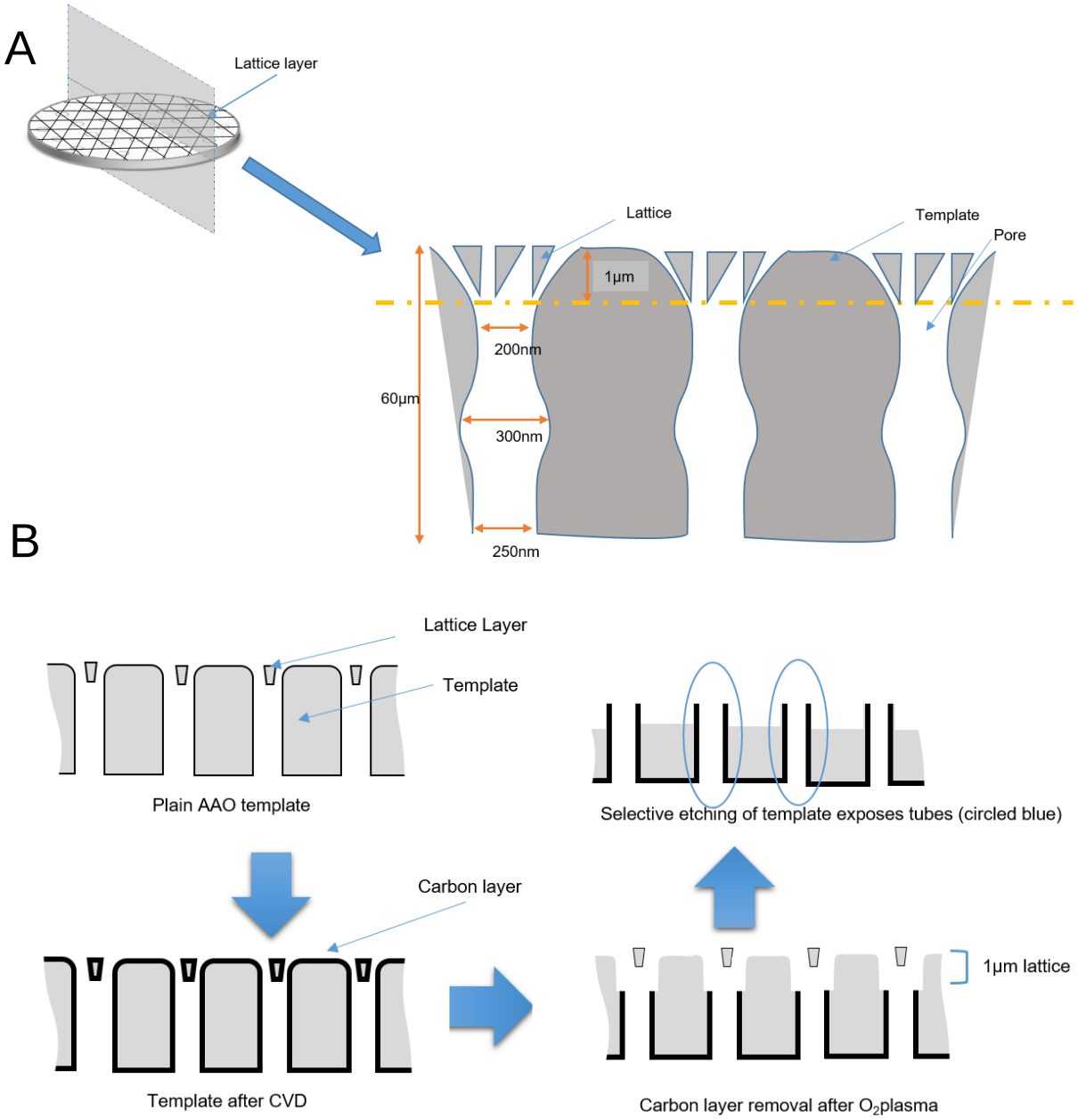

Figure 2.10: Schematic representation of a cross section view for the Whatman Anodisc AAO membrane **(A)** Magnified cross section view of template with dimensions. Dotted line indicates end of lattice layer **(B)** fabrication process with lattice shown

Fig. 2.10 is a schematic showing the cross section view of AAO membranes used as templates. These membranes consist of ordered pores which run the entire thickness of the membrane and open at both ends. Pore diameter at the top is close to 200nm and 250nm at the bottom surface. The top is also characterized by presence of a mesh like AAO layer we call ‘lattice structure’. This lattice structure hinders direct access to the pores and is non-functional for our use. During etching, considerable time is spent in removing this lattice layer since ordered carbon nanotubes are not found in this region. The required length of nanotube exposure is only ~200nm but time spent in clearing away this layer slows the fabrication process. Removal of this layer prior to manufacturing is desirable because not only will it reduce etching but potentially improve the quality of the array fabricated using wet etching. The use of ion milling, wet etching and mechanical polishing are prospective methods of removing the lattice.

3. Selection of Alternative Nanofabrication Process

In order to reduce fabrication time and increase yield, it became important to study and evaluate a number of fabrication processes which could replace the current process. This chapter discusses the process of selecting a feasible alternative nanomanufacturing method. Fig. 3.1 below shows the alternative processes that were proposed to replace current methods.

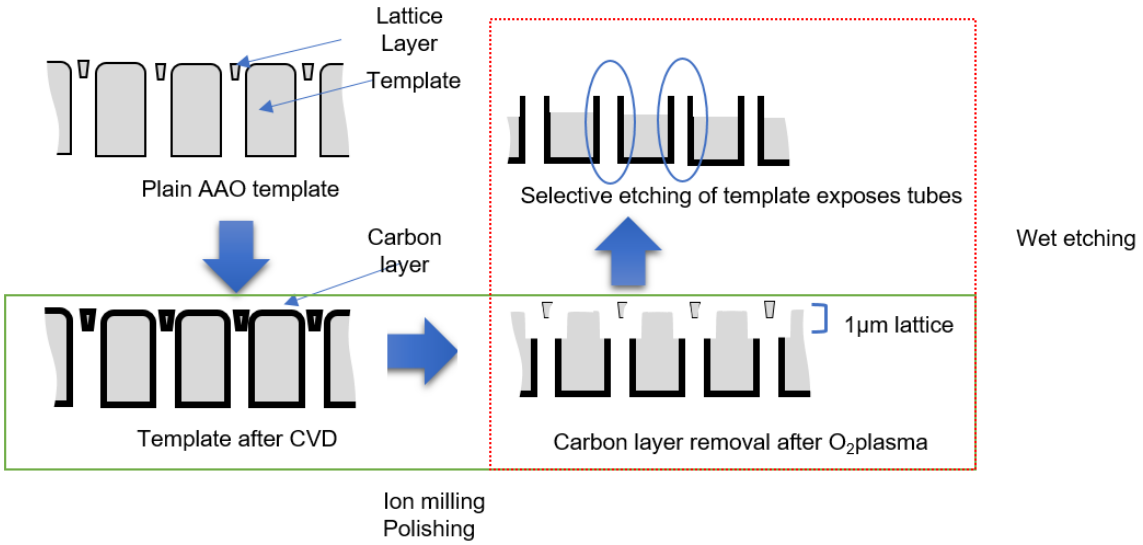

Figure 3.1: Alternative proposed fabrication processes

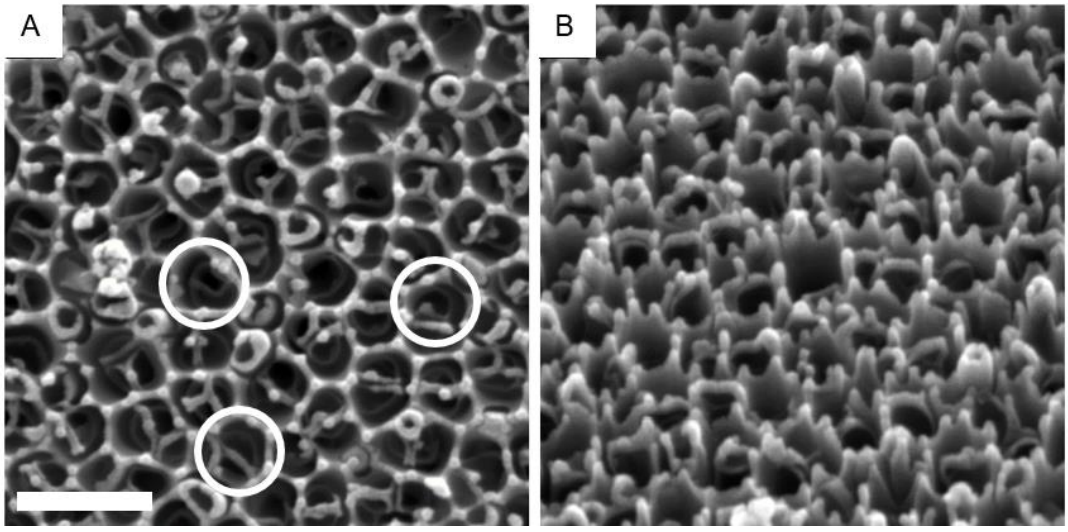

Figure 3.2: SEM micrograph of array after etching with 1M NaOH for 6 minutes. Tubes can be seen embedded inside pores (circled). **(A)** Normal view **(B)** 35° tilt view. Scale bar 500nm

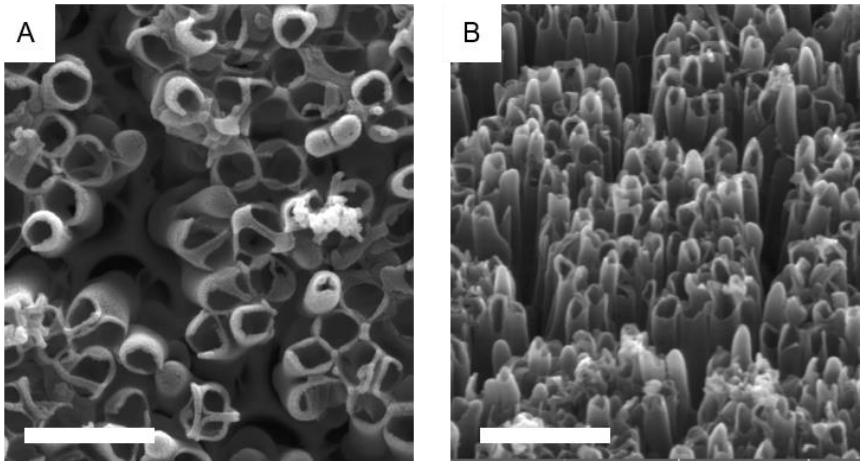

Figure 3.3: SEM micrograph of array after etching with 1M NaOH for 20 minutes. Tubes can be seen coalesced together. (A) 35o tilt view (B) Normal view. Scale bar (A) 500nm (B) 1µm

3.1 Wet Etching

Reactive ion etching, being the most expensive and time-consuming process, was of highest priority in elimination. The wet etching of Aluminum oxide can be carried out by using easily obtainable compounds such as sodium hydroxide and phosphoric acid. These compounds also present the advantage of easy disposal and relatively safe handling. This makes wet etching a promising alternative to reactive ion etching. Initial trials were carried out for the above process using O_2 plasma followed by etching in 1M NaOH.

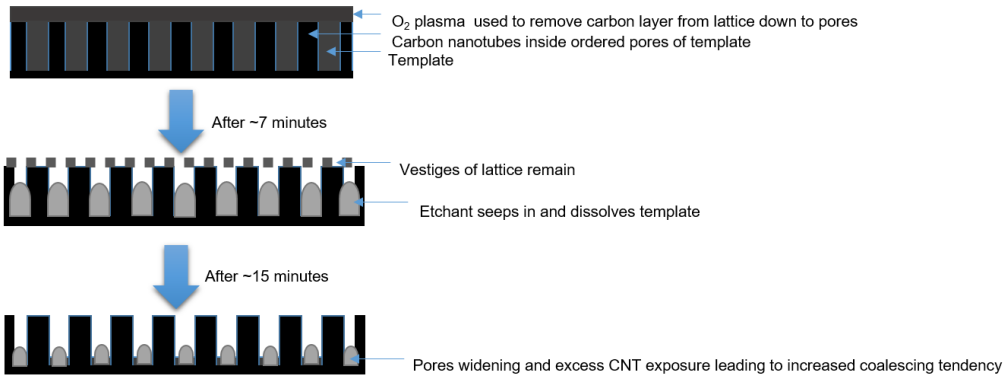

Figure. 3.4: Schematic showing the progression of wet etching

It was observed that despite the rapid speed of etching, its isotropic nature leads to a condition referred to as pore widening. In Fig 3.2, we observe that after 6 minutes of etching the CNT array, part of the lattice layer remains, covering the tubes. Tubes can be seen within the pores but they have not been exposed. At 20 minutes of etching, tubes are very clearly exposed however, the template has been excessively etched and the thinner sections of AAO separating the pores have also been dissolved in the NaOH. This is illustrated in Fig. 3.3 above. The lack of support resulted in CNTs collapsing upon one another and forming a coalesced clump instead of an ordered array, depicted in Fig. 3.4. Another observation critical to our application was the formation of towers on the surface which implied that etching was not evenly carried out.

Based upon the above results, the following conclusions were drawn

1. In a short timeframe, wet etching is sufficient to expose a limited number of tubes. But, the lattice structure will remain dominant with random peaks across the surface. With extended duration of etching, pore widening becomes the dominant feature, this leads to a loss of support for the nanotubes and eventual clumping together, most likely due to the surface tension of etchant.
2. If the lattice layer can be removed prior to etching the CNT arrays or prior to beginning the fabrication process, wet etching can potentially expose the required length of CNTs in a short amount of time without pore widening.

From the above conclusions, it could be inferred that a method to eliminate the lattice layer would be beneficial prior to wet etching. Thus, a number of attempts were made to eliminate the lattice layer.

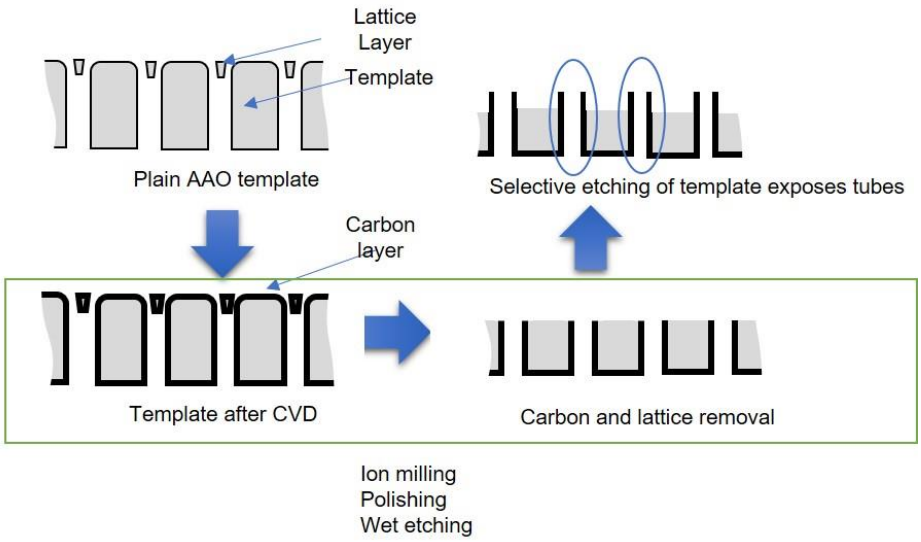

Figure 3.5: Removing lattice layer before etching

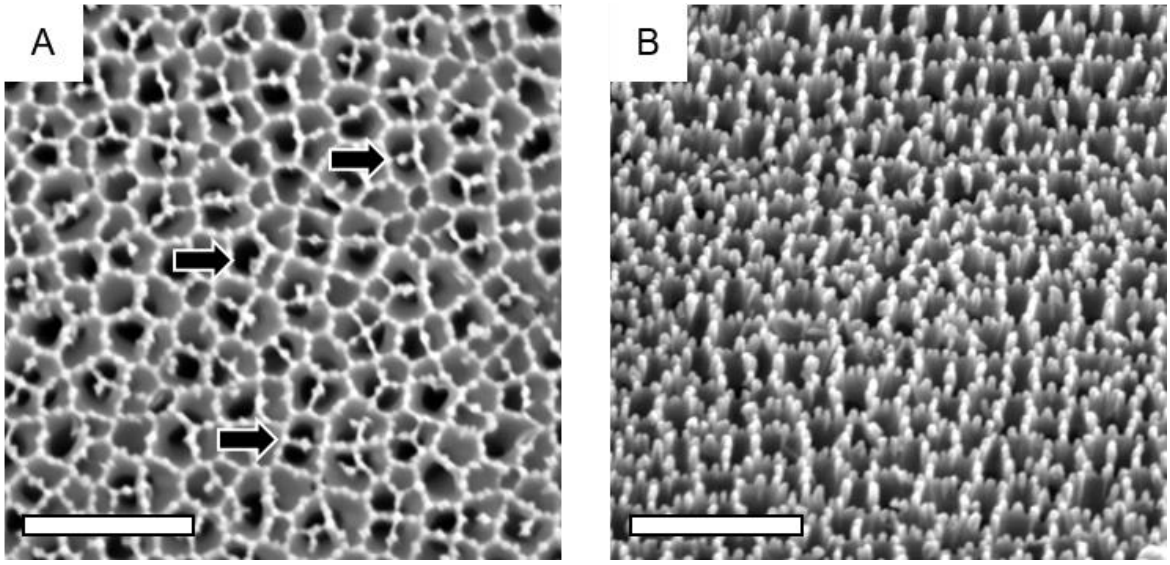

Figure 3.6: SEM micrograph of bare AAO membrane after wet etching for 7 minutes in 1M NaOH **(A)** top down view, arrows showing pores under partially etched lattice **(B)** 35 tilt view showing pillars. Scale bar 1µm

Figure 3.5 depicts the fabrication process proposed, involving the removal of lattice layer. The lattice layer could be removed after the CVD process or prior to it. The first attempt was carried out using NaOH to etch away the lattice from a bare AAO membrane. The images in Fig. 3.6 show that compared to an unetched membrane, there is a significant reduction in the lattice, however, the presence of pillars is observed. Since a smooth surface is required for the exposure of coplanar CNTs, alternative methods were considered.

3.2 Ion Milling

A potential method to eliminate the lattice layer was to utilize ion milling. Initial studies carried out using ion milling have provided proof of concept and encouraging results for removing the lattice layer. As mentioned in Sec 2.4.2, the process of dry etching for AAO is not well documented. A method of wet etching (referred to as the drop method) followed by dry etching was studied to observe the prospects of using a hybrid method. This involved placing a small amount of etchant (in this case 1M NaOH) upon the membrane to form a drop as shown in Fig. 3.7. It was done so to minimize etching from the bulk of the template by reducing the rate of replenishment for available etchant in the pores. This sample was later exposed to ion milling.

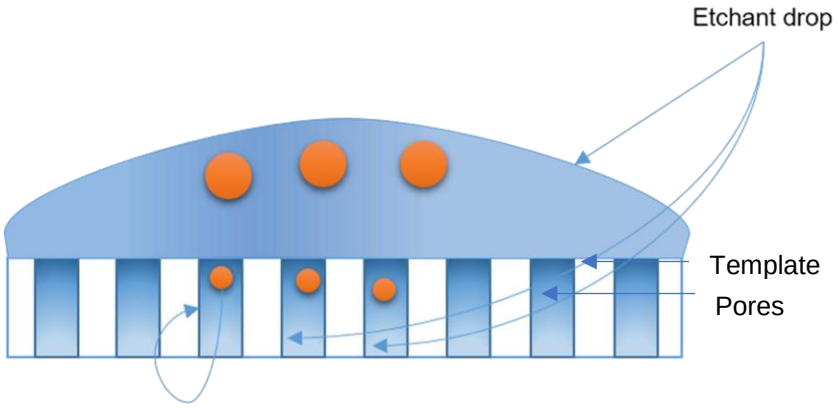

Figure 3.7: Utilization of minimal etchant or 'drop method'. This is tried to reduce dissolution from bulk of membrane

SAMCO RIE 1C, benchtop reactive ion etching machine was used to carry out all ion milling procedures. Ion milling with multiple conditions was attempted, mentioned in Table 2 below:

	Temperature	Power	Flow Rate	Pressure
Case 1	25°C	100 W	45 SCCM	31.45 Pa
Case 2	25°C	200 W	10 SCCM	12.97 Pa
Case 3	25°C	200 W	74.21 SCCM	54 Pa

Table 2: Process parameters for Ion Milling experiments

3.2.1 Case 1:

Temperature - 25°C, Power- 100 W, flow rate- 45 SCCM, Pressure- 31.45 Pa

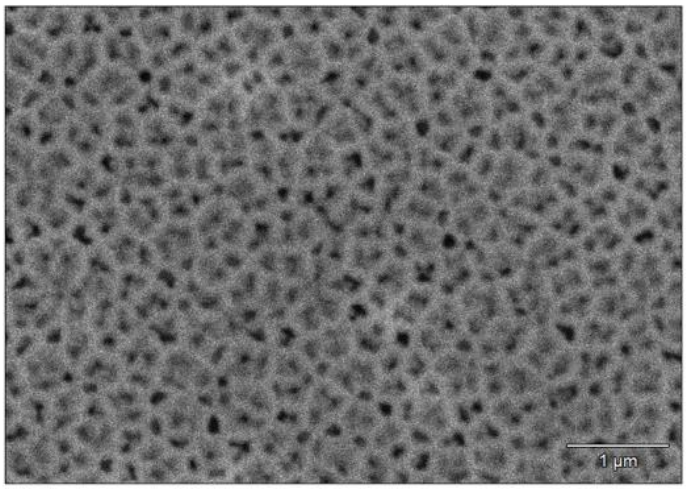

Figure 3.8: SEM micrograph, normal view of carbon coated membrane after 30-minute ion milling. No material removal is observed.

Samples were of both types; bare AAO membranes and carbon coated membranes, with amorphous carbon layer present. The experiment was run for 10, 20 and 30 minutes.

Its observed that Ion milling at this specification did not have much effect on the membranes. Both samples, even after 30 minutes did not show significant signs of material removal as seen in Fig. 3.8.

3.2.2 Case 2

Temperature – 25 C, Power- 200W, Flow rate- 10 SCCM, Pressure – 12.97 Pa

Using a lower pressure as recommended by SAMCO Engineers, etching was carried out again on similar samples, both bare and carbon coated. Using a lower pressure increases the mean free path of gases. This increases the probability of an ion striking the surface of the membrane. Also since inter-ionic collisions are reduced, it is expected that ions with higher energy will strike the surface, leading to more material removal. Etching under these conditions was carried out for 30 minutes, 60 minutes and 90 minutes. The

SEM micrographs in Fig. 3.9 show that considerable material removal took place at the end of 90 minutes. In contrast, carbon coated membranes showed very little material removal as compared to bare membranes, promoting the idea that removal of lattice layer prior to CVD might be easier.

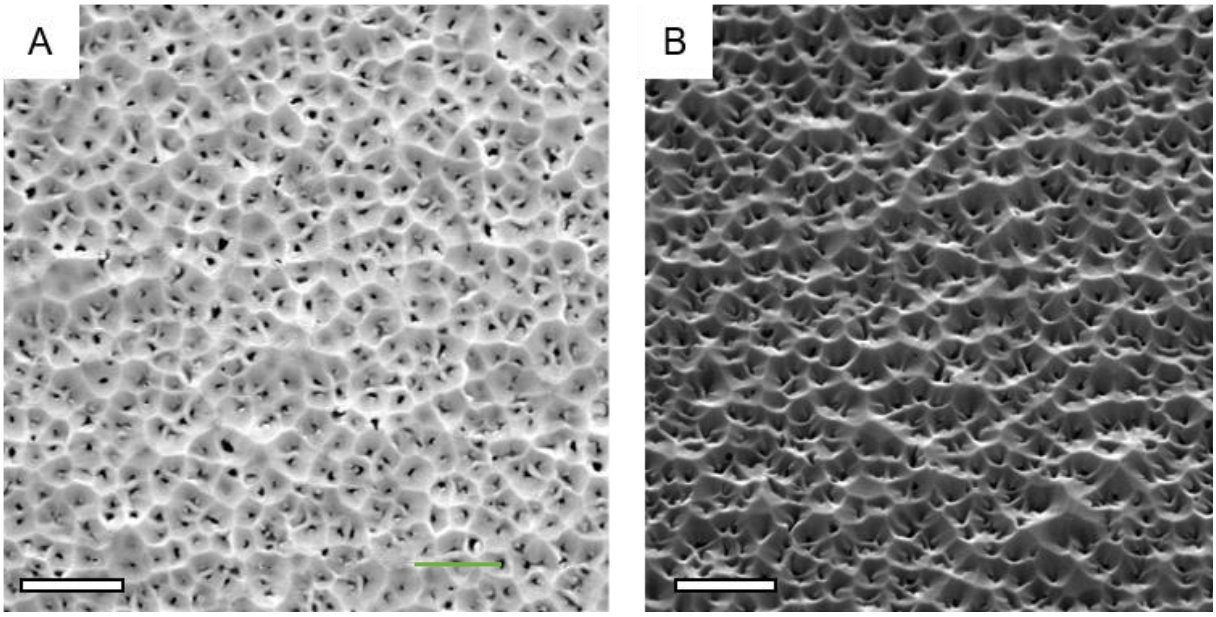

Figure 3.9: SEM micrograph of plain AAO membrane after 1.5-hour ion milling. Pits and craters can be seen, indicating material removal. **(A)** Normal View **(B)** 35° Tilt view showing non-uniform etching. Scale bar 1µm

3.2.3 Case 3

Wet etched 7 minutes, 1M NaOH

Temperature – 25 C, Power- 200W, Flow rate- 74.21 SCCM, Pressure – 54 Pa

Membranes were first etched for 7 minutes using 1M NaOH. The method of etching was different because a small volume of etchant utilised to minimize etching from inside open pores as shown in Fig. 3.7. This time, a higher pressure was utilised i.e. a higher gas flow rate to have a larger number of free radicals in the plasma and thus more etching. Ion milling was carried out for 1 hour with the above-mentioned parameters in 4 runs of 15 minutes. This was done to prevent the machine from overheating. It was observed that there was significant exposure of the pores. The pores also appear to be clogged by

debris, which can be seen in Fig. 3.10. However, this is an encouraging result since removal of lattice layer is explicit and ordered pores can be identified.

In the above processes, it was observed that ion milling had the potential to remove the lattice later but left the membrane with an uneven surface morphology. Ion milling is also not a physical process but a

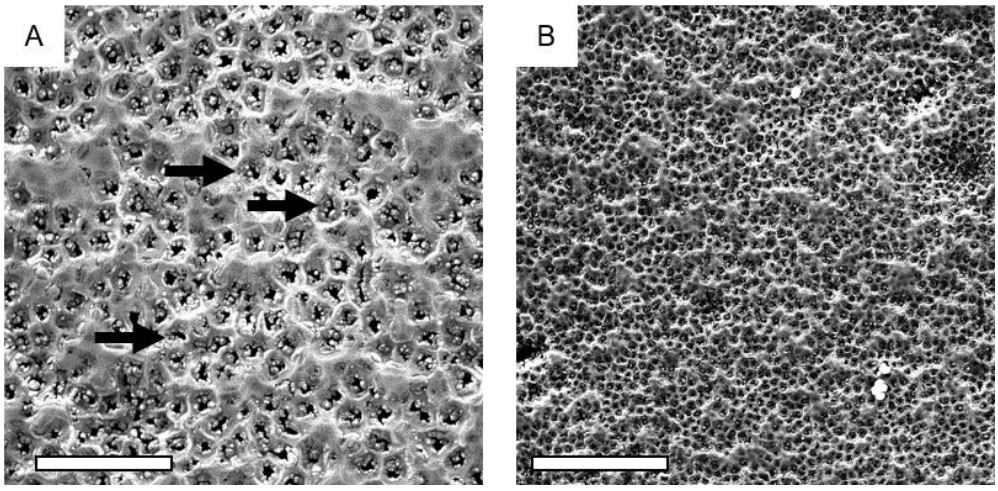

Figure 3.10: SEM Micrographs of bare AAO membranes after 7 minutes wet etching using 'drop method' and subsequent ion milling for 1 hour. **(A)** scale bar 5µm **(B)** scale bar 2µm. Material removal is comparatively uniform and pores are beginning to show (marked with arrows)

plasma based process which can potentially vary on different equipment. It is also important to note that carrying out CVD on clogged membranes with an uneven morphology would not result in coplanar CNTs. To overcome these disadvantages, other methods were considered.

3.3 Mechanical Polishing

The most desirable fabrication process is one that poses least variability, easy scale up opportunities and preferably can be carried out without the use of cleanroom facilities. Since the lattice layer is about 1µm deep from the top of the surface, polishing was considered as a potential option. Mechanical polishing poses the advantage that it is easy to scale up, is free of cleanroom requirements and is not subject to variations due to plasma or other dynamic systems.

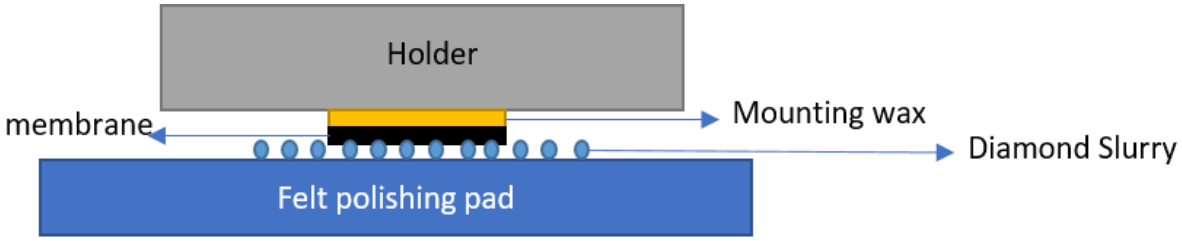

Figure 3.11: Polishing set up schematic

3.3.1 Case 1: Polishing bare AAO membranes:

Bare AAO membranes were polished on a Struers TegraPol using 1µm DiaPro diamond suspension. The polishing set up is shown in Fig. 3.11. Bare membranes were subjected to 12 minutes of polishing at 150RPM.

In Fig 3.12 and 3.13 it is seen that the lattice layer seems to have been eliminated and pores are visible. The pores are clogged with debris from polishing. Further trials were carried out using polishing followed

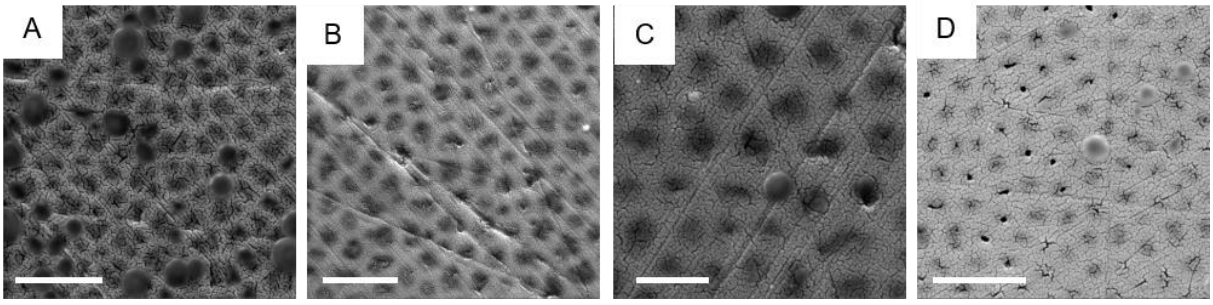

Figure 3.12: top down view micrographs of polished membranes, 15N, 150RPM (A) 3 minutes (B) 6 minutes (C) 9 minutes (D) 12 minutes, scale bar: 1um (A, B), 500nm (C, D)

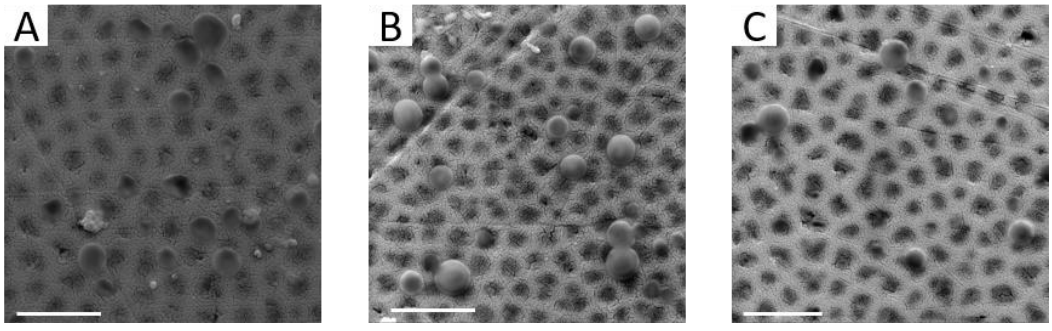

Figure 3.13: Top down micrographs of polished membranes with increasing force **(A)** 20N **(B)** 25N **(C)** 30N, for 5 minutes. Dark spots are covered pores. Scale bar 1um

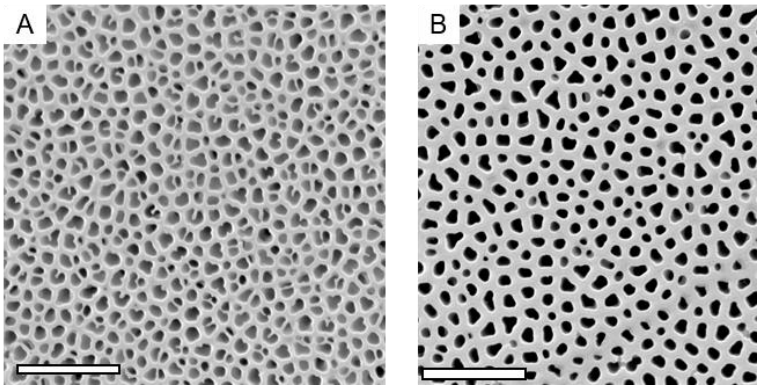

Figure 3.14: SEM micrographs showing polished bare membranes **(A)** 12 minutes, 15N **(B)** 18 minutes, 30N.Both were followed by 3 min etching with 1M NaOH Scale 2µm

by wet etching. After 3 minutes of polishing at 15N, there is significant reduction in the lattice, shown in Fig. 3.14 (A) By increasing force to 30N and stepping up the time to 18 minutes, there is a very clear elimination of lattice from the surface of membranes seen in Fig. 3.14 (B). This brings us to a definite conclusion that polishing is a very promising process for this task.

These membranes were then annealed in preparation for CVD. Polished membranes after annealing resulted in curling of the membranes which rendered them imperfect for cell culture studies. Since polishing is a non-selective process, it can be carried out after the CVD step thereby leading to the

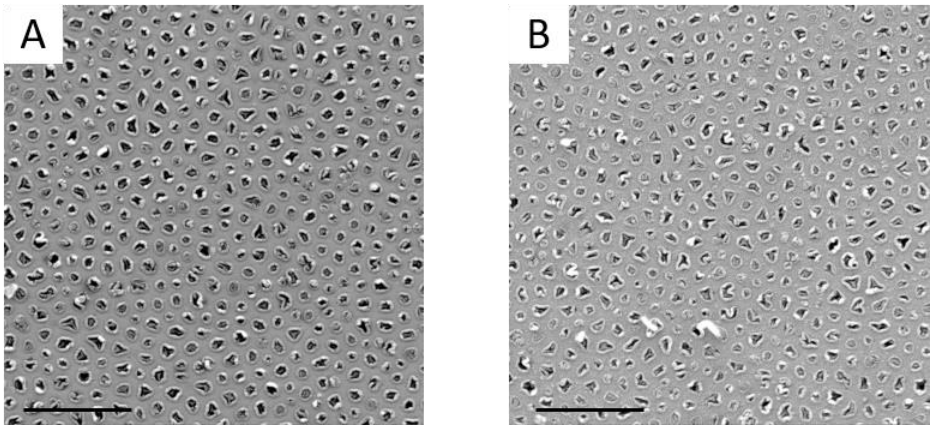

Figure 3.15: Top down micrographs of CNT arrays. Polished for 20 minutes at 30N, etched with 1M NaOH. **(A)** 3 mins **(B)** 5 mins. Scale 2um

reduction in steps, increasing yield by reducing damage to membranes during the polishing process and preventing polished and annealed membranes from curling during the CVD process.

3.3.2 Case 2: Polishing carbon coated devices

In Fig. 3.15 polished and etched CNT arrays are shown. The crusty appearance of the CNT arrays was found to be due to excessive sputter coating in preparation for electron imaging. Some amount of clogging can be observed within the CNTs. The cause and solution to clogging will be further discussed in the following chapter.

From the above images, following conclusions can be drawn:

1. Polishing is a simple and effective technique to eliminate the lattice layer.
2. There exists control over the polishing process through mutually independent variables such as time and force
3. Clean room facilities are not required for polishing
4. Scaling up of polishing will be a much simpler operation than scaling up of a dry etching process
5. Polishing poses a higher risk of damaging membranes

Based upon the above points, it was decided that polishing, combined with wet etching is the most feasible fabrication technique for mass production of CNT arrays. Hence, further studies were dedicated to the optimization of this process and understanding the variables that affect it.

Chapter 4: Effects of Synthesis Parameters on Carbon Nanotubes

After analyzing the observations made during experiments mentioned in chapter 4, it was clear that mechanical polishing was a viable alternative solution for the fabrication of CNT arrays. To effectively implement a fabrication process, it becomes important to comprehend in totality the behavior of the process under varying conditions. It was also important to understand the extent to which this process could be controlled in order to yield CNT array devices of required dimensions such as tube height and diameter. In this chapter, effects of the different process parameters with respect to physical properties of CNTs are discussed. During the polishing – wet etching process, the following parameters can be controlled:

Polishing: Force, time, size of polishing particles

Wet etching: Etchant, concentration of etchant, time

4.1 Effect of Polishing Parameters

Mechanical polishing was shown to potentially eliminate the lattice layer and overcome the issues associated with plasma based processes. The image in Fig. 5.1 depicts the polishing set up:

1. Mounting of carbon deposited membranes on aluminum stubs: Aluminum stubs were cleaned thoroughly with acetone to make sure they were free of impurities and leftover wax from earlier processes. The stubs were then heated to 150 – 160°C on a hot plate, this is twice the flow point (78°C) of the 7071 Blanchard wax used. When stubs are warmed up, a stick of 7071 Blanchard holding wax (acquired from the J.H Young Co.) is used to apply a thin layer of wax on their surface. The wax so applied should be even thickness and have no air bubbles. The device is placed on the wax and let allowed to settle down for 45s – 1 minute, until it is seen that the entire surface of the devices contacts wax (this is confirmed by observing the wetting of the devices by

the wax which can be visibly observed). Any section of the membrane not in contact with that wax poses an increased risk of the device cracking during polishing. Care should be taken at this point to make sure that the wax film is even, this is imperative to prevent high and low spots on the mounted device and ensure even polishing. The stub is then allowed to cool down to room temperature. Excess wax can be cleaned by rubbing gently on a Kim wipe wetted with acetone.

2. Polishing: The stub is placed in the holder of the Struers TegraPol and polished with set force for a given time. The MD-Floc polishing pad should be lubricated with 4-5 drops of green water based lubricant for every 5 minutes of polishing. After polishing, stub is placed under running water to clean off polishing slurry and allowed to dry under an air dryer.
3. Dismounting of polished device from stub: The stub with the device on it is heated to 140°C on a hot plate. When the stub is warmed up, acetone is poured using a dropper on the stubs to help dissolve wax and free the device. Using constant addition of acetone via a dropper, the device is picked up using tweezers and rapidly transferred to a vessel containing 99% acetone. This is carried out rapidly with great care to prevent the solidification of wax on the device which can result in the contraction of the wax and excess strain on the device resulting in damage or curling. The device is left in the acetone bath for 5 minutes to dissolve remaining wax. The device can now be removed from the acetone bath and allowed to dry. If visible traces of wax remain on the device surface, it should be immersed in fresh acetone for another 5 minutes while stirring.

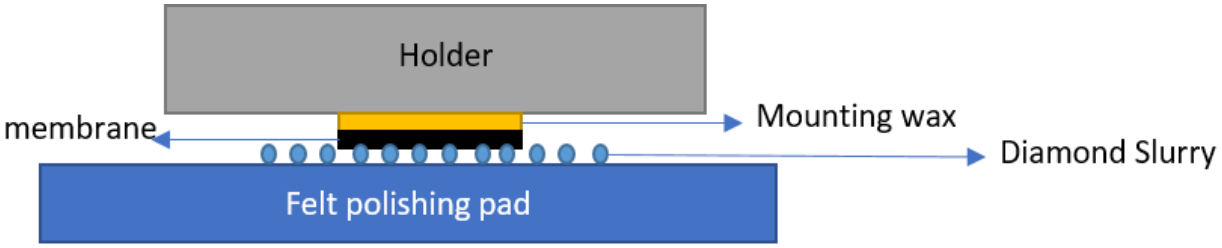

Figure 4.1: Polishing set up for CNT arrays

4.1.1 Effect of Polishing Time:

The AAO template does not have pores with a constant diameter through the cross section. The diameter of pores varies along the thickness of the membrane. This is illustrated in Fig. 3.10. With an increase in polishing time, it was hypothesized the diameters of exposed CNTs can be controlled due to an increased removal of template material and exposure of wider or narrower pores.

Experiment:

AAO membranes without carbon on them were mounted on aluminum stubs using 7071 Blanchard wax acquired from Stronghold Wax Company. They were then polished for time periods ranging from 5 minutes to 30 minutes in increments of 5 minutes using Struers DiaPro 1µm polishing suspension. Membranes were then etched in 1M NaOH for 3 minutes to clear polishing debris from the surface and expose pores while minimizing the effect of pore widening. They were then sputter coated for 3.5 minutes with Pd/Au to prepare for SEM imaging. Imaging was carried out on Tescan Mira 3 FESEM, 20kV gun voltage and 9mm working distance. All images were captured at a magnification of 40kx.

Measurement of pore sizes was carried out using NIH ImageJ. Images were adjusted for threshold and pore areas and perimeter recorded. Hydraulic diameter was calculated using the equation H= $\frac{4\,Area}{Perimeter}$. Depending upon the number of pores in an image, between 700-800 measurements were taken from each image. 2 images from different regions of the same membrane were analyzed.

Results:

Figure 4.2 shows SEM micrographs of the membranes after polishing and wet etching. The dark and light bands on the edges are caused due to charge build up during imaging. Visually, the pores appear to have

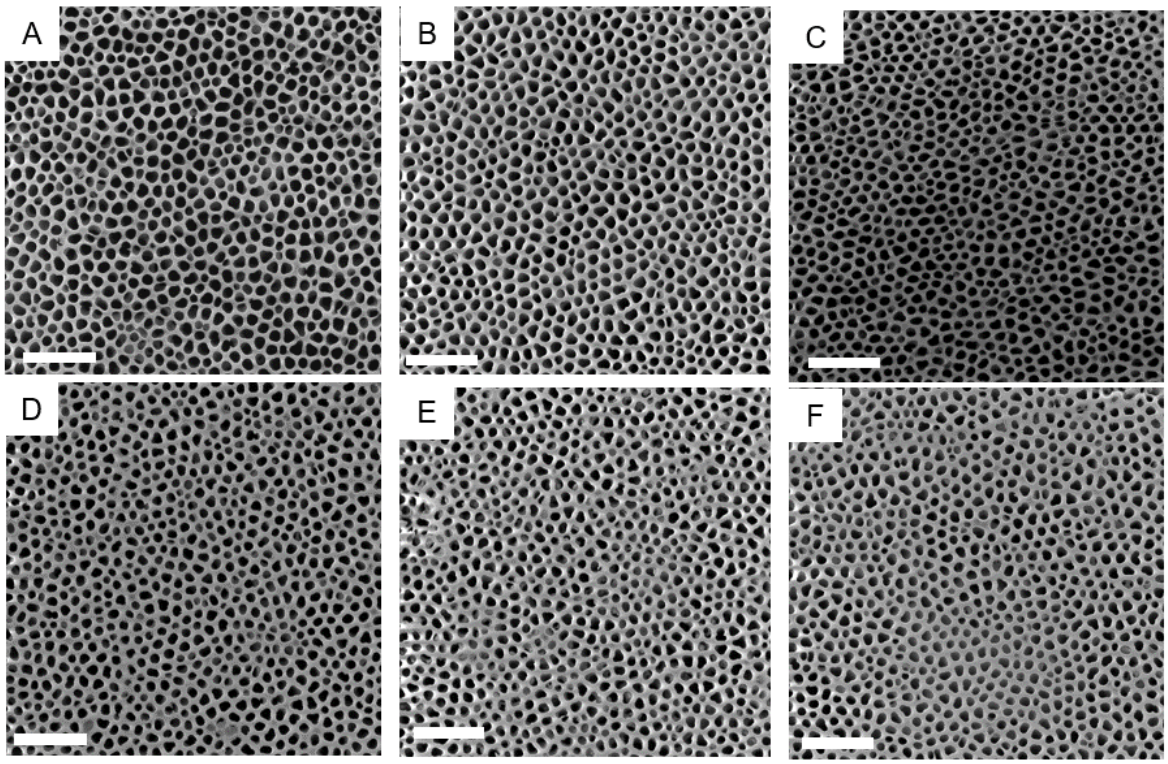

Figure 4.2: Membranes polished at 30N for **(A)** 5minutes **(B)** 10 minutes **(C)** 15 minutes **(D)** 20 minutes **(E)** 25 minutes **(F)** 30 minutes, scale bar 2µm

been perfectly exposed with no sign of the lattice layer. The graphs in Fig. 4.3 show average pore size and pore size distribution for each of the specimens.

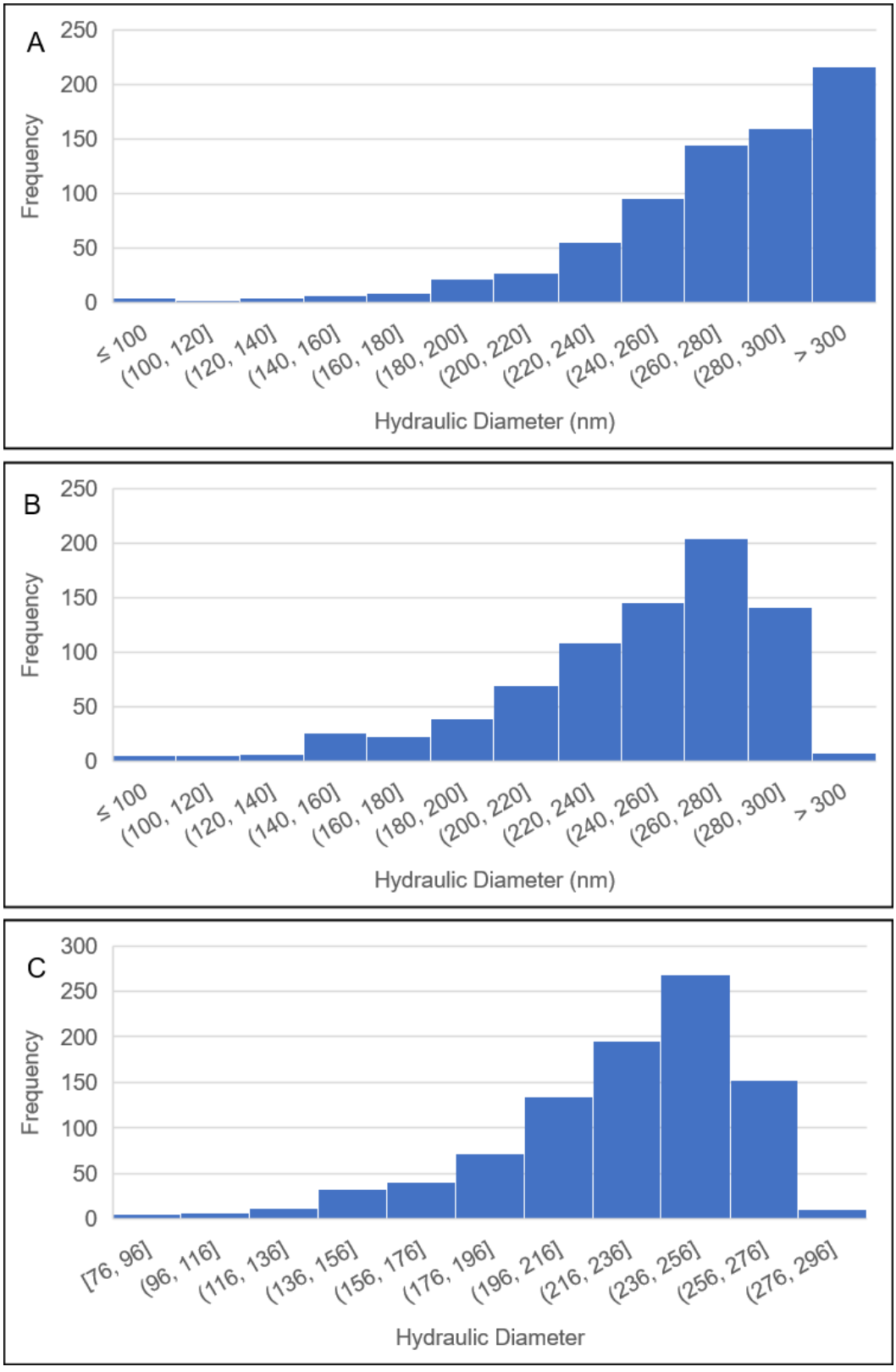

Figure 4.3a: Variation of pore hydraulic diameter with increasing polishing time at 30N **(A)** 5 min **(B)** 10 min **(C)** 15 min

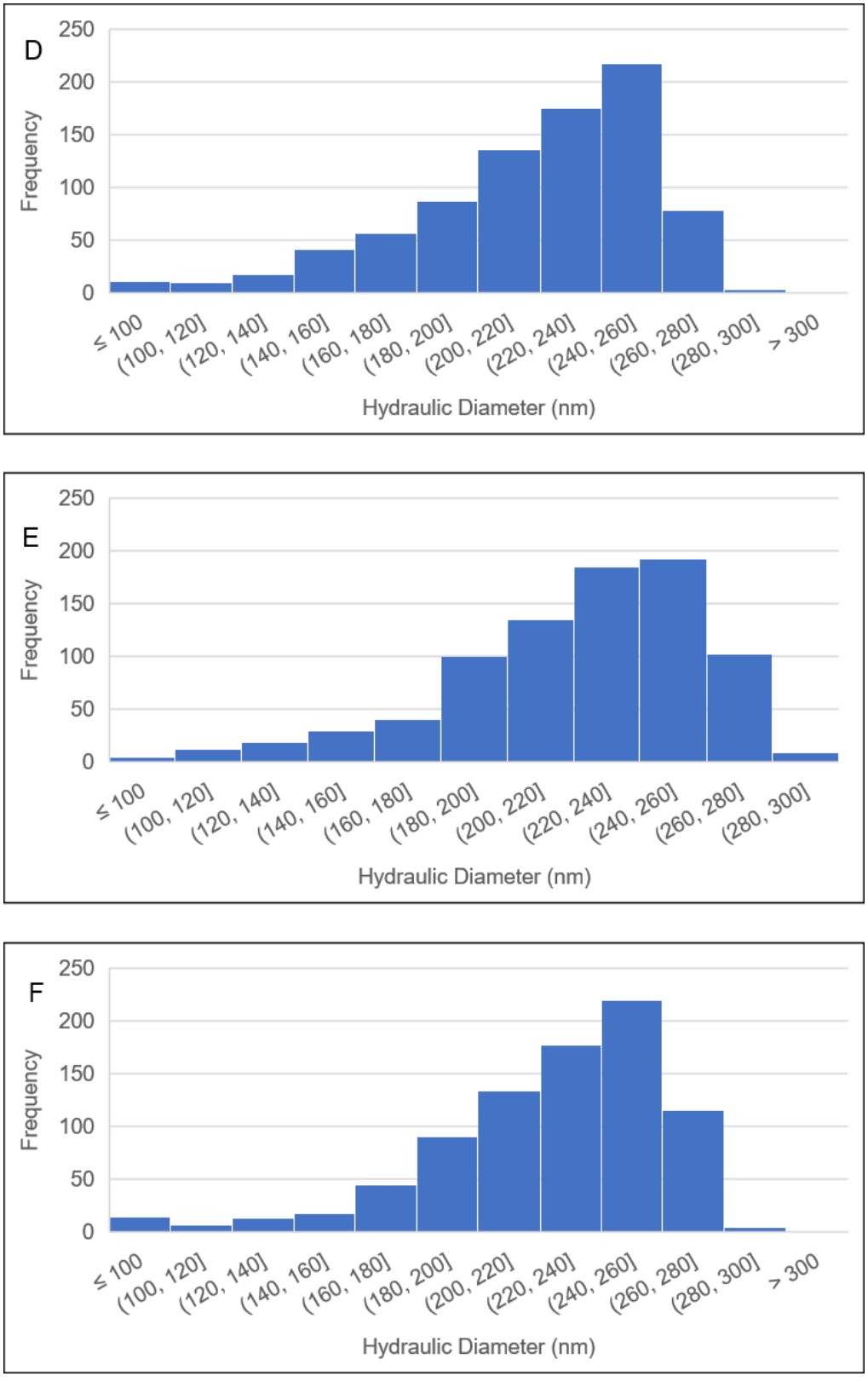

Figure 4.3(b): Variation of pore hydraulic diameter with increasing polishing time **(D)** 20 min **(E)** 25 min **(F)** 30 min

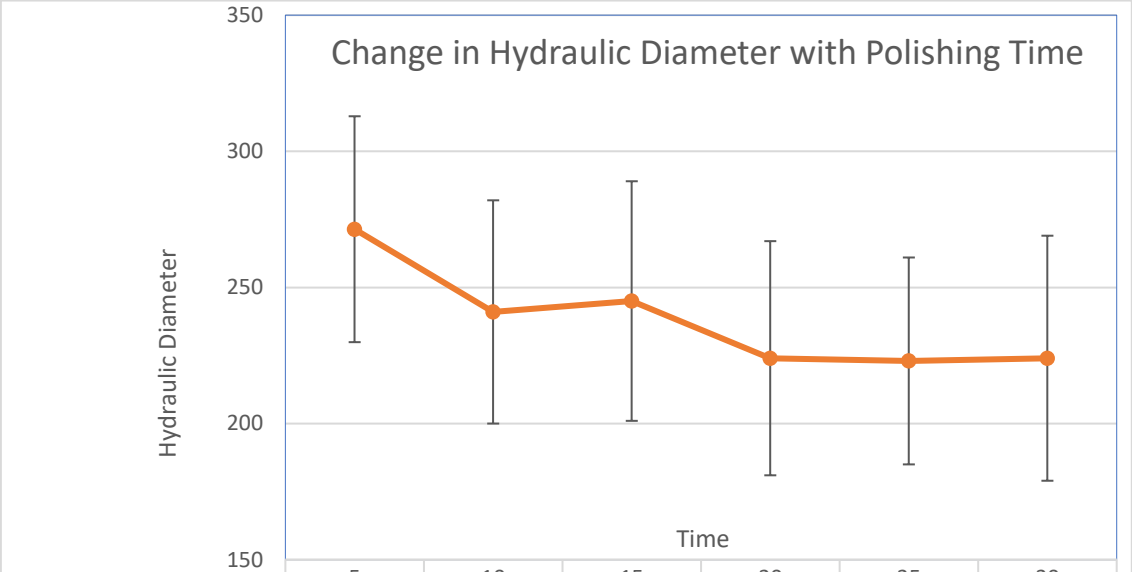

	5	10	15	20	25	30
Hydraulic Diameter (nm)	271	241	245	224	223	224
Standard Error of Mean	1.07	1.09	1.08	1.07	0.93	1.11

Figure 4.4: Change in Hydraulic Diameter with Polishing Time. Error bars show SD.

Observations and conclusions:

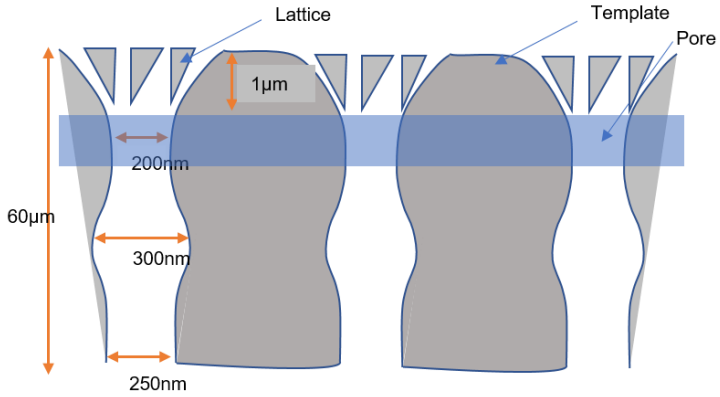

Figure 4.5: Cross section view of membrane showing region exposed by polishing in blue. Not to scale

From the above data, a slight decrease in the average pore size is observed with increase in polishing time. This suggests that after just 5 minutes, the membrane has been polished to expose pores higher than 250nm in diameter and as polishing continues, a decrease in pore size can be observed. This indicates that polishing is taking place within the 'neck' area of the pores, after the lattice layer. The error bars indicate the standard deviation of pore sizes within a sample. The standard error value indicates that there is significant difference between pore sizes when polishing time is raised from 5 minutes to 10 minute and

further on to 20 minutes. There is no increase in the hydraulic diameter with polishing, suggesting that material is not removed to more than a few microns below the lattice layer as shown in fig. 4.5.

4.1.2 Effect of Polishing force

The geometry of pores through the AAO membrane cross section has been well documented by (Golshadi 2016). The pores are shown to have a vase like geometry beyond the lattice layer, starting with a wide opening leading to a narrower neck and a wider body, depicted in Fig. 4.5. It can be deduced that by controlling the depth to which the membrane is polished, exposed CNT diameters can be controlled. The depth of polishing could be controlled by either polishing at a higher force or polishing for longer times.

In this experiment, AAO membranes were exposed to 7 hours of CVD at 705 °C. Membranes were then polished for 5 minutes using the DiaPro 1µm diamond suspension at 10N, 30N and 50N. membranes were then wet etched in 1M NaOH for 5 minutes at room temperature. SEM imaging was carried out using the Mira TESCAN FESEM at a beam voltage of 20kV. The hydraulic diameter of the tube lumen was calculated using ImageJ particle analysis tool. Area and perimeter of pores were recorded and hydraulic diameter calculated as $\frac{4\,Area}{Perimeter}$. 2 images from difference regions on each membrane were analyzed and Students t-test assuming equal variance was used to make sure that the difference in data from the 2 images was not statistically significant. Fig. 4.6 shows the images used for analysis followed by graphs in Fig. 4.7 showing the distribution of CNT inner diameters.

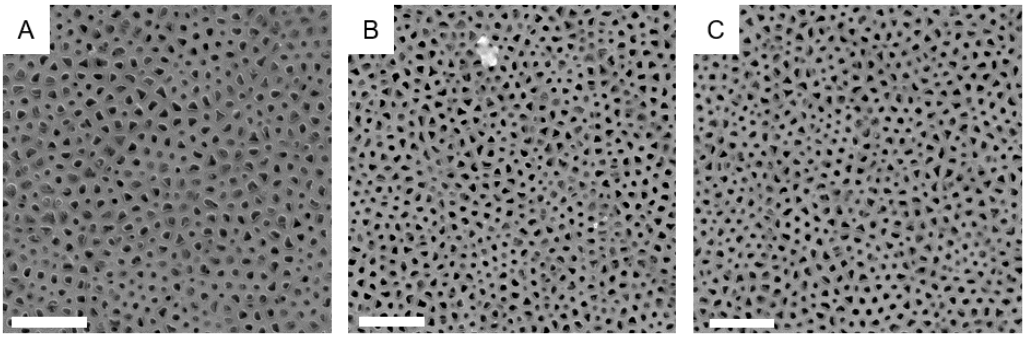

Figure 4.6: Top down view SEM micrographs of CNT arrays after polishing at **(A)** 10N **(B)** 30N **(C)** 50N Scale bar 2µm

Observations and conclusions:

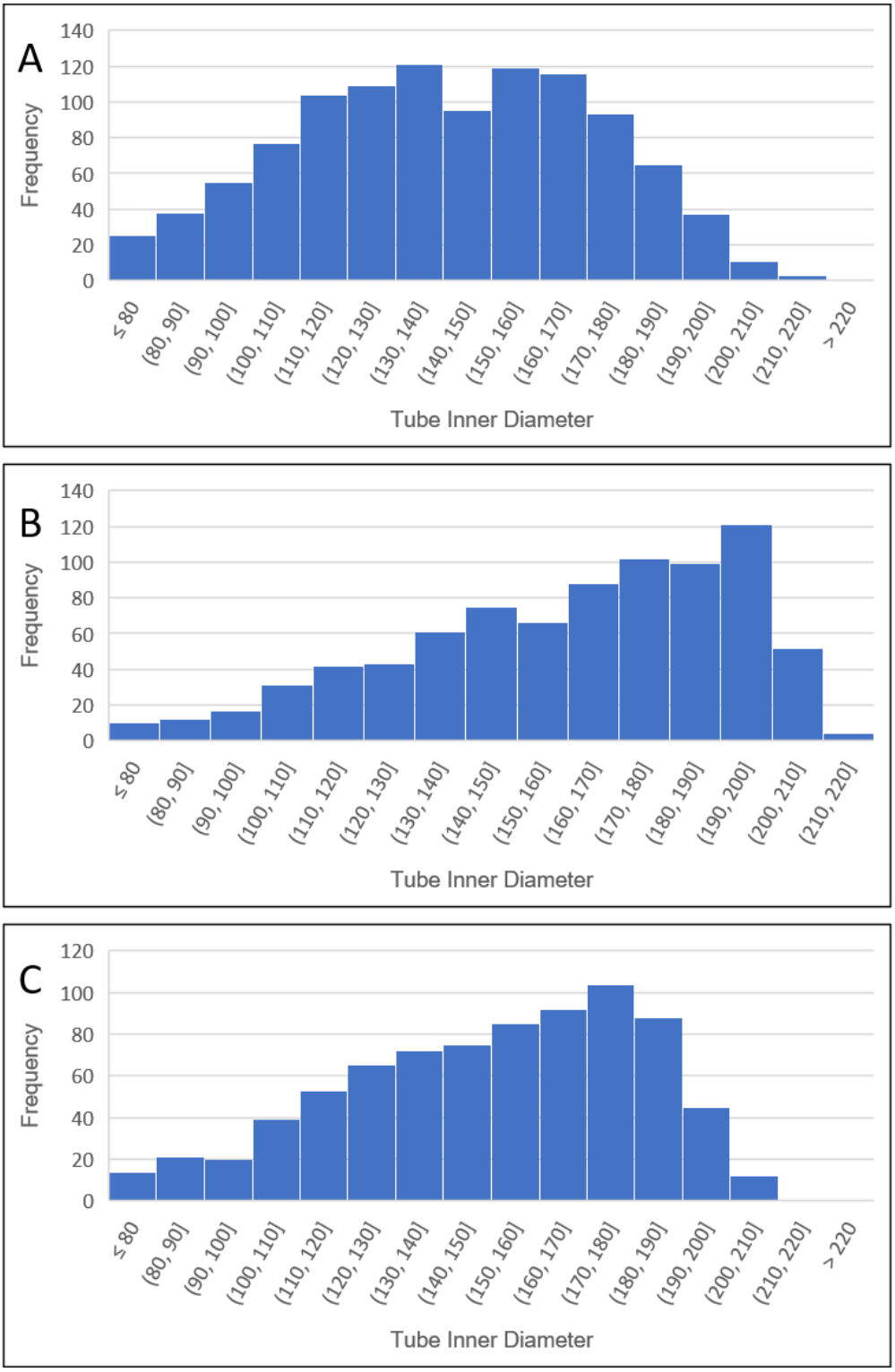

Figure 4.7: Variation of inner hydraulic diameter of CNT with polishing force after 5 minutes of polishing **(A)** 10N **(B)** 30N **(C)** 50N

Recordings of tube diameters from the same membrane on different regions of the membrane were not statistically different from each other indicating that the polishing process could result in even polishing across the surface. There was little difference observed between the CNT inner diameters between devices polished with different forces, strongly suggesting that increasing force does not necessarily increase the depth to which polishing occurs. With increased polishing force, the membranes were found to be more likely to curl during the etching step, likely due to increased internal stresses. Increasing the polishing force also increased the likelihood that a membrane could get stripped off the polishing stub or develop cracks, thus compromising its functionality or leading to a complete loss. Therefore, a polishing force of not more than 30N was considered ideal for the process while keeping time as the variable parameter to adjust depth of polishing.

4.2 Wet Etching:

The aluminum oxide template used is an amphoteric oxide, soluble in both acids and bases. Wet etching of aluminum oxide is commonly carried out using NaOH or H_3PO_4. In this section, the effect of etching time and etchant molarity upon CNT height is discussed.

4.2.1 Effect of etchant concentration:

To better understand etch rates with respect to changing concentration etchants, CNT array devices were etched with NaOH ranging from 1M to 9M concentration after polishing for 5 minutes at 30N. CNT height measurements were carried out manually using ImageJ on SEM micrographs captured at 35° stage tilt. 200 data points were recorded from each image. Fig. 4.8 shows the qualitative change in array devices with increasing molarity of etchant. Pore widening is observed to be the limiting factor for tube heights when wet etching is used. Tube height distribution is shown in Fig. 4.9.

Results and Observations:

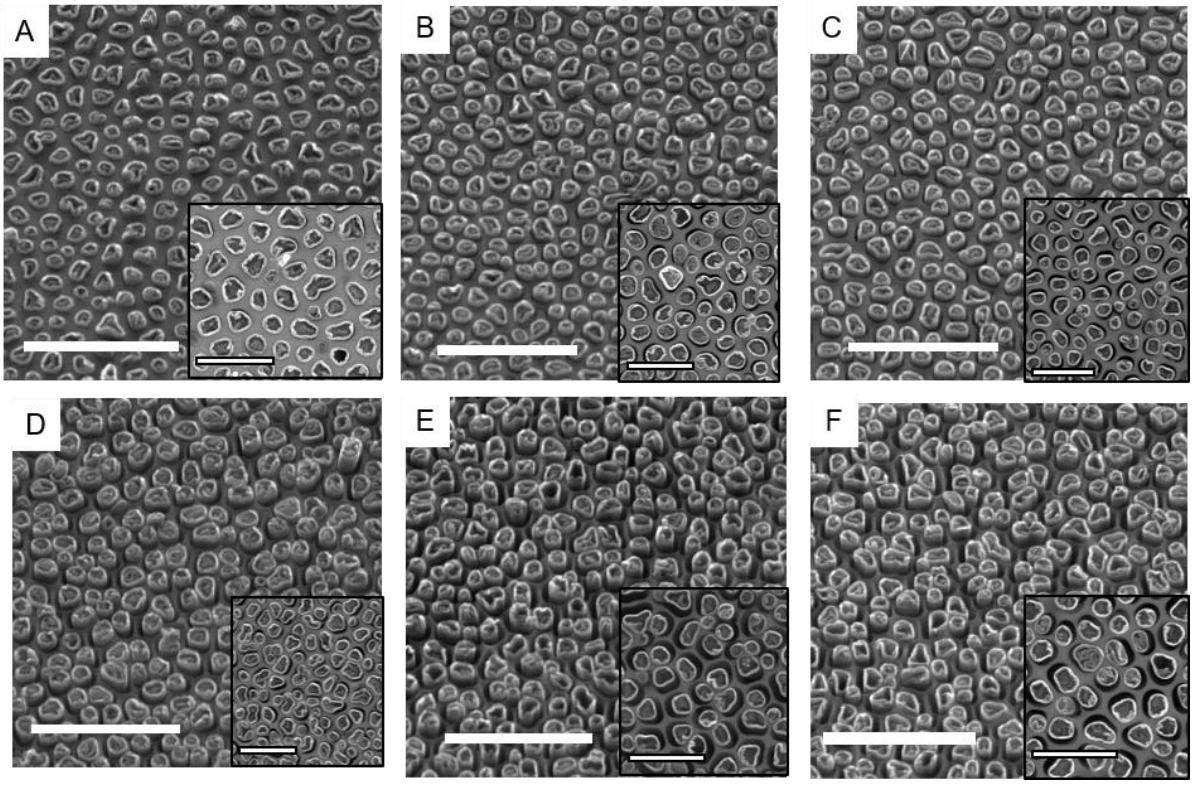

Figure 4.8: 35° tilt micrographs of CNT array devices etched with NaOH (A) 1M (B) 2M (C) 3M (D) 5M (E) 7M (F) 9M Inlets showing top down view and pore widening. Scale bar 2µm, inlet scale bar 1µm

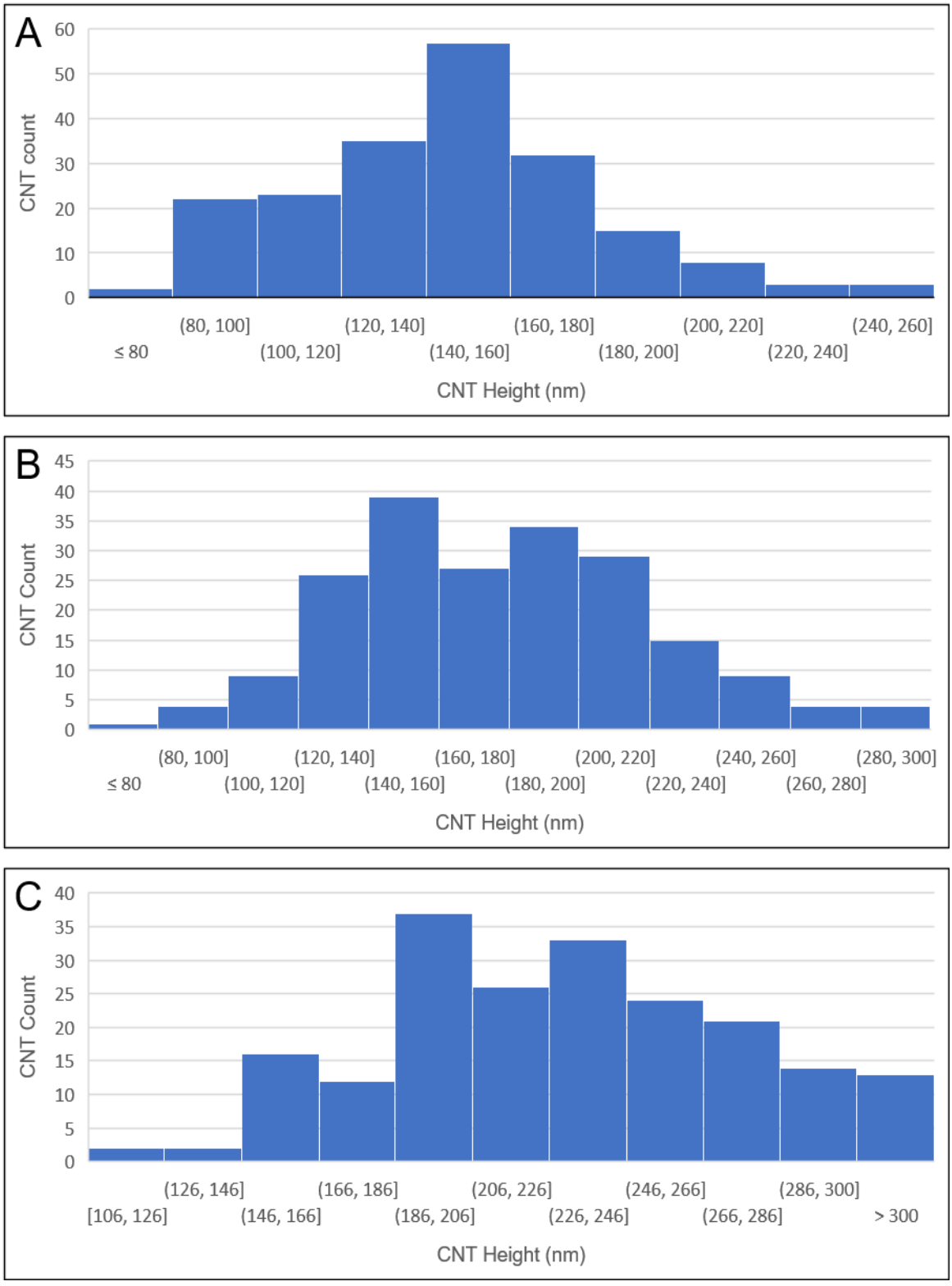

Figure 4.9: CNT height distribution after etching 5 minutes with NaOH **(A)** 1M **(B)** 2M **(C)** 3M

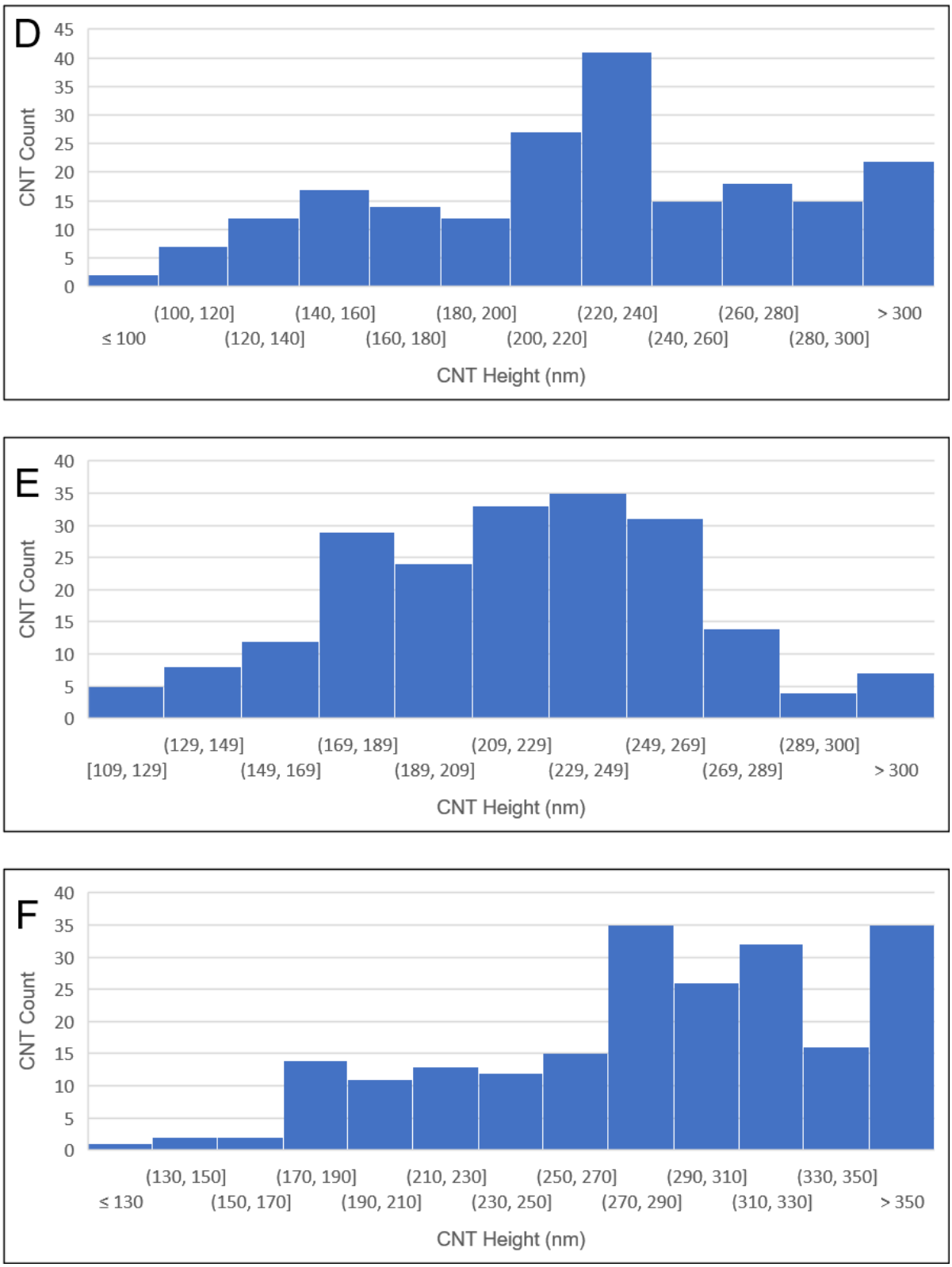

Figure 4.9(b): CNT height distribution after etching 5 minutes with NaOH **(D)** 5M **(E)** 7M **(F)** 9M

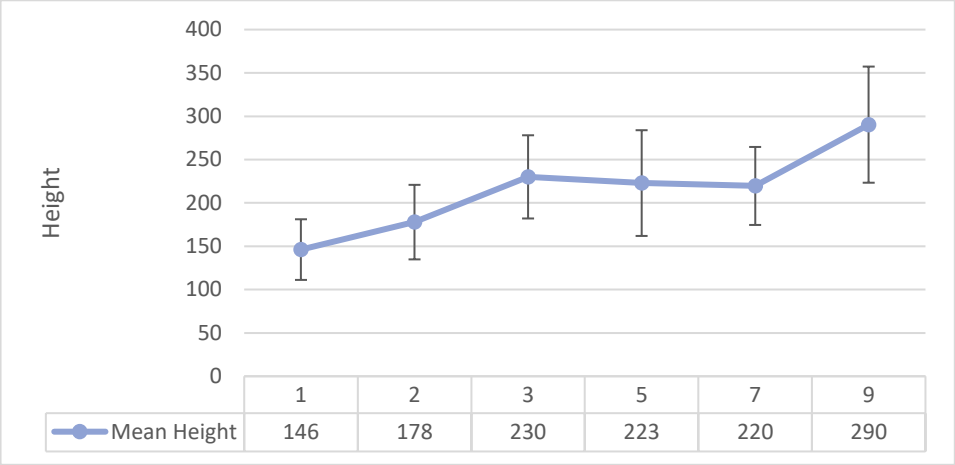

Figure 4.10: Mean CNT height after etching for 5 minutes with varying NaOH

A consistent increase is observed in the CNT heights up to 3M concentration, as seen in fig. 4.10. The regime between 3M and 7M concentration does not show significant difference in tube heights. This is attributed to the isotropic nature of wet etching and resulting pore widening. Both the edges around the tubes and the bulk of the membrane experience the same etch rates. However, there is much lesser material to etch at the edges as compared to the bulk. Therefore, in a given amount of time, more of the edge gets etched, leading to a rapid widening of the pore instead of uniform top-down etching.

Pore widening poses the risk of CNTs losing their structural support from the template and potentially clumping, if excess etching is carried out. It also adds ambiguity to the measurement of CNT heights because the actual point of intersection between the template surface plane through the CNT cannot be identified. Thus, CNT measurements from devices with significant pore widening cannot be accurately judged.

4.3 Conclusion

Polishing and wet etching can be controlled to yield CNT arrays of desirable physical parameters in a fraction of the time as compared to reactive ion etching. A typical polishing process will take 10 minutes of process time to yield 6 membranes compared to 6 hours for RIE. Thus, polishing and wet etching are significantly quicker and cheaper processes.

Chapter 5: CNT Quality Control

CNTs fabricated through polishing and wet etching display quality issues unique to the polishing process. Polishing, being an abrasive process, poses the risk of damaging CNT arrays due cracks induced in the template during the process, uneven polishing due to improper mounting of CNT devices on polishing stub and microscale damage to CNTs from polishing particles. This chapter presents a qualitative assessment of CNT arrays using electron microscopy as the primary investigative tool. All SEM micrographs were captures on the TESCAN Mira3 FESEM, with an accelerating voltage of 20kV unless mentioned otherwise.

5.1 Clogging of CNTs

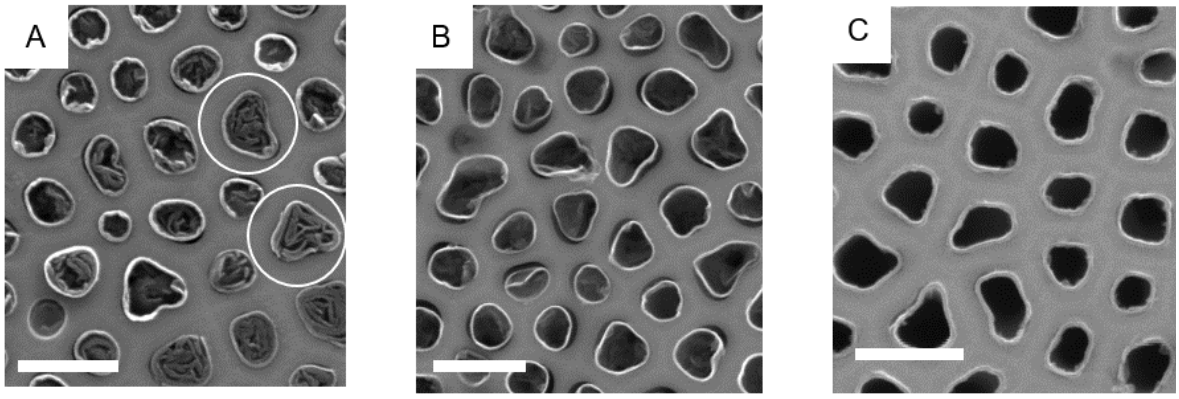

Figure 5.1: SEM micrographs of CNT arrays showing possible clogging **(A)** Type 1: Highly clogged and damaged, white circles show clogging in tubes **(B)** Type 2: Light clogging and minimal damage **(C)** Type 3: No clogging, no damage. Scale 500nm

As seen in Fig. 4.1 earlier, the polishing set up consists of a number of materials which are directly involved in contact with the polishing pad and may lead to clogging of nanotubes. Clogging throughout this chapter is classified as 3 types, shown in fig. 5.1. Type 1 clogging indicates highly clogged pores which are often found alongside damaged tubes. Type 2 clogging is less compared to type 1 and less tube

damage is observed. Type 3 indicates well formed, unclogged CNTs with no damage. The presence of obstructions in CNTs can be undesirable if CNT devices are used for fluidic applications such as intracellular delivery or as a component of a microfluidic system. In order to understand the cause of clogging and methods to eliminate it, a number of experiments were carried out.

Membranes during polishing come in contact with several materials. Blanchard holding wax, a commonly used wax for polishing silicon wafers in the microchips industry, is used to hold the AAO membranes onto the polishing stubs machined out of aluminum. The polishing pad used is a Struers MD FLOC non-woven fiber pad. Polishing slurries used were 1µm, ¼ µm Struers DiaPro (Diamond) and 0.05µm alumina (powder suspended in water). With the above set up, 4 major elements can be identified as the potential source of clogging in CNT arrays:

- Diamond – from polishing suspension
- Wax – Used to hold the devices on the stub
- Alumina
- Carbon – from CNT devices

5.1.1 Identification of clogging source - Wax

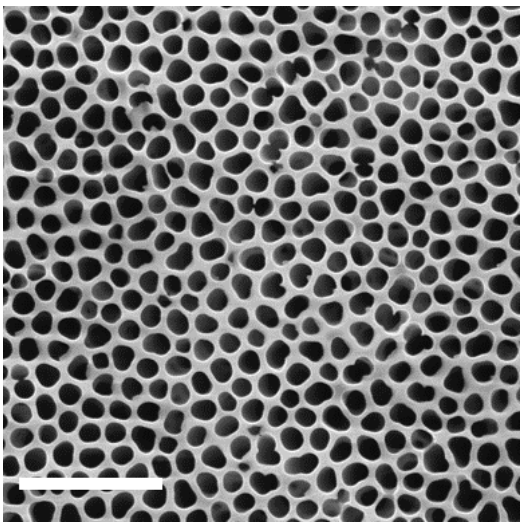

Figure 5.2: Bare membrane polished for 5 minutes, 30N. No clogging observed. Scale 2µ

Initial hypothesis suggested that due to improper cleaning, residual wax was responsible for clogging the CNTs. This problem was not observed when plain membranes were polished with or without wax suggesting that the decreased diameter of lumen after carbon deposition was affecting the ability of acetone to completely remove wax. Since wax is soluble in acetone, longer acetone wash times, higher temperatures and ultrasonication in acetone were experimented with to understand its effect on clogging. Fig. 5.3 shows the results after the different rinsing processes.

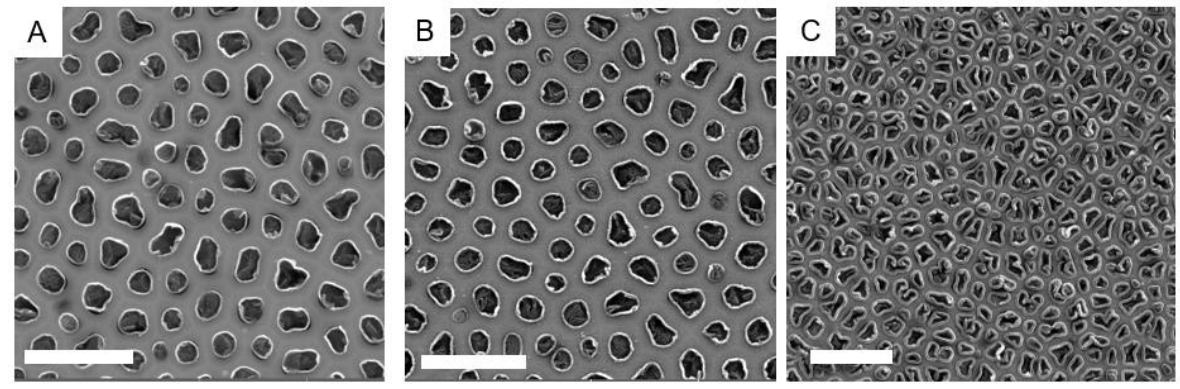

Figure 5.3: Top down micrographs of CNT arrays after **(A)** rinsing in acetone (40°C) **(B)** Rinsing in water (100°C) **(C)** After forcing acetone through CNTs using syringe. Type 2 clogging observed in all specimens. Scale 1µm

In the images shown in Fig. 5.3, it can be observed that clogging is persistent in all CNT devices despite the processing technique utilized. These experiments indicated that the hypotheses of wax clogging the nanotubes was likely to be a weak hypothesis and other causes should be considered. However, the experiments did not indicate a complete breakdown of the hypothesis since it could not be confirmed whether the acetone was truly effective at dissolving wax from the CNTs. Thus, these experiments assumed that acetone is 100% effective at dissolving all wax. To confirm the hypothesis, polishing was carried out without using wax as a mounting agent for 5 minutes and 30N followed by 5 minutes of etching with 1M NaOH. CNT arrays were mounted using Kapton tape on to aluminum stubs and polished. The resulting micrographs, shown in fig. 5.4, showed type 1 clogging in the CNTs, thereby confirming the hypothesis that wax was not responsible for clogging the CNTs.

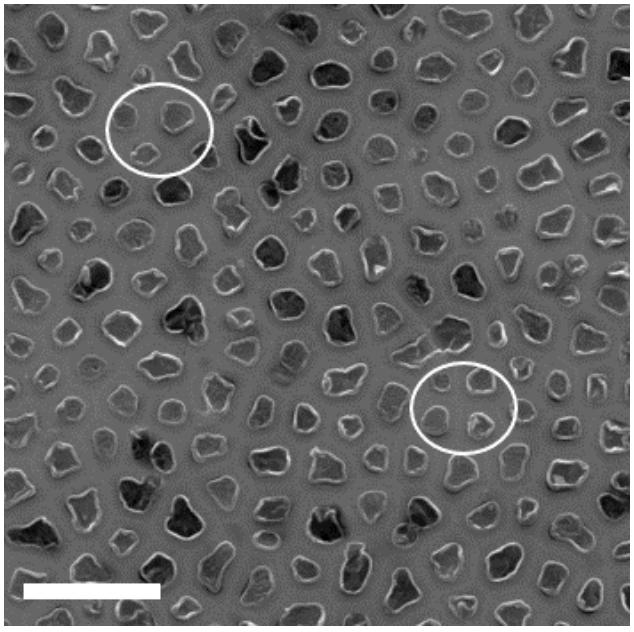

Figure 5.4: Top down micrograph of CNT array, polished without wax, 5mins, 30N. Clogged tubes encircled.

5.1.2 Identification of Clogging Source – Aluminum Oxide

Aluminum oxide, if involved in clogging the CNTs, should ideally have been dissolved by the action of wet etchants such as NaOH or phosphoric acid. It is possible that due to the small diameters of CNTs, etchants were not able to access the lumen and dissolve the alumina.

To overcome this, X-ray microanalysis using scanning electron microscopy (SEM) was utilized.

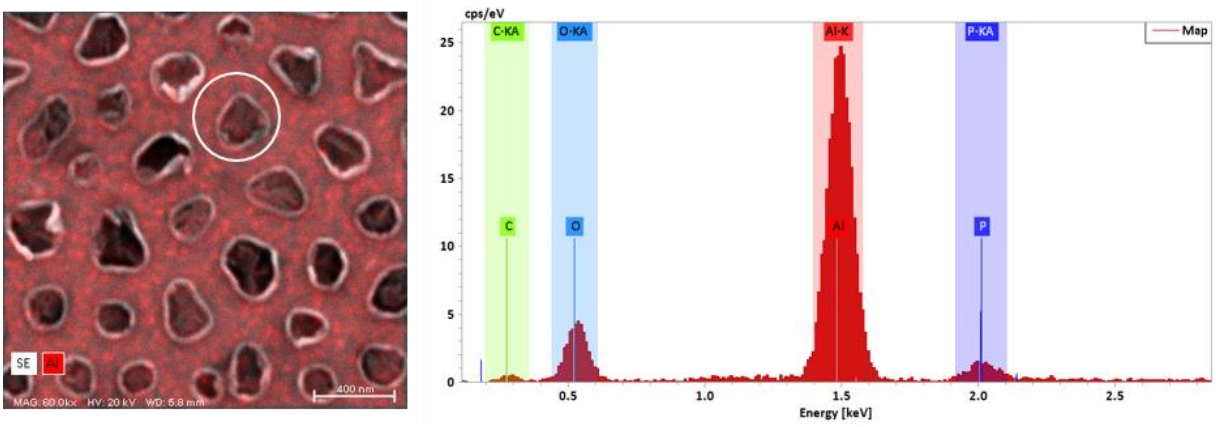

Figure 5.5: EDX spectra overlay - showing aluminum in red. Clogged pore circled. Red color suggests presence of aluminum

The image in Fig. 5.5 strongly suggests that alumina is present in some quantities in the clogged pores. It must be noted that EDX results cannot be taken as conclusive but were used as a guide for future experiments. To eliminate traces of alumina from the clogging, devices were exposed to reactive ion etching using BCl_3 and wet etching techniques. It was expected that BCl_3 will result in selective etching of AAO and a reduction in clogging can be observed.

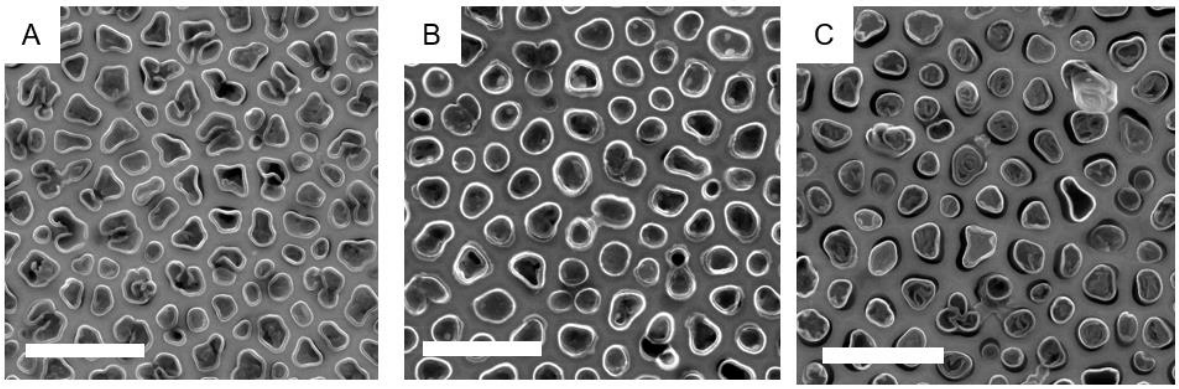

Figure 5.6: Top down micrographs of CNT devices processed with RIE for **(A)** 15 minutes **(B)** 30 minutes **(C)** 45 minutes followed by wet etching for 5 minutes with 1M NaOH. **A**, **B** show type 2 clogging and **C** shows type 3 clogging. Scale 1µ

Reactive ion etching was carried out for 15, 30 and 45 minutes at a flow rate of 20SCCM argon and 80SCCM BCl_3 on different devices immediately after polishing. The devices were then subject to wet etching with 1M NaOH for 5 minutes. It was expected that reactive ion etching will selectively etch away aluminum oxide, thereby unclogging the tubes to some degree. The images in Fig. 5.6 show that RIE has influenced the clogging of CNT arrays but type 1 clogging is seen in Fig. 5.6 (C) and type 2 in panels A, B. The devices used for this batch of experiments also show some variability in polishing but clogging is observed in all sections of the devices irrespective of the quality of polishing. Further experiments were carried out using by using variations of wet etching.

In Fig. 5.7, all devices were etched using 1M NaOH for 5 minutes unless specified. Significant etching has taken place when using higher concentration of NaOH or warm NaOH, indicated by the presence of

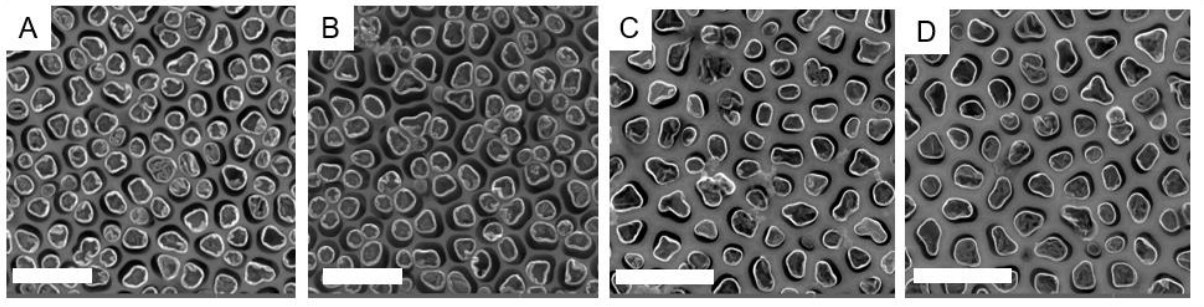

Figure 5.7: Top down micrographs of CNT devices etched with **(A)** 7M NaOH for 5 minutes **(B)** 9M NaOH for 5 minutes **(C)** 1M NaOH for 5 minutes followed by 0.1M NaOH for 5 minutes **(D)** 1M NaOH, ~40°C, 5 minutes, Scale 1µ

pore widening. However, clogging is still observed in the CNTs. With the increase in NaOH concentration, an increase in the viscosity and surface tension of solution is observed. To enable better access to the CNT lumen, a lower molarity of NaOH was used to etch the device for a second round. Using a lower molarity of NaOH for a second round of etching after 5 minutes of etching with 1M NaOH also did not show any reduction in clogging.

5.1.3 Identification of Clogging: Carbon

Since all the methods above selectively dissolve or etch away aluminum oxide, it could be concurred that aluminum oxide was not the primary element responsible for clogging of CNTs because there appeared to be negligible change in the number of clogged CNTs in each experiment. This in conclusion implied that the clogging was most likely being caused by carbon being smeared from damaged CNTs during the polishing process.

In order to confirm the hypothesis, attempts were made to oxidize carbon using oxygen plasma etching. The 2 routes to eliminate carbon from the polishing process are shown in Fig. 5.8 below. In route A, carbon is etched away prior to polishing and therefore is not involved in the polishing process, eliminating any possibility of it clogging the CNTs. In route B, carbon is etched after CNTs have been exposed. In an ideally controlled process, just the right amount of etching would take place to eliminate the clogging. In the case of excessive etching, the CNT array could be further wet etched to dissolve more of the membrane and re-expose nanotubes. Since, neither of the processes provide an advantage over the other, the selection criteria were limited to the route which would offer better control over the geometry of CNT array device.

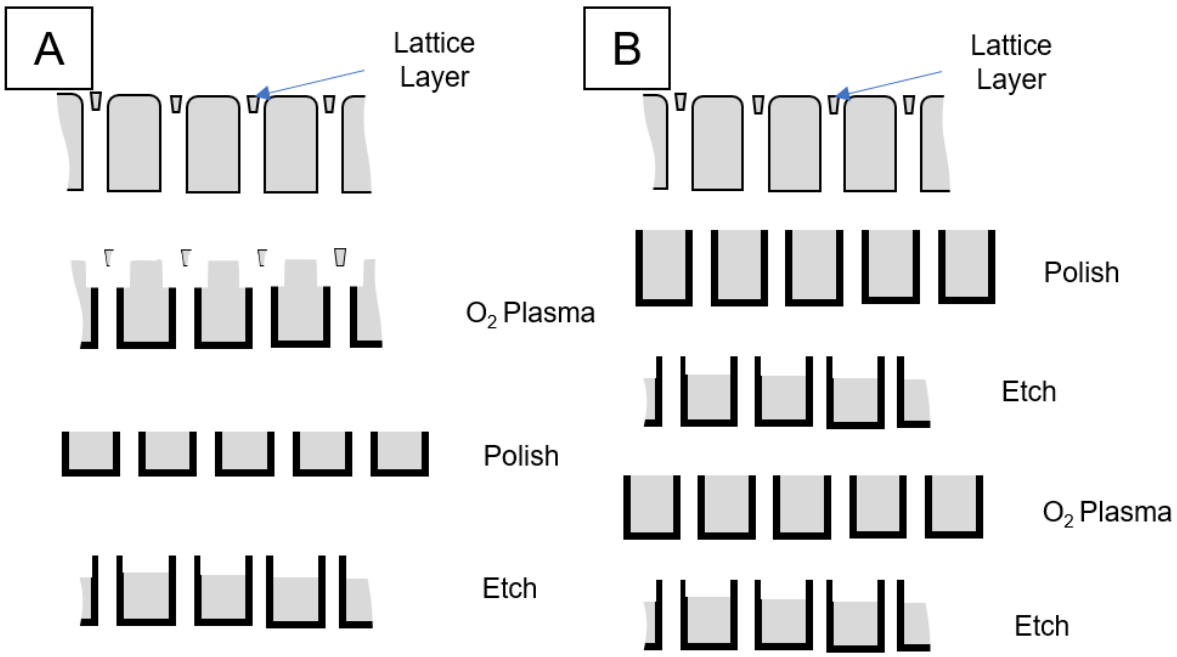

Figure 5.8: Schematic depicting two methods of implementing oxygen plasma to remove carbon **(A)** O_2 plasma is used to eliminate carbon from the polishing process **(B)** O_2 plasma is used to etch the top of CNTs which can then be exposed again by etching

In Fig. 5.9 below, results from method A are shown. Initially oxygen plasma (SAMCO RIE-1C) was carried out for 2 and 4 minutes at 50SCCM flow rate and 200W RF power on carbon coated membranes prior to polishing. The devices were then polished for 25 minutes at 30N and etched in 1M NaOH for 5, 8minutes. It is seen that carbon is completely etched off in some regions from the membranes and no clogging is observed. Plasma treatment therefore resulted in excessive etching. To better control the process, oxygen plasma was carried at 50W and 50SCCM on carbon coated devices and followed by 25 minutes of polishing at 30N 5, 7 minutes of etching in 1M NaOH. In fig. 5.10 (A, B) are images from 2 different membranes. (A) displays clogging while minimal tubes are observed in (B). Since the etch rate of amorphous carbon within the geometry of porous membrane is not documented, it was not possible to estimate the depth to which carbon was being etched. From 5.10 (A, B) it is clear that the process presents variability. Owing to the above factors, it was decided to try route B shown in fig. 5.8.

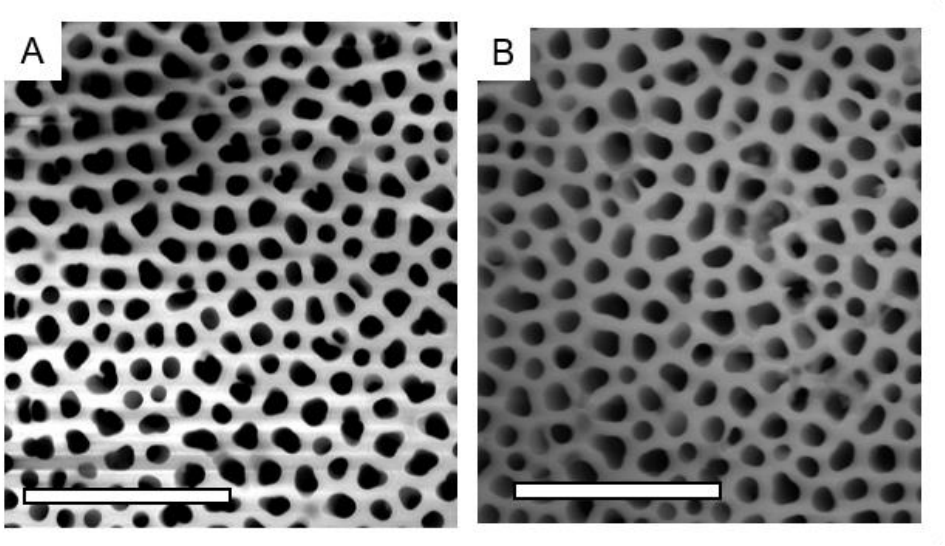

Figure 5.9: SEM micrographs of devices after O_2 plasma at 50SCCM, 200W **(A)** 2 minutes **(B)** 4 minutes followed by polishing for 25 minutes at 30N and wet etching for **(A)** 5 minutes **(B)** 8 minutes. Scale 2µm

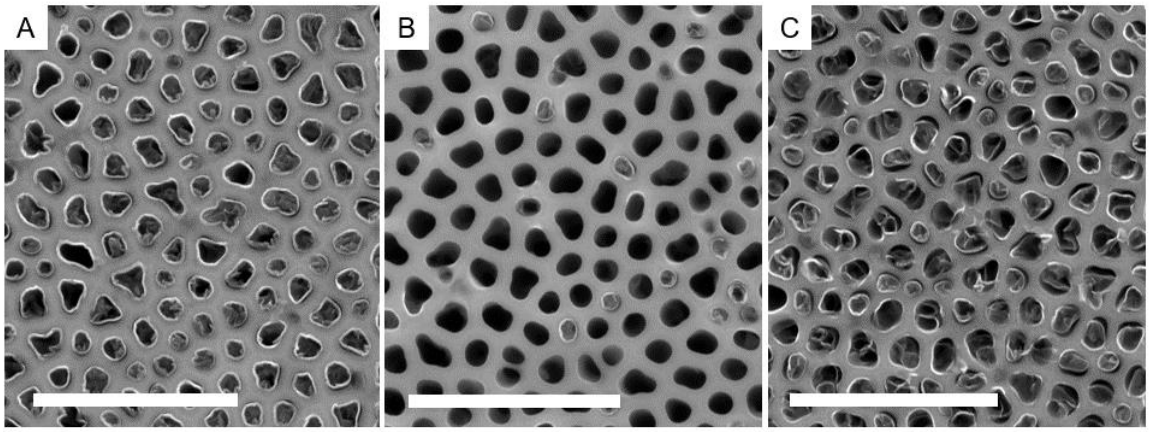

Figure 5.10: CNT arrays fabricated using procedure outlined in fig. 6.8 (A). O_2 plasma carried out at 50SCCM, 50W for 1 minute followed by polishing for 25 minutes, 30N **(A, B)** Wet etched 3 minutes **(C)** 7 minutes with 1M NaOH. Scale 2µm

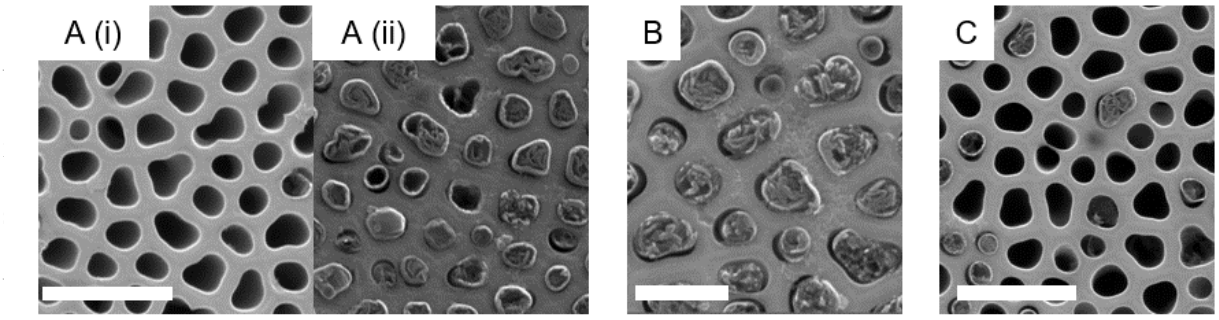

Figure 5.11: Devices polished for 5 minutes, 30N followed by wet etching for 5 minutes with 1M NaOH. O_2 plasma carried out for **(A)** 60s **(B)** 90s **(C)** 120s at 50W, 50SCCM flow rate followed by etching again for 5 minutes with 1M NaOH. Scale **(A)** 1µm **(B)** ½ µm **(C)** 1 µm

Oxygen plasma was also carried out on polished devices after etching, to understand whether the process of eliminating clogging could be controlled when nanotubes are exposed. Fig. 5.11 shows the resulting devices after 60, 90, 120 seconds of oxygen plasma at 50W, 50SCCM of oxygen flow. The devices were etched again in NaOH after oxygen plasma to increase the length of exposed tubes. After 1 minute of treatment with oxygen plasma, seen in Fig. 5.11 A (i), certain regions of the membranes show excessive etching and no tubes are observed. In Fig. 5.11 (A (ii)) clogged tubes of type I are observed. After 2 minutes of treatment and more, almost all carbon is etched away and no nanotubes are observed on the surface, implying excessive etching.

Although oxygen plasma treatments were successful to a limited extent in helping unclog the CNT devices, a high level of variability and lack of control made the use of O_2 plasma unfeasible.

Corona plasma treatment was also briefly explored as an aid to unclog the CNT arrays. A corona discharge is formed when a highly charged conductor ionizes the insulating fluid around it, in most cases this fluid is air. The corona discharge will result in the production of ozone and other ions. A handheld corona discharge device known as the plasma wand was used for this task. Since CNT devices are conductive, an arc was formed between the conducting tip of the corona device and CNT device. Membranes were treated either before etching or after etching for 30s and 120s. Fig. 5.12 shows the

results of the experiment. In Fig. 5.12 (A, C) we can see that corona treatment immediately after polishing for 30 seconds does not result in a significant reduction in the clogging of carbon nanotubes in some region while other regions show a complete elimination of nanotubes. After 120s of corona treatment, CNTs have been etched and bare AAO can be observed. The process exhibits a high amount of localized variability.

5.2: Effect of CVD Time and Membrane Position in Furnace on CNTs

It was found that the position of membranes on the CVD holder, referred to as the 'boat' and CVD time had a major effect on the clogging of CNT arrays. The following experiments were carried out to qualitatively observe how CVD time and membrane placement affects CNT quality.

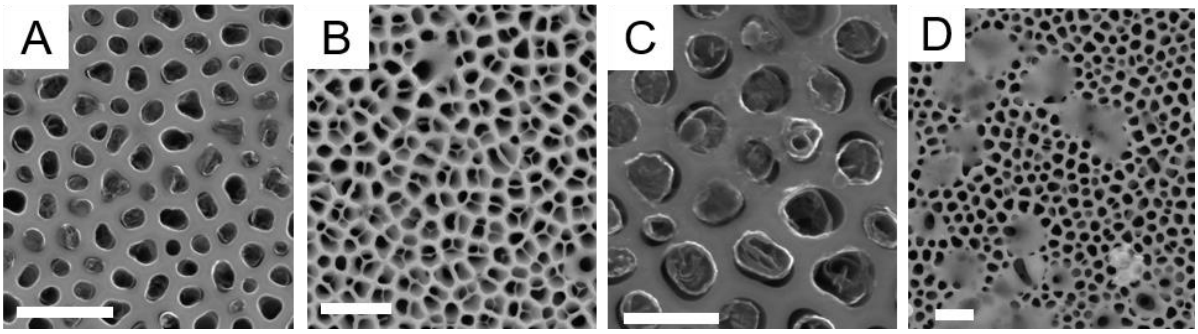

Figure 5.12: Plasma wand used before etching **(A)** 30s **(B)** 120s, Plasma wand used after etching **(C)** 30s **(D)** 120s, followed by etching for 1 minute with 1M NaOH. Scale 1µm, **(C)** scale 500nm

Experiment 1:

The CVD boat consists of 35 slots, of which 9 were filled as shown in fig. 5.13. The membranes were put through CVD for 5 hours and 7 hours. Membranes were then taken in groups of three, depending on their position in the boat (near gas inlet, center, near exhaust). 1 membrane in each group was polished with

15N force for 5 minutes while the other two in the group were polished at 30N for 5 minutes followed by 5 minutes of wet etching with 1M NaOH. The results are shown in fig. 5.14 and 5.15 below.

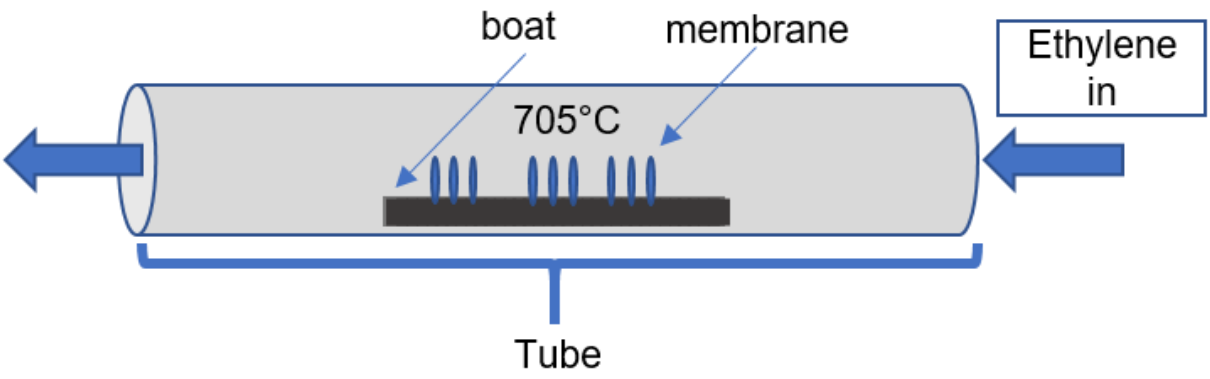

Figure 5.13: Arrangement of membranes to study CNT quality changes due to position in tube furnace and CVD time

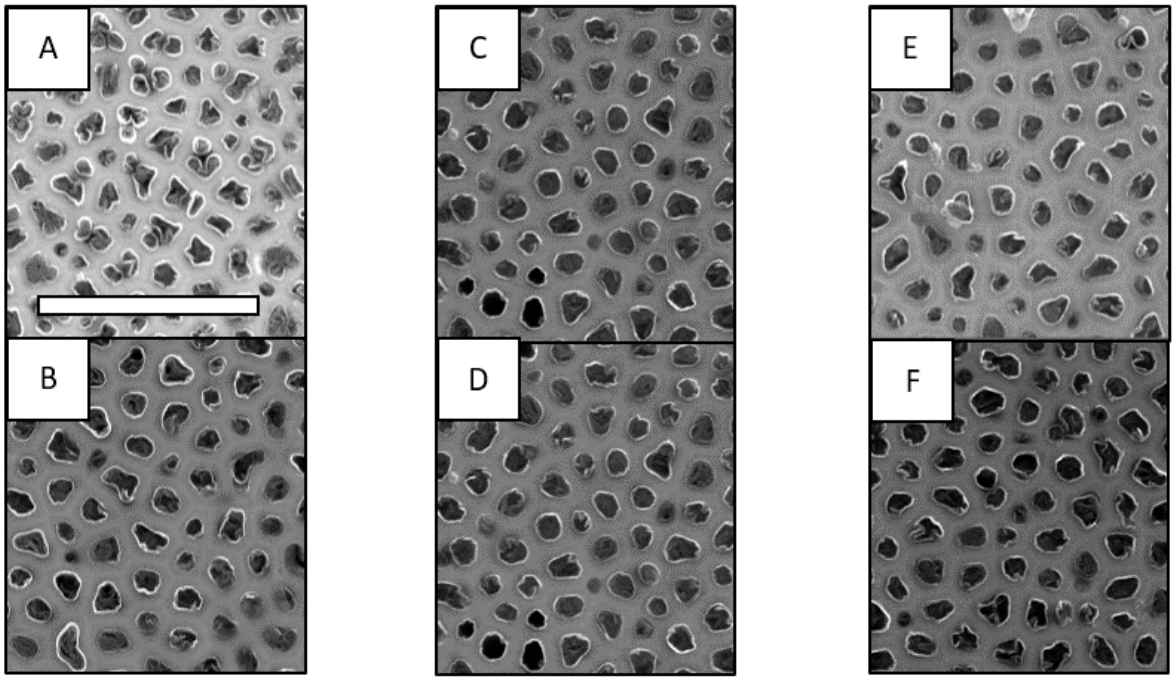

Figure 5.14: SEM micrographs of 5-hour CVD **(A, C, E)** 15N 5 min polished devices **(B, D, F)** 30N 5 min polished devices **(A, B)** near exhaust **(C, D)** center **(E, F)** near inlet. Scale 2µm

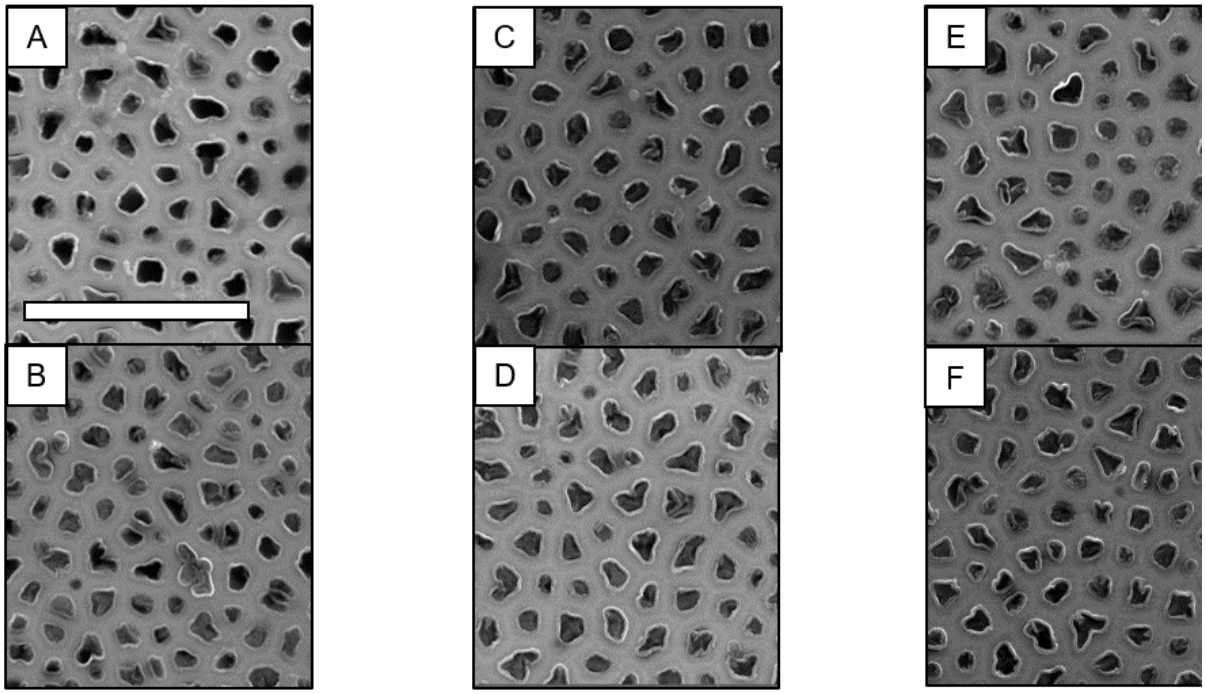

Figure 5.15: SEM micrographs of 7-hour CVD **(A, C, E)** 15N 5 min polished devices **(B, D, F)** 30N 5 min polished devices **(A, B)** near exhaust **(C, D)** center **(E, F)** near inlet. Scale 2µm

The position of devices in the polishing equipment holder was also tracked to rule out any variability due to the polishing set up.

Results: It was observed that after 5 hours of CVD, irrespective of polishing force, CNTs were easily damaged during the polishing process and appeared to be clogged. CNT wall thicknesses appear to be consistent across all samples indicating uniform carbon deposition. After 7 hours of CVD, an interesting observation was made. Specimens closer to the exhaust seem to have lesser clogging in the

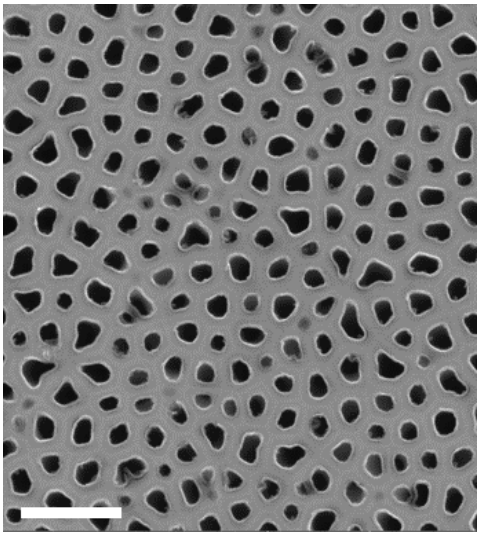

Figure 5.16: Unclogged, undamaged tubes after 7 hours CVD. Device was placed near exhaust during CVD. Scale 1000nm

tubes and displayed lower tube damage, despite equivalent tube wall thicknesses. This experiment was repeated to confirm results, seen in fig. 5.16.

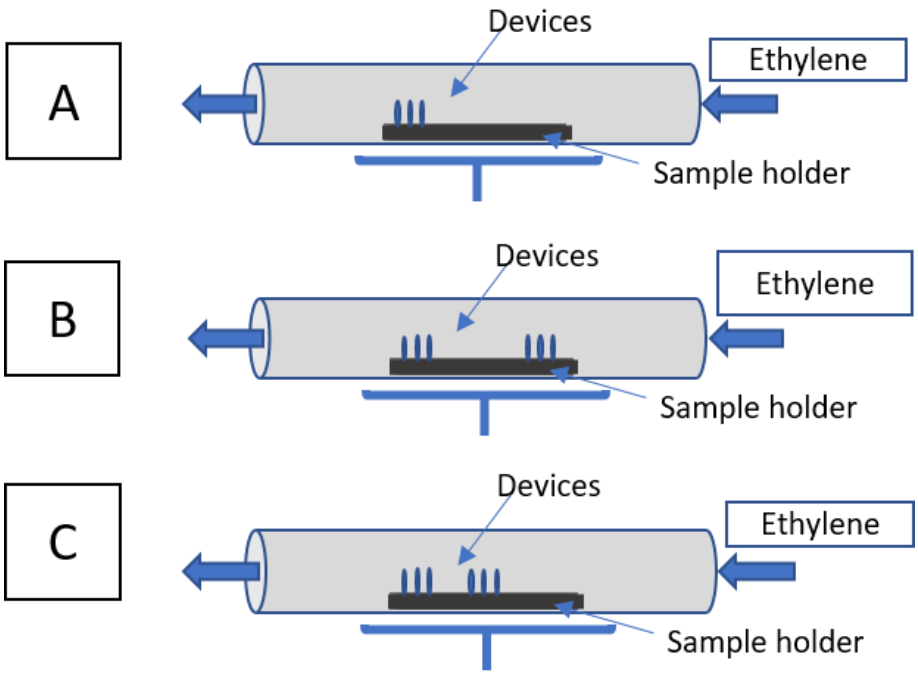

Figure 5.17: Experimental set up to study variation in CNT quality after polishing due to membrane positioning in sample holder and interdependence of membranes in different positions. CVD carried out for 7 hours

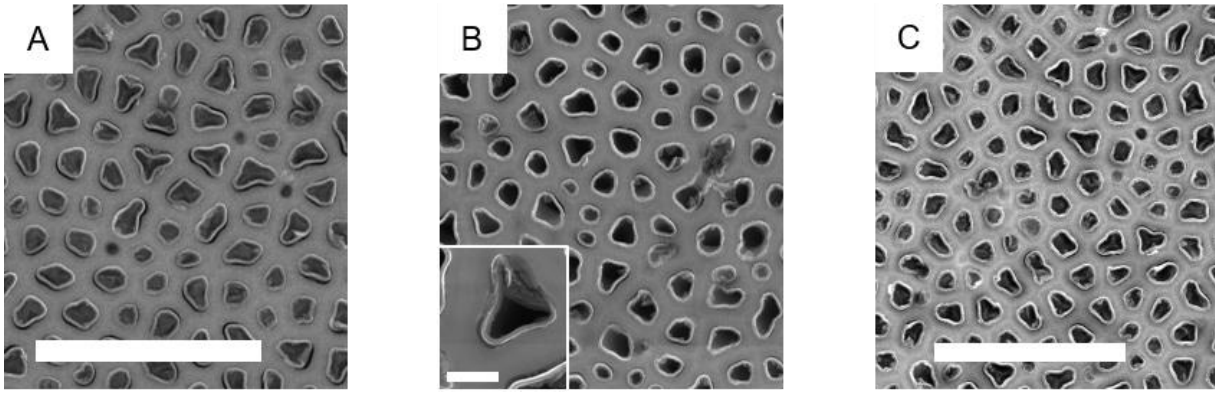

Figure 5.18: Membranes imaged corresponding experiments described by fig. 6.17. **(A)** Type 1 clogging observed in all samples **(B)** No clogging in one sample (shown here). Inlet shows tube damage **(C)** Type 2 clogging observed. All specimens imaged were from the group near the exhaust. Scale 2µm (A, B scale is the same), **(B inlet)** 200nm

A third experiment was designed to study whether the removal of membranes from other positions in the boat would yield similar results. In this experimental set up the boat was filled with membranes as shown in figure 5.17. The membranes were then exposed to 7 hours of CVD and polishing at 30N for 5 minutes using 1µm diamond slurry followed by etching using 1M NaOH for 5 minutes. Fig. 5.18 shows the results of this experiment. Only the marked membrane showed unclogged tubes. This result strongly suggested an interdependence of membranes in different positions with respect to how devices reacted to polishing.

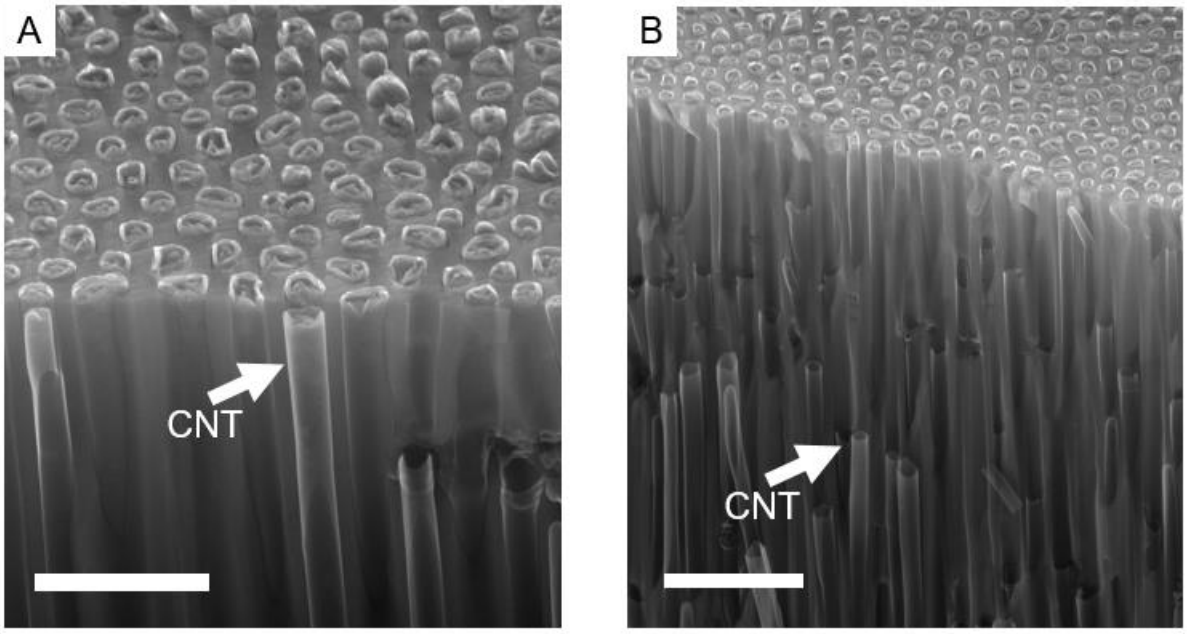

Figure 5.19: Cross section view of membranes **(A)** No clogging is observed in the tubes below the surface **(B)** Unclogged membrane, no clogging in tubes below surface. Thus, clogging is only on the surface. Scale (A) 1µ (B) 2µ

To verify that CNTs were unclogged all the way through, cross section of etched, broken membranes was imaged. In Fig. 5.19, the CNTs show no clogging, neither at the upper opening of the CNTs nor in the lower sections. In the clogged CNT arrays, it is seen that the clogging does not extend down below the very top, implying that there are no impurities that remain in the tubes from the polishing process. This is an important observation since the presence of impurities within the nanotubes would pose larger problems for the purposes of cleansing as compared to impurities at the very openings.

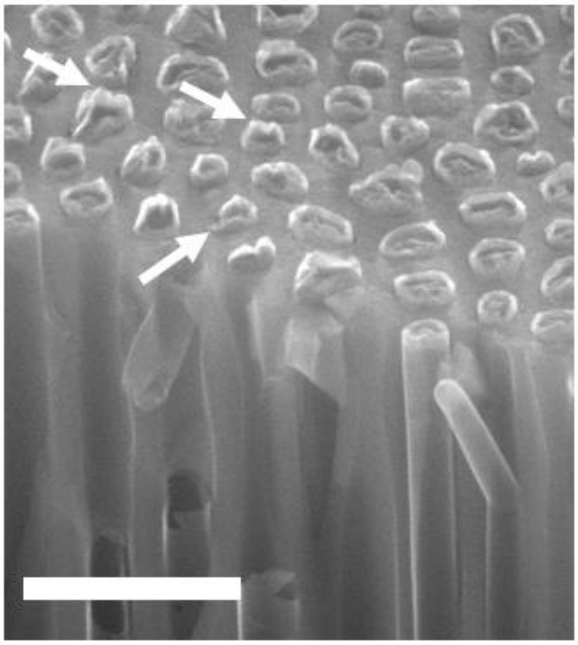

Figure 5.20: Arrows showing jagged tube walls

Although unclogged CNTs could be obtained by the above-mentioned method, it added time to the process while reducing yield by 50% because only 3 membranes at a time could be obtained unclogged. Unclogged membranes also displayed signs of tube damage and jugged CNT walls as shown in fig. 5.20.

The issue of clogging was also studied with respect to the grain size of polishing slurry used. The following solutions were available for use:

1. Struers DiaPro Nap 1µm
2. Struers DiaPro Nap ¼ µm

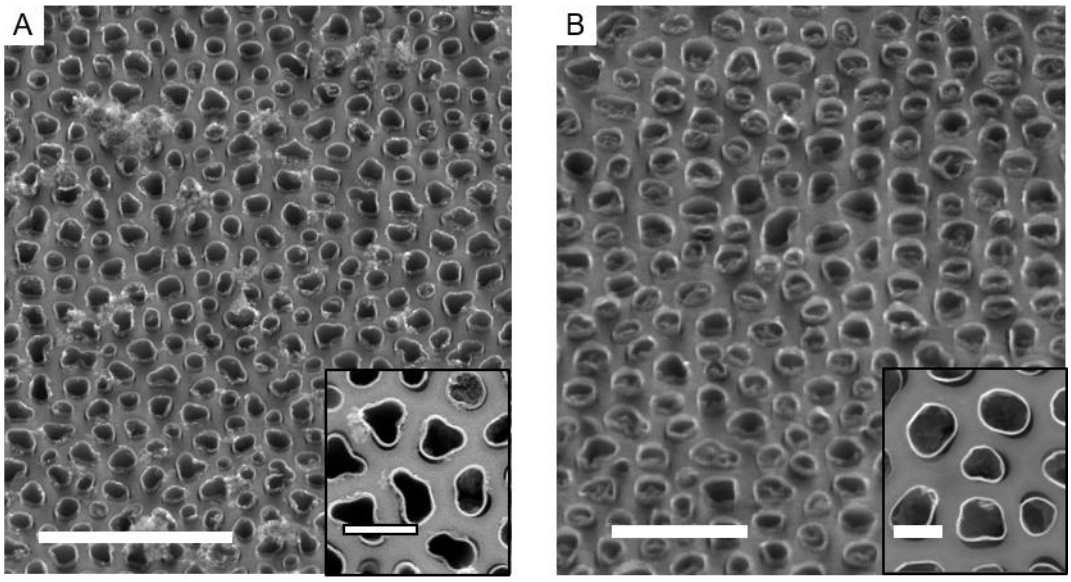

Figure 5.21: 35° tilt micrographs of CNT arrays polished using **(A)** 50nm Alumina for 5 minutes at 30N, inlet shows top down view of tubes **(B)** ¼ µ DiaPro for 5 minutes, 30N, inlet shows top down view. Scale **(A)** 2µ, inlet 500nm **(B)** 1µ, inlet 250nm

3. Electron Microscopy Sciences: Type DX alpha alumina powder 0.05µm

The Struers acquired suspensions are proprietary suspensions of mono-crystalline diamonds, coolant and lubricant to minimize heat generation during the process and increase the life of the polishing pad. The Alumina powder was mixed with water or Struers proprietary DP Green Lubricant. Results of polishing from the different suspensions are shown in Fig. 5.21. A marked observation is that the reduction in suspension size has a marked increase upon the smoothness of tube walls and reduction of clogging within CNTs. The DX alpha alumina powder shows the best results with respect to clogging, however, due to the lack of lubrication, coolant and imperfect concentration of particles, accelerated polishing pad wear was observed along with increased damage to membranes during the polishing process.

In conclusion, alternative processes of fabrication have been developed which can produce CNT arrays of quality comparable to CNT arrays produced via dry etching in a fraction of the time. The use of smaller suspension particles for polishing results in increased coplanarity of tubes and decrease in clogging of CNTs.

Chapter 6: Cell Culture on CNT arrays and Transfection

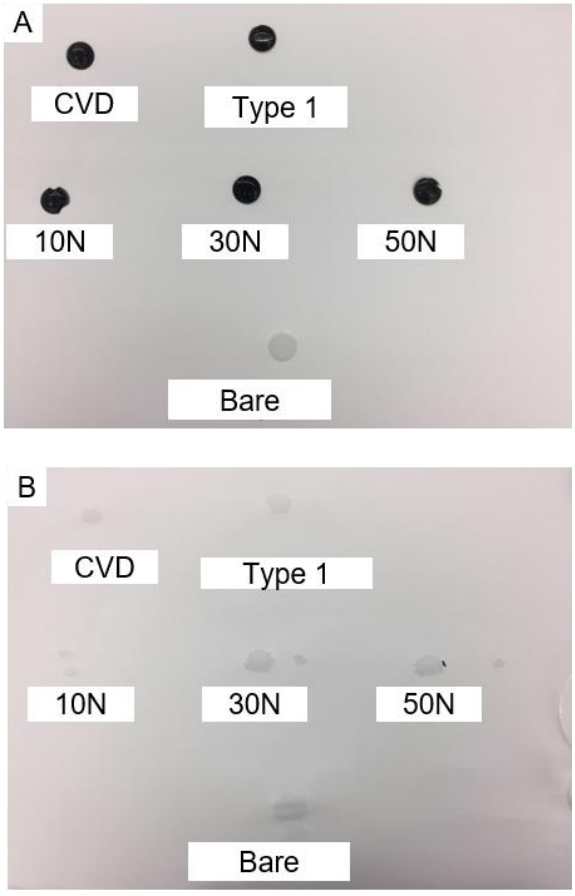

Figure 6.1: (A) Devices placed on dry paper with water droplet **(B)** wetting observed under device after 2 hours, confirming fluid flow capability

To confirm that CNT array devices were ready for use with cell transfection, basic fluid flow experiments were carried out. These experiments were not designed to quantify fluid flow parameters through nanotubes but rather to confirm that flow of fluid was possible through the devices. The experiment was set up as follows.

Devices were placed cell growth side down on a sheet of paper and a drop of DI water was placed on the device. The device was covered to prevent evaporation of the drop. After 2 hours, wetting of paper under the device confirmed that water had gone through the CNT array, depicted in Fig. 6.1 below.

6.1 Cell culture – Experiment 1: 3T3 Cell Growth on CNT arrays

The first experiment to study cell growth was carried out on devices that had been exposed to 3 minutes of oxygen plasma at 300 mTorr, 250W RF power and 100 sccm of oxygen flow. The devices were then wet etched using 1M NaOH for 15, 17 and 20 minutes. The aim of this experiment was to understand basic cell culture protocols and handling of equipment in a tissue culture room.

Cells used were of the NIH/3T3 type fibroblasts. Cells were detached from cell flask by letting them sit in trypsin for 7 minutes. Trypsin was aspirated and Dulbecco's Modified Eagle's Medium (DMEM) was added to neutralize the effects of trypsin. 20µl of cells in media was taken and dyed blue with 20µl of trypan blue to identify dead cells. 0.5µl of cells was put into a hemocytometer for counting. Each device was to be coated with 40,000 cells which was calculated as approximately 500µl.

2 of 17 minute and 15-minute etched devices each were coated with cells. Devices were rinsed with ethanol prior to use. The devices were left to dry for 5 minutes and PBS used to rinse devices to remove leftover ethanol if any. 0.5ml of cell solution was added to each well and allowed to incubate for 24 hours. To observe cells under a microscope, they were fixed using paraformaldehyde diluted in PBS (unknown concentration) and stained with a green actin filament dye. Images in Fig. 6.2 show cells growing on the devices.

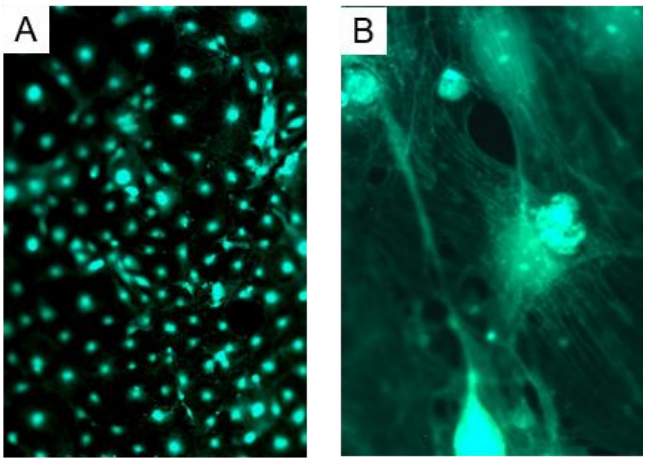

Figure 6.2: Fluorescent image of fixed 3T3 cells on CNT array etched for 17 minutes with 1M NaOH **(A)** 20x **(B)** 100x

The images in Fig. 6.2 show that cells adhered to the surface of the CNT array device and appear to be healthy as per their morphology.

6.2 Cell Culture – Experiment 2: HE293 Cell growth and EYFP transfection attempt

HEK 293 cells were cultured on CNT array devices fabricated using mechanical polishing. Devices were fabricated by carrying out CVD for 5 hours followed by polishing for 5 minutes at 30N of force using DiaPro 1µm diamond suspension. The devices were then etched using 1M NaOH for 3 minutes, 5

minutes and 7 minutes. The CNT heights were measured as 104 ± 30nm, 114±30nm and 134±39nm for 3 min, 5 min and 7 min etched devices respectively. The distribution of tube heights can be seen in fig. 6.3.

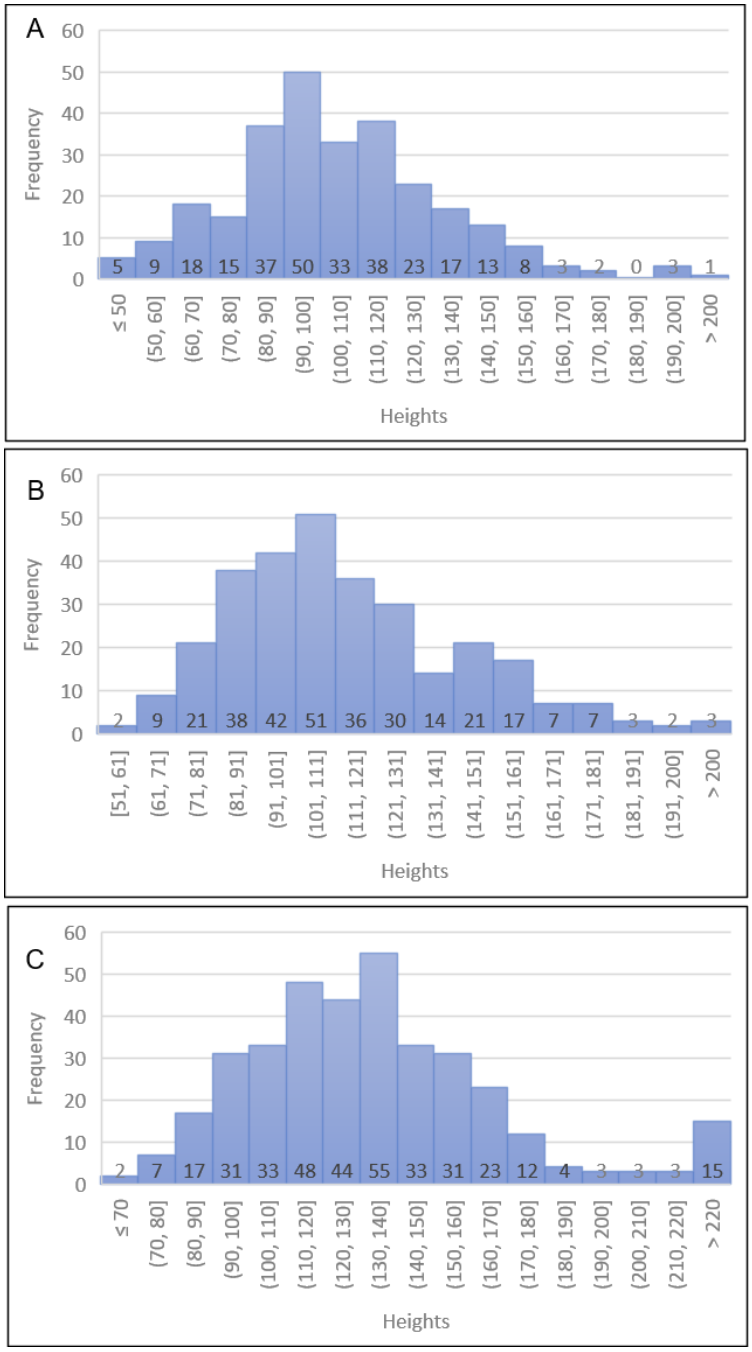

Figure 6.3: CNT height distribution after etching with 1M NaOH (A) 3 min (B) 5 min (C) 7 min

48,000 cells were added to each device as a drop on the CNT devices facing cell growth side up. The cells were allowed to adhere onto the device for 2 hours. 1ml of DMEM was added to the wells and cells

allowed to incubate for 48 hours. Cells were stained using Calcein AM green to view under fluorescent microscope. Confluency was observed ranging between 50-70% on different locations of the devices. This can be seen in fig. 6.4 below.

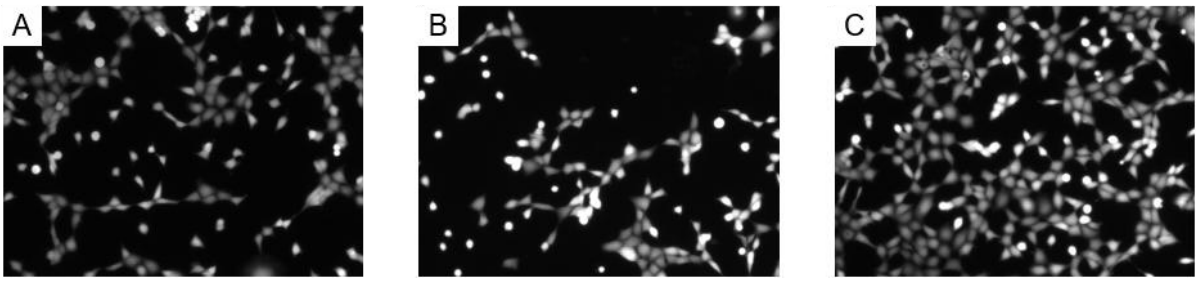

Figure 6.4: HEK293 cells harvested after 48 hours from CNT arrays **(A)** from 3 min etched device **(B)** from 5 min etched device **(C)** from 7 min etched device

The devices were then transferred to the transfection set up shown in Fig. 6 and transfection was attempted using Venus Enhanced Yellow Fluorescent Protein (EYFP). EYFP was prepared by adding 36µl of Venus DNA in 600µl of patch clamp buffer. 100µl of DNA was added to each device and they were allowed to incubate for 2 hours.

Cells were harvested from device using trypsin after 2 hours and transferred to tissue culture plastic. They were allowed to incubate for 24 hours and then viewed under a fluorescent microscope. The cells were found to show no fluorescent activity and it could be concluded that transfection was not successful. The cause of failure was hypothesized as a combination of multiple issues. As seen in Fig. 3, the devices can be seen to possess clogging within nanotubes. CNTs were also observed to have peaks and jagged edges unlike the smooth coplanar surfaces of devices fabricated through RIE. In order to increase chances of success, the above issues were addressed in preparation for the next experiment.

6.3 Cell Culture – Experiment 3: HEK293 Cell growth and EYFP transfection attempt

HEK 293 cells were cultured on arrays devices fabricated via 7 hours of CVD followed by polishing for 5 minutes at 30N. Devices were etched using 1M NaOH for 5 minutes and 7.5 minutes. As mentioned in Chapter 6, this method of fabrication resulted in unclogged CNTs. 5 devices were used for this

experiment. 3 were etched for 5 minutes and 2 were etched for 7.5 minutes. Devices were coated with 48,000 cells and allowed to incubate for 2.5 hours. 2ml of DMEM was added to each of the 5 wells containing CNT devices after 2.5 hours and 1 ml of DMEM was added to the control well in a 24-well plate. Cells were dyed red using CellTracker CMTPX. Dye was prepared by adding 50µg of CellTracker red to 70µl of Dimethyl Sulfoxide (DMSO). 2µl dye was added to 2ml of media in 6 well plates and allowed to sit for 30 minutes. Cells were then viewed under a rhodamine filter and had appeared to have achieved confluency of 90%. Lipofection was used for the control experiment. 50µl Jet Prime buffer was mixed with 1µl jet prime reagent and 0.5µg of Venus YFP. Control well media was aspirated and 0.5ml of fresh media added and the lipofection solution added. For transfection using CNT devices, 600µl patch clamp buffer was mixed with 36µl Venus DNA. Each device received 100µl of Venus DNA solution.

Devices were pulled out of the incubator after 2.5 hours and transferred to new well plates. They were viewed again under the rhodamine filter and appeared to be confluent. It should be noted at this point that the microscope was not equipped with a camera and thus images were not acquired. Devices were washed with trypsin and cells were transferred to 6 well plates, allowed to incubate for 24 hours. Very few cells were observed after 24 hours and no fluorescence was observed either. In contrast, the control well cells fluoresced bright yellow. This indicated another failure in transfection. The leading cause for this failure was identified as mishandling when cells were harvested from CNT array devices to well plates after transfection. Also, cells were plated on the device for only 24 hours prior to transfection. According to Golshadi, the time that cells were allowed to grow on devices prior to transfection had a significant impact on transfection efficiency. The low concentration of DNA was as also cited as a major reason for lack of fluorescence. Transfection using CNT array device requires a much higher concentration of DNA as compared to lipofection.

In parallel with this experiment, the following set up was also tested for transfection. Fig. 6.5 shows a Whatman paper which has been wetted with DMEM. Instead of laying CNT devices on cylinders, the device was laid down cell side down on the Whatman paper. Protocols for cell culture, dye preparation

and DNA preparation followed were the same as above in this experiment. Cells were transfected in the same method as above. Cells were found to adhere well to the device and did not adhere to the Whatman paper. However, no transfection was observed. This method has potential for reducing device damage and improve ease of handling during the transfection process.

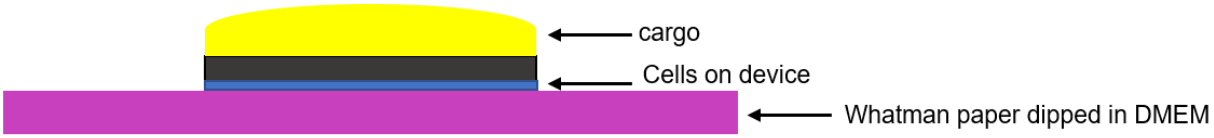

Figure 6.5: Set up for transfection using Whatman paper

Keeping in mind the above-mentioned drawbacks, the next cell culture experiment was carried out using propidium iodide (PI), a cell impermeable dye and cells allowed to culture for 48 hours.

6.4 Cell culture – Experiment 4: HEK293 Cell Growth, PI injection

3 devices were used for this cell culture experiment. The devices were exposed to CVD for 7 hours, followed by 5 minutes of polishing at 30N using 1µm DiaPro diamond suspension. The devices were then wet etched for 5 minutes and 7.5 minutes with 1M NaOH. Each device came from 3 distinct regions of the boat. Calcein AM purple was used to stain cells for fluorescence and Propidium Iodide was used as cargo for delivery inside cells. Calcein Purple was created by adding 42µl of sterile DMSO to 25µg of dye. 40µl of this solution was added to 1250µl of buffer to create 200x working solution. For 6 wells, at 1ml per well, 30µl of working solution was needed. Propidium Iodide was used at 75µm concentration in patch clamp buffer (PCB). A 100x stock solution was made by adding 5mg of PI per 1ml of PBS. Therefore, the final solution required 300µl of PCB in 3µl of 100x PI.

Each device was coated with 24,000 cells by placing a 100µl drop of cells in media on the top surface of device. The cells were then allowed to attach for 2 hours on the surface in an incubator and 2ml of media was added to each well with the devices. Cells were allowed to incubate for 48 hours before transfection. Due to a handling error, excess PI was added on the devices, leading to quick cell death since high concentrations of PI can be toxic to cells. Transfection data was thus not obtained. PI was seen to have

been transferred to through CNTs. After only a small number of cells could be harvested from the device again.

A critical observation from the above experiments was the small number of cells harvested after transfection from CNT devices. This lead to re-evaluation of the experimental set up and identification of potential problems.

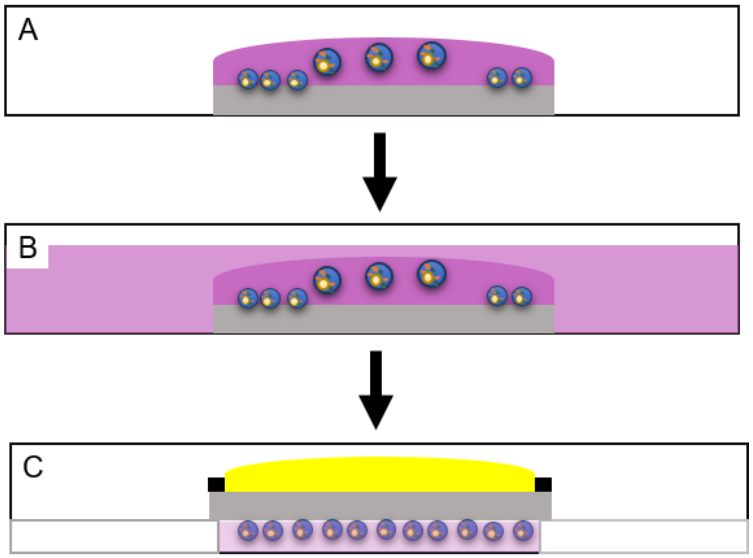

Figure 6.6: Schematic showing steps involved in transfection process **(A)** Cell adherence by placing a drop of cells on device (2 hours) **(B)** Adding media to let cells grow (48 hours) **(C)** Placing device upside down in cylinder, cell side in DMEM, cargo placed on top (2 hours)

Fig. 6.6 shows the handling and manipulation required throughout the process. CNT arrays are first placed in a 6 well plate and sterilized using ethanol. The ethanol is allowed to dry, followed by rinsing with PBS. A 100-150µl drop of media containing the required number of cells is placed on the device. This is preferred over immersing the device in 1-2ml of media with cells to prevent cells from adhering and growing on the underside of the device where cargo to be transfected will be placed. Cells are allowed 2 hours to adhere on to the surface before each well is filled with 1-2ml of media and left to incubate for 24-48 hours. Devices are then transferred into the transfection set up. Each cylinder in is

filled with 150µl of fresh media and device is placed such that the cell adherent surface is immersed in media. A drop of solution (PCB or DMSO) containing the required cargo is placed on the other side of the device with great care to prevent the drop from breaking and leaking into the media or sliding off the device. The set-up is placed in the incubator for 2 hours. After this step, devices are washed with PBS and cells trypsinized. The cells are then transferred to a new 6 well plate with 1-2ml of media and allowed to incubate for 24 hours to show transfection.

In the above protocol, the first step of attaching cells to the device is rife with ambiguity about cells adhering to the CNT surface. Golshadi et. al had immersed CNT devices in media for 24 hours to allow cells to grow on the device. However, this poses the risk of cells growing on the bottom surface too. Moreover, due to the extremely smooth surface finish of polished CNT arrays, it is difficult to make sure that the drop of cells in media remains completely upon the device and much of it can slide off with ease. This can potentially lead to a loss of cells on the device. With a thin layer of cells on the device and high variability in confluency, it is likely that the cargo takes the path of least resistance like any other fluid flow system, allowing cargo to leach into the media below.

6.5 3D Printed Nanofluidic Device

Whatman Anodisc 13 alumina membranes are 60µm in thickness. This results in extreme fragility and in turn results in easy loss of devices by cracking during handling and manipulations carried out during experiments. In order to ease handling of the CNT devices, three-dimensional (3D) printing was used to create a support structure for the membranes. 3D printing was utilized to encapsulate the CNT array in a microfluidic device. In Fig. 6.7 shows the geometry of the proposed structure and different sizes of rings printed around a bare AAO membrane.

The 3D printed rings around CNT devices served multiple purposes during the course of culturing cells and subsequent transfection. Apart from developing cracks or due to handling errors in dry conditions, during the production of devices, CNT devices were found to adhere to wet surfaces due to

surface tension. This required very delicate handling, which was operator dependent and could not be standardized for large-scale use. This problem was further exacerbated when the liquid in question was of higher viscosity as is commonly observed in with growth media in cell culture or wet etchants during production such as phosphoric acid (H_3PO_4). This lead to the device being damaged when lifting off from a wet surface while transferring from one culture dish to another. The 3D printed ring provided an uneven surface, which easily breaks surface tension and can be easily held by tweezers while minimizing the risk of damage to CNT device.

During the process of transfection, the ring not only could provide physical support but also serve as a reservoir for the purpose of holding cargo to be delivered into cells. The thickness of 3D printed ring may potentially be increased to accommodate larger volumes of reagent and this also prevents tweezer - cell contact, thereby minimizing the risk of cell death due to any stress that might be inflicted upon them by

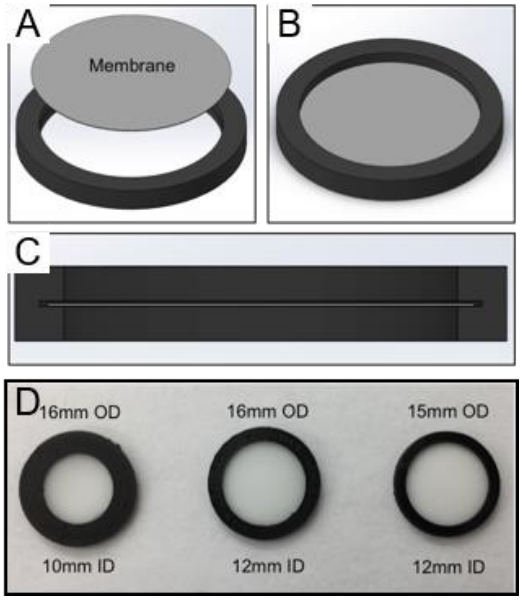

Figure 6.7: (A, B, C) CAD illustrations of proposed 3D printed rings **(D)** 3D printed prototypes of different sizes on plain AAO membranes

tweezers. Moreover, since the active area of the device is now defined by the inner diameter of the ring, it provides for a more confident analysis of cell growth and transfection. This is because the edges of the device display imperfections, which can hinder functionality.

To demonstrate cell culture on 3D printed devices, HEK 293 cells were cultured on the 3D printed CNT array devices for 48 hours and stained with CellTracker Green to observe cell growth and morphology. Devices were coated with Polylysine to aid in cell adhesion. Cells displayed morphology similar to devices without support structure or standard tissue culture plastic as shown in Fig. 6.8.

The cell growth results were as expected due to the nature of the process used to fabricate the rings. The PLA does not contact the bulk of CNT device surface during 3D printing and serves purely as a

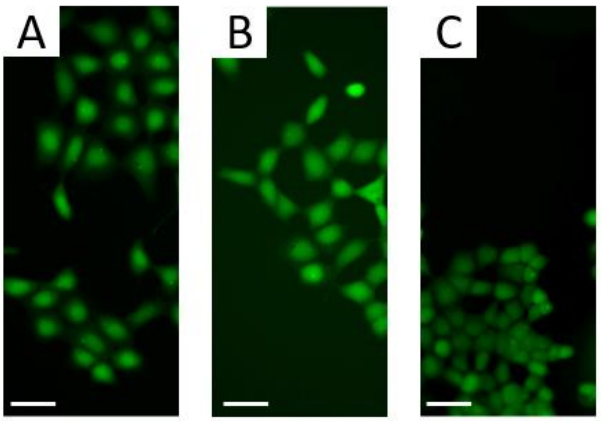

Figure 6.8: HEK 293 cells stained with CellTracker Green on **(A)** standard tissue culture plastic **(B)** CNT device **(C)** CNT device with support structure. Scale: 50 µm

holder for these devices without affecting cell culture on the surface of the device. Thus, the presence of a support structure had no detrimental effect on cell growth.

Conclusion

It can be concluded that cells grow on CNT array devices using regular cell culture protocol. However, more work needs to be done to establish a technique which will minimize loss of cells from the device to maximize transfection. A 3D printed support was developed to aid in handling of device and cell culture was demonstrated on the device.

Chapter 7: Conclusion

7.1 Research Summary

Carbon nanotube arrays have shown the potential to be used as a device for intracellular delivery of biomolecules of different size and charges into immortalized cell lines and also hard to transfect cells such as stem cells, neurons and macrophages. With an increased demand for novel therapeutics which offer features such as targeted drug delivery, personalized treatments and combination of gene therapy and stem cell therapy, the CNT array device can potentially be an indispensable tool for the future of medicine. Since carbon is a conductive material, this device also offers the potential of being used an intracellular probe which can carry out single cell analysis on multiple cells simultaneously. This makes it highly desirable for use in biomedical research applications as an aid to study cell functioning. However, a major limiting factor for the development of this device and expansion of its use in the scientific and medical community was the expensive and time-consuming fabrication process involved in their manufacture. Depending upon the physical requirements of the device, the time spent in etching 8 devices could go up to 12 hours using reactive ion etching.

In this thesis, a number of alternative nanofabrication processes have been outlined for the production of CNT array with the aim of reducing time for production and increasing yield. An emphasis was given on avoiding processes which required clean room facilities or plasma based processes in order to minimize variability due to environmental and equipment based factors. This was also important to keep costs low and enable scaling up the production of devices. Mechanical polishing, a purely physical and economically feasible method, along with wet chemical etching were selected as an alternative to reactive ion etching. Both processes require minimal resources and can be scaled up in a linear manner at low cost. The effects of parameters such as polishing force, time, etching time and etchant molarity on physical dimensions of CNT arrays were documented. It was shown that the presented alternative processes could control CNT height distribution to a fine degree in a relatively short processing time ranging from 5-30

minutes of polishing followed by 5-30 minutes of wet etching. Compared to the reactive ion etching process, this implies a time saving of nearly 97%. It also has the advantage of being able to increase yield by using equipment with a larger holding capacity since polishing and wet etching are not dependent upon the scale of the device.

The quality of CNTs was qualitatively analyzed using scanning electron microscopy. Issues associated with the polishing process included clogging of nanotubes, damaged tubes, cracked and broken membranes during polishing and rough CNT wall edges. The use of process variables such as CVD time, positioning of samples in CVD furnace tube and change in polishing particle size to control CNT quality was shown. CNTs could be produced with clogged or unclogged tubes depending upon the need of application.

Lastly, cell growth has been demonstrated on CNT arrays and attempts made to transfect with EYFP and Propidium Iodide dye. Potential causes of failure and variability were identified.

7.2 Future work:

7.2.1 Future work in nanofabrication technique:

The newly developed fabrication process can save up time by up to 97%. However, a number of issues such as variability in polishing due mounting membranes on the polishing set up and loss of devices due to formation of cracks were identified. Future work can be carried out to refine the technique and scale up the process. The use of alumina slurry had shown potential in producing CNTs with smooth edges, minimal damage and no clogging. The alumina particles in turn lead to accelerated wear of the polishing pad. Work on studying the right amount and type of polishing lubricant and coolants to be added would be a valuable input.

Whatman Anodisc AAO membranes are extremely fragile and are easily damaged during handling over the course of experiments. To aid in handling the device and also providing a built-in reservoir for fluid over the device, fused deposition modeling 3D printer was used to print a ring around the CNT arrays.

This provided the CNT array device with added rigidity and ease of handling. Future work on incorporating more extensive 3D printed devices using CNT devices is of great interest. Development of microfluidic chips with CNT devices can eliminate the need to for multiple handling steps during experiments and provide a simple, sterile and disposable platform for carrying out transfection.

7.2.2 Future work in cell culture and transfection

In this thesis, only devices polished with 1µm DiaPro were used to study cell growth on CNT arrays. This resulted in devices that were clogged with damaged tubes or CNTs with jagged walls. The presence of variability in cells adhering to the device also was a potential issue that was identified. With respect to cell growth, a number of parameters need to be understood such as the ideal CNT height for transfection and cell growth, use of membranes with different pore spacing or diameters as the CVD template to study cell growth when CNT diameters and CNT spacing changes.

The effect of time and cell growth is also not documented in depth for CNT arrays. It was noted by Golshadi that an increase in cell culture time prior to transfection would lead to an increase in transfection efficiency. An in-depth study to understand the correlation between transfection efficiency and culture time can lead to interesting insights about CNT – cell interfacing. It has also been shown that stem cells are highly sensitive to their physical surroundings. Therefore, it will be required to understand the effect of CNT arrays on stem cell differentiation

REFERENCES

[1] "Gene Therapy." *Gene Therapy*. American Medical Association. Web. 04 Mar. 2016.

[2] Hunt, K.K., Vorburger, S.A., Swisher, S.G., 2006, "Gene Therapy for Cancer," Humana Press, Totowa, NJ, .

[3] Liu, S., Xia, Z., and Zhong, Y., 2014, "Gene Therapy in Pancreatic Cancer," World Journal of Gastroenterology : WJG, **20**(37) pp. 13343-13368.

[4] Sinn, P. L., Anthony, R. M., and McCray, J., Paul B, 2011, "Genetic Therapies for Cystic Fibrosis Lung Disease," Human Molecular Genetics, **20**(R1) pp. R86.

[5] Tebas, P., Stein, D., Tang, W. W., 2014, "Gene Editing of CCR5 in Autologous CD4 T Cells of Persons Infected with HIV," New England Journal of Medicine, **370**(10) pp. 901-910.

[6] Berkhout, B., Ertl, H.C.J., Weinberg, M.S., 2015, "Gene Therapy for HIV and Chronic Infections," Springer New York, New York, NY, .

[7] Bennett, J., 2009, "Gene Therapy for Color Blindness," New England Journal of Medicine, **361**(25) pp. 2483-2484.

[8] Kootstra, N. A., and Verma, I. M., 2003, "Gene Therapy with Viral Vectors," Annual Review of Pharmacology and Toxicology, **43**pp. 413-439.

[9] Woods, N., Muessig, A., Schmidt, M., 2003, "Lentiviral Vector Transduction of NOD/SCID Repopulating Cells Results in Multiple Vector Integrations Per Transduced Cell: Risk of Insertional Mutagenesis," Blood, **101**(4) pp. 1284-1289.

[10] Kay, M. A., Thomas, C. E., and Ehrhardt, A., 2003, "Progress and Problems with the use of Viral Vectors for Gene Therapy," Nature Reviews Genetics, **4**(5) pp. 346-358.

[11] Walther, D. W., and Stein, U., 2012, "Viral Vectors for Gene Transfer," Drugs, **60**(2) pp. 249-271.

[12] FUCHSLUGER, T., 2011, "Viral Vectors for Gene Transfer," Acta Ophthalmologica, **89**(s246) pp. 0.

[13] Neumann, E., Schaefer-Ridder, M., Wang, Y., 1982, "Gene Transfer into Mouse Lyoma Cells by Electroporation in High Electric Fields," The EMBO Journal, **1**(7) pp. 841-845.

[14] Potter, H., 2001, "Transfection by Electroporation," Current Protocols in Neuroscience / Editorial Board, Jacqueline N. Crawley ... [Et Al.], **Appendix 1**pp. Appendix 1E.

[15] Niidome, T., and Huang, L., 2002, "Gene Therapy Progress and Prospects: Nonviral Vectors," Gene Therapy, **9**(24) pp. 1647-1652.

[16] Henry, S., McAllister, D. V., Allen, M. G., 1998, "Microfabricated Microneedles: A Novel Approach to Transdermal Drug Delivery," Journal of Pharmaceutical Sciences, **87**(8) pp. 922-925.

[17] Ali, R. R., 2004, "Prospects for Gene Therapy," Novartis Foundation Symposium, **255**pp. 165.

[18] Li, S., and Huang, L., 2000, "Nonviral Gene Therapy: Promises and Challenges," Gene Therapy, **7**(1) pp. 31-34.

[19] Golshadi, M., and Schrlau, M. G., 2013, "Template-Based Synthesis of Aligned Carbon Nanotube Arrays for Microfluidic and Nanofluidic Applications," ECS Transactions, **50**(33) pp. 1-14.

[20] Golshadi, M., Wright, L. K., Dickerson, I. M., 2016, "High-Efficiency Gene Transfection of Cells through Carbon Nanotube Arrays," Small, pp. n/a.

[21] Wirth, T., Parker, N., and Ylä-Herttuala, S., 2013, "History of Gene Therapy," Gene, **525**(2) pp. 162-169.

[22] Karson, E. M., 1990, "Prospects for Gene Therapy." Biology of Reproduction, **42**(1) pp. 39-49.

[23] ROGERS, S., and PFUDERER, P., 1968, "Use of Viruses as Carriers of Added Genetic Information," Nature, **219**(5155) pp. 749-751.

[24] Cross, D., and Burmester, J. K., 2006, "Gene Therapy for Cancer Treatment: Past, Present and Future," Clinical Medicine and Research, **4**(3) pp. 218-227.

[25] Cavazzana, M., Ribeil, J. A., Payen, E., 2014, "Outcomes of Gene Therapy for Beta Thalassemia Major Via Transplantation of Autologous Hematopoietic Stem Cells Transduced Ex Vivo with a Lentiviral Beta A T87Q Globin Vector," Human Gene Therapy, **25**(11) pp. A22.

[26] Ylä-Herttuala, S., and Martin, J. F., 2000, "Cardiovascular Gene Therapy," The Lancet, **355**(9199) pp. 213-222.

[27] Escors, D., and SpringerLink (Online service), 2012, "Lentiviral vectors and gene therapy," Springer, New York; Basel, .

[28] Kaiser, J., 2009, "GENE THERAPY Beta-Thalassemia Treatment Succeeds, with a Caveat," Science, **326**(5959) pp. 1468-1469.

[29] Aubourg, P., Hacein-Bey-Abina, S., Bartholomae, C., 2011, "Hematopoietic Stem Cell Gene Therapy with Lentiviral Vector in X-Linked Adrenoleukodystrophy," Blood, **118**(21) pp. 80.

[30] Cavazzana-Calvo, M., Hacein-Bey, S., Basile, G. d. S., 2000, "Gene Therapy of Human Severe Combined Immunodeficiency (SCID)-X1 Disease," Science, **288**(5466) pp. 669-672.

[31] National Institutes of Health [NIH] (United States). Recombinant DNA Advisory Committee, 2002, "NIH Report: Assessment of Adenoviral Vector Safety and Toxicity: Report of the National Institutes of Health Recombinant DNA Advisory Committee," .

[32] Anderson, W. F., 2002, "Adenoviral Vector Safety and Toxicity," Human Gene Therapy, **13**(1) pp. 1.

[33] Felgner, P. L., Gadek, T. R., Holm, M., 1987, "Lipofection: A Highly Efficient, Lipid-Mediated DNA-Transfection Procedure," Proceedings of the National Academy of Sciences of the United States of America, **84**(21) pp. 7413-7417.

[34] C. Madeira, R. D. Mendes, S. C. Ribeiro, 2010, "Nonviral Gene Delivery to Mesenchymal Stem Cells using Cationic Liposomes for Gene and Cell Therapy," Journal of Biomedicine and Biotechnology, **2010**pp. 735349-13.

[35] Onishi, A., Iwamoto, M., Akita, T., 2000, "Pig Cloning by Microinjection of Fetal Fibroblast Nuclei," .

[36] Brinster, R. L., Chen, H. Y., Trumbauer, M. E., 1985, "Factors Affecting the Efficiency of Introducing Foreign DNA into Mice by Microinjecting Eggs," Proceedings of the National Academy of Sciences of the United States of America, **82**(13) pp. 4438-4442.

[37] Kaushik, S., Hord, A. H., Denson, D. D., 2001, "Lack of Pain Associated with Microfabricated Microneedles," Anesthesia and Analgesia, **92**(2) pp. 502-504.

[38] Prausnitz, M. R., 2004, "Microneedles for Transdermal Drug Delivery," Advanced Drug Delivery Reviews, **56**(5) pp. 581-587.

[39] Bariya, S. H., Gohel, M. C., Mehta, T. A., 2012, "Microneedles: An Emerging Transdermal Drug Delivery System," Journal of Pharmacy and Pharmacology, **64**(1) pp. 11-29.

[40] Yang, N., Burkholder, J., Roberts, B., 1990, "In Vivo and in Vitro Gene Transfer to Mammalian Somatic Cells by Particle Bombardment," Proceedings of the National Academy of Sciences of the United States of America, **87**(24) pp. 9568-9572.

[41] Gómez-Chiarri, M., Livingston, S. K., Muro-Cacho, C., 1996, "Introduction of Foreign Genes into the Tissue of Live Fish by Direct Injection and Particle Bombardment," Diseases of Aquatic Organisms, **27**pp. 5-12.

[42] Shalek, A. K., Robinson, J. T., Karp, E. S., 2010, "Vertical Silicon Nanowires as a Universal Platform for Delivering Biomolecules into Living Cells," Proceedings of the National Academy of Sciences of the United States of America, **107**(5) pp. 1870-1875.

[43] Kim, W., Ng, J. K., Kunitake, M. E., 2007, "Interfacing Silicon Nanowires with Mammalian Cells," Journal of the American Chemical Society, **129**(23) pp. 7228-7229.

[44] McKnight, T. E., Melechko, A. V., Griffin, G. D., 2003, "Intracellular Integration of Synthetic Nanostructures with Viable Cells for Controlled Biochemical Manipulation," Nanotechnology, **14**(5) pp. 551-556.

[45] VanDersarl, J. J., Xu, A. M., and Melosh, N. A., 2012, "Nanostraws for Direct Fluidic Intracellular Access," Nano Letters, **12**(8) pp. 3881.

[46] Park, S., Kim, Y., Kim, W. B., 2009, "Carbon Nanosyringe Array as a Platform for Intracellular Delivery," Nano Letters, **9**(4) pp. 1325.

[47] Lau, K. K. S., Bico, J., Teo, K. B. K., 2003, "Superhydrophobic Carbon Nanotube Forests," Nano Letters, **3**(12) pp. 1701-1705.

[48] F. H.H. Gojny, M H G Wichmann, 2004, "Gojny, F.H., Et Al.: Carbon Nanotube-Reinforced Epoxy-Composites:Enhanced Stiffness and Fracture Toughness at Low Nanotube Content. Compos. Sci. Technol. 64, 2363-2371," Composites Science and Technology, **64**(15) pp. 2363-2371.

[49] Yang, W., Thordarson, P., Gooding, J. J., 2007, "Carbon Nanotubes for Biological and Biomedical Applications," Nanotechnology, **18**(41) pp. 412001.

[50] Lim, H. D., Park, K. Y., Song, H., 2013, "Enhanced Power and Rechargeability of a LiO2 Battery Based on a Hierarchical-Fibril CNT Electrode," Advanced Materials, **25**(9) pp. 1348-1352.

[51] Li, L., Yang, H., Zhou, D., 2014, "Progress in Application of CNTs in Lithium-Ion Batteries," Journal of Nanomaterials, **2014**pp. 1-8.

[52] Wang, X. H., Sun, L. N., Susantyoko, R. A., 2014, "Ultrahigh Volumetric Capacity Lithium Ion Battery Anodes with CNT-Si Film," Nano Energy, **8**pp. 71-77.

[53] O'Connell, M., Wisdom, J. A., Dai, H., 2005, "Carbon Nanotubes as Multifunctional Biological Transporters and Near-Infrared Agents for Selective Cancer Cell Destruction," Proceedings of the National Academy of Sciences of the United States of America, **102**(33) pp. 11600-11605.

[54] Khawli, L. A., and Prabhu, S., 2013, "Drug Delivery Across the Blood-Brain Barrier," Molecular Pharmaceutics, **10**(5) pp. 1471.

[55] Harrison, B. S., and Atala, A., 2007, "Carbon Nanotube Applications for Tissue Engineering," Biomaterials, **28**(2) pp. 344-353.

[56] Kohli, P., and Martin, C. R., 2003, "The Emerging Field of Nanotube Biotechnology," Nature Reviews Drug Discovery, **2**(1) pp. 29-37.

[57] Wang, J., 2005, "Carbon-nanotube Based Electrochemical Biosensors: A Review," Electroanalysis, **17**(1) pp. 7-14.

[58] Li, J., Ng, H. T., Cassell, A., 2003, "Carbon Nanotube Nanoelectrode Array for Ultrasensitive DNA Detection," Nano Letters, **3**(5) pp. 597-602.

[59] Brigger, I., Dubernet, C., and Couvreur, P., 2002, "Nanoparticles in Cancer Therapy and Diagnosis," Advanced Drug Delivery Reviews, **54**(5) pp. 631-651.

[60] Cherukuri, P., Gannon, C. J., Leeuw, T. K., 2006, "Mammalian Pharmacokinetics of Carbon Nanotubes using Intrinsic Near-Infrared Fluorescence," Proceedings of the National Academy of Sciences of the United States of America, **103**(50) pp. 18882-18886.

[61] Singh, R., Pantarotto, D., Lacerda, L., 2006, "Tissue Biodistribution and Blood Clearance Rates of Intravenously Administered Carbon Nanotube Radiotracers," Proceedings of the National Academy of Sciences of the United States of America, **103**(9) pp. 3357-3362.

[62] Saltzman, W. M., and Olbricht, W. L., 2002, "Building Drug Delivery into Tissue Engineering," Nature Reviews. Drug Discovery, **1**(3) pp. 177-186.

[63] Abarrategi, A., Gutiérrez, M. C., Moreno-Vicente, C., 2008, "Multiwall Carbon Nanotube Scaffolds for Tissue Engineering Purposes," Biomaterials, **29**(1) pp. 94-102.

[64] Yang, N., Chen, X., Ren, T., 2015, "Carbon Nanotube Based Biosensors," Sensors and Actuators B: Chemical, **207**pp. 690-715.

[65] Gelain, F., 2008, "Novel Opportunities and Challenges Offered by Nanobiomaterials in Tissue Engineering," International Journal of Nanomedicine, **3**(4) pp. 415-424.

[66] Che, G., Lakshmi, B. B., Martin, C. R., 1998, "Chemical Vapor Deposition Based Synthesis of Carbon Nanotubes and Nanofibers using a Template Method," Chemistry of Materials, **10**(1) pp. 260-267.

[67] Xu, J., Zhang, X., Chen, F., 2005, "Preparation and Modification of Well-Aligned CNTs Grown on AAO Template," Applied Surface Science, **239**(3) pp. 320-326.

[68] Williams, K. R., Gupta, K., and Wasilik, M., 2003, "Etch Rates for Micromachining Processing-Part II," Journal of Microelectromechanical Systems, **12**(6) pp. 761-778.

[69] Zhou, B. R., W.F, 1996, "Kinetics and Modeling of Wet Etching of Aluminum Oxide by Warm Phosphoric Acid," Journal of the Electrochemical Society, **143**(2) pp. 619.

[70] Guofeng Hu, Haiming Zhang, Wenwen Di, 2009, "Study on Wet Etching of AAO Template," Applied Physics Research, **1**(2) pp. 78.

[71] Xiao, Z. L., Han, C. Y., Welp, U., 2002, "Fabrication of Alumina Nanotubes and Nanowires by Etching Porous Alumina Membranes," Nano Letters, **2**(11) pp. 1293-1297.

[72] Kim, N. H., Kim, D. S., Lee, H. U., 2007, "Fabrication of Microchannel Containing Nanopillar Arrays using Micromachined AAO (Anodic Aluminum Oxide) Mold," Microelectronic Engineering, **84**(5) pp. 1532-1535.

[73] Jee, S. E., Lee, P. S., Yoon, B., 2005, "Fabrication of Microstructures by Wet Etching of Anodic Aluminum Oxide Substrates," Chemistry of Materials, **17**(16) pp. 4049-4052.

[74] Lee, K. H., Huang, Y. P., and Wong, C. C., 2011, "Nanotip Fabrication by Anodic Aluminum Oxide Templating," Electrochimica Acta, **56**(5) pp. 2394-2398.

[75] Park, S., Kim, Y., Kim, W. B., 2009, "Carbon Nanosyringe Array as a Platform for Intracellular Delivery," Nano Letters, **9**(4) pp. 1325.

[76] Nojiri, K., and SpringerLink (Online service), 2014, "Dry Etching Technology for Semiconductors," Springer International Publishing, Cham, .

[77] Anonymous "Electroporation," **2016**.

[78] https://commons.wikimedia.org/w/index.php?curid=350191, "Chirality of Carbon Nanotube," **Public Domain**.